Microfurnace Design for Fabrication of Tapered Optical Fiber Conveyor Belts

A Major Qualifying Project Report:

Submitted to the Faculty

of the

WORCESTER POLYTECHNIC INSTITUTE

in partial fulfillment of the requirements for the

Degree of Bachelor of Science

by

Brandon Bozeat

Jonathan Stump

Advisor:
Professor Yuxiang Liu

Date: April 27th, 2017

Abstract

Fiber optics are widely used in optical telecommunications, including internet signals, to transmit information. Through special fabrication methods, the same optical fibers can be used for microscale biological applications, such as sensing and manipulating cells. These methods include heat-and-draw processes that reduce the diameter of the fiber to approximately 1 micrometer, resulting in a tapered profile. Particle manipulation is possible through light-matter interaction that occurs outside the physical boundary of the fibers throughout the tapered section. Common flame-based tapering processes are poorly repeatable and susceptible to instabilities, which cause losses of power transmission and diminish the taper's ability to manipulate particles.

Our goal was to develop an improved and repeatable fabrication process to produce tapered fibers that have low losses in water and therefore have reliable particle trapping capabilities. We designed and built an electrical microfurnace that produced tapered fibers with up to 96% optical transmission in air and with a max of 10% deviation in transmission between subsequent trials. Compared to ~80% transmission with the flame fabrication and no guarantee that the next fiber produced will be of similar quality. In water, these fibers lost no more than an additional 33% of optical power, compared with ~80% loss with the flame method. With this significantly improved optical transmission, an optical conveyor belt has been experimentally demonstrated in water, with microscale particles trapped and propelled along the fiber taper.

Table of Contents

Chapter 1: Introduction

Optical fibers, shown in Figure 1, are used to transmit light by the mechanism of total internal reflection. They are commonly used in telecommunications to transmit data such as internet connections over long distances via electromagnetic carrier waves. In a single optical fiber, layers of glass and plastic with different indices of refraction act as a waveguide such that light is confined to the innermost layer of the fiber.

Figure 1: A bundle of optical fibers [1]

Tapered optical fibers, also called optical fiber nanowires, are specially fabricated optical fibers with two transition regions where the diameter of the fiber changes as a function of position along the length of the fiber, shown in Figure 2. These regions meet at a narrow waist having a diameter around 1µm. [2] Tapered fibers exhibit unique optical and mechanical properties which are essential their numerous applications.

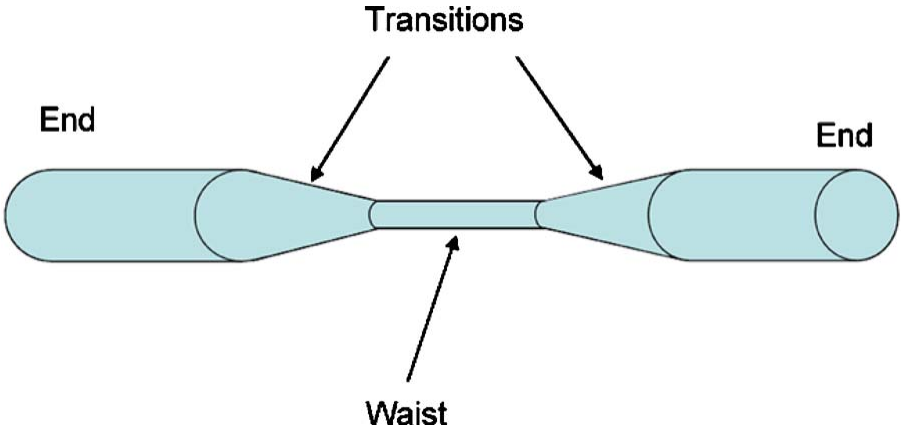

Figure 2: Optical fiber taper [3]

1.1 Motivation

Although conventional fiber optics are widely used in applications of telecommunications, imaging, and sensing, tapered fibers are still an emerging technology. Literature cites many applications of optical fibers with tapered regions, particularly in the field of microfluidics [4] due to the presence of large evanescent fields, which can be exploited for particle manipulation, sensors, and high-Q resonators. [3, 5] These applications are the topics of ongoing research that depends on the fabrication of such tapered fibers.

Conventional optical fibers are appealing because they offer low losses over large distances. This property of high transmission is due to total internal reflection, which results from a difference in refractive indices between the core of a fiber and its cladding. In the process of creating a tapered fiber, however, the optical boundary between the fiber's core and cladding is either removed or damaged. While this is necessary to create a fiber with the desired properties, particularly that of having a large evanescent field, it can significantly reduce the transmission through the fiber. The primary limitation of research requiring optical fiber nanowires is the perceived difficulty in creating low-loss fiber tapers. [3]

Power loss is of paramount concern for applications exploiting the large evanescent field present in tapered regions of optical nanowires because these applications utilize power that propagates outside the physical boundary of the fiber. [3] Since the cladding is modified during tapering, the ambient medium can strongly affect the transmission through a tapered fiber; for example, a fiber with losses of approximately 1 dB in air may experience losses between 2 and 5 dB in water. [4] Other causes of transmission loss in tapered fibers are low diameter uniformity and high surface roughness. [6]

Many properties of tapered optical fibers that affect transmission are a result of the process by which they were produced. It is therefore the goal of this project to develop a process for repeatedly fabricating low-loss optical fiber tapers.

Chapter 2: Background

Tapered optical fibers share many properties with conventional optical fibers with some additional benefits due to their geometry, which make them uniquely suitable for special applications. These properties are the result of a variety of methods for creating optical fiber tapers. This section discusses and compares the various properties, applications, and fabrication methods of tapered optical fibers with standard optical fibers.

2.1 Standard Optical Fibers

A typical single-mode fiber (SMF) consists of three layers: a silica glass core, a silica glass cladding layer, and a polymer buffer, as shown in Figure 3. The core layer is typically made of pure silica glass, while the cladding layer contains impurities to increase its refractive index and allow total internal reflection to occur. [7]

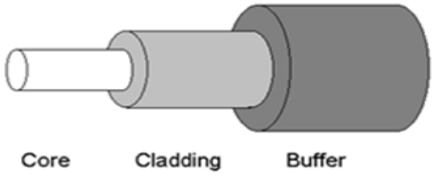

Figure 3: Single-mode fiber cross-sections [8]

In a single-mode fiber, the core, cladding, and buffer layers are around 9 µm, 125 µm, and 250 µm in diameter, respectively. Multi-mode fibers have cores with diameters up to 100 µm, but are not considered in this report as they are not commonly used for fiber tapering. In both types of fibers, the purpose of these layers is to confine light to the core, which maximizes transmission for carrying a signal.

By substituting the expressions for electromagnetic fields in optical fibers into Maxwell's equations, two sets of wave equations are derived [9]:

$$\frac{\partial^2 E_z}{\partial r^2} + \frac{1}{r}\frac{\partial E_r}{\partial r} + \frac{1}{r}\frac{\partial^2 E_z}{\partial \theta^2} + [k^2 n(r,\theta)^2 - \beta^2]E_z = 0 \quad (1)$$

$$\frac{\partial^2 H_z}{\partial r^2} + \frac{1}{r}\frac{\partial H_z}{\partial r} + \frac{1}{r^2}\frac{\partial^2 H_z}{\partial \theta^2} + [k^2 n(r,\theta)^2 - \beta^2]H_z = 0 \quad (2)$$

Where $E_r, E_\theta, H_r,$ and H_θ are:

$$E_r = -\frac{j}{[k^2 n(r)^2 - \beta^2]}\left(\beta \frac{\partial E_z}{\partial r} + \frac{\omega \mu_0}{r}\frac{\partial H_z}{\partial \theta}\right) \quad (3)$$

$$E_\theta = -\frac{j}{[k^2 n(r)^2 - \beta^2]}\left(\frac{\beta}{r}\frac{\partial E_z}{\partial \theta} - \omega \mu_0 \frac{\partial H_z}{\partial r}\right) \quad (4)$$

$$H_r = -\frac{j}{[k^2 n(r)^2 - \beta^2]}\left(\beta \frac{\partial H_z}{\partial r} - \frac{\omega \varepsilon_0 n(r)^2}{r}\frac{\partial E_z}{\partial \theta}\right) \quad (5)$$

$$H_\theta = -\frac{j}{[k^2 n(r)^2 - \beta^2]}\left(\frac{\beta}{r}\frac{\partial H_z}{\partial \theta} + \omega \varepsilon_0 n(r)^2 \frac{\partial E_z}{\partial r}\right) \quad (6)$$

These equations describe how light propagates through an optical fiber. The solutions described by the above four equations imply that light guided by a cylindrical waveguide (such as an optical fiber taper) can be single mode or multimode, determined by the diameter of the waveguide. [9] These modes were observed during our work of tapering down the fiber diameter, which will be described in Chapter 3.

2.2 Current State of Fiber Taper Fabrication

Most existing methods of producing tapered optical fibers involve a heat-and-draw process, wherein a heating element softens the glass of a standard optical fiber while it is pulled in tension axially. The buffer layer is first stripped away such that the polymer does not burn and deposit any debris on the surface of the tapered region. Since the viscosity of vitreous silica used in optical fibers is a function of temperature, heating fibers causes them to stretch when pulled. [10] As the fiber is stretched longer, it becomes thinner due to conservation of mass.

The fiber is stretched such that its waist diameter decreases to around 1 µm, as shown in Figure 4. Tapered fibers with diameters below 1 µm are often referred to as optical nanowires, whereas fibers with diameters larger than 1 µm are referred to as microwires. [3] The length of the tapered region may vary depending on the process by which the taper is made. The transition regions, where the original diameter of the fiber decreases to the waist diameter, provide the added benefit of enabling the tapered fiber to be spliced together with unmodified conventional fibers. This also allows for in-situ transmission monitoring during the tapering process.

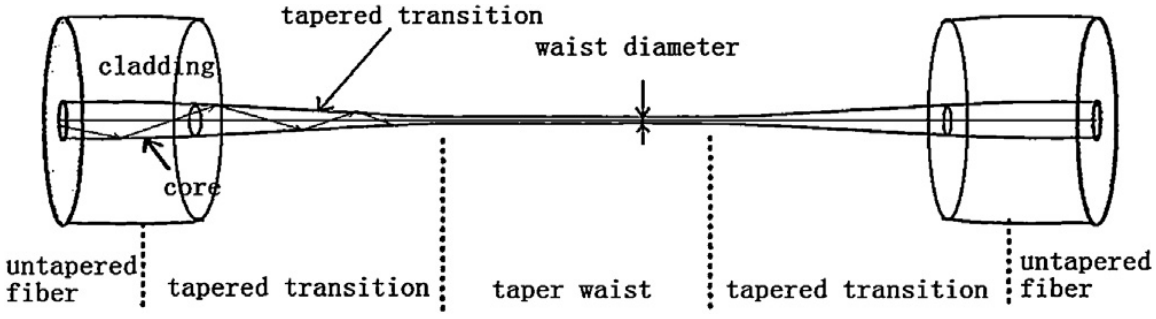

Figure 4: Schematic of tapered optical fiber [11]

Several methods for fabricating optical fiber tapers have emerged in recent research efforts. Primarily, optical fiber tapers are created using a brushed-flame approach, although alternative heat sources such as lasers and electrical elements have been studied in similar setups. [3, 12]

The variety of methods that have been studied ultimately attempt to create low-loss optical nanowires by adiabatically stretching fibers to have low surface roughness and a high degree of uniformity. [3, 12, 13] Although fibers with submicrometer diameters have been created through "bottom-up" fabrication processes, they have exhibited poor optical and mechanical properties compared with nanowires created from conventional optical fibers by heat-and-draw methods. [6, 13]

2.2.1 Flame Methods

Optical fiber tapers fabricated using flame-based method typically utilize a flame fed by oxygen and isobutane. [3, 6, 13] It is important to use a clean-burning flame to avoid depositing particulate matter on the optical fibers that may affect its optical performance [13, 14] The temperature of the flame can also be controlled by monitoring the flow of fuel. As the flame heats a portion of the fiber, motorized stages to which the fiber is clamped pull the fiber in opposite directions along its axial length. An illustration of a flame-based tapering method is shown in Figure 5.

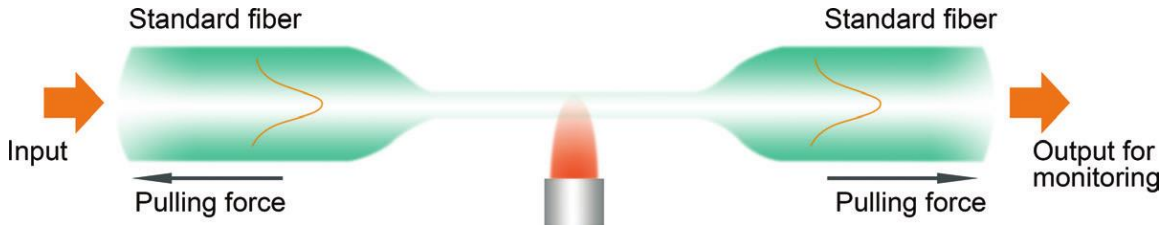

Figure 5: Flame-heated taper drawing [12]

Typical flame sources produce flames with widths around 3mm. [3, 6] However, creating longer tapers requires heating larger volumes of glass more uniformly, which has led to the development of a brushed flame method. [15] In brushing setups, the flame is moved back and forth between two points in a scanning or sweeping motion; the volume of glass heated is now determined by the brushing distance rather than the width of the flame itself. The variables added by this method such as the speed and length of the sweeping motion add more control to the tapering process. [16] As the fiber is drawn and the waist diameter decreases, modifying the parameters of flame sweep length and speed can change the profile of the transition regions.

Prior to the development of the flame brushing method, a two-step process using a static flame and heated sapphire rod was used to create optical fiber tapers. [3] Optical fibers were first drawn to near micrometer diameters using a stationary flame and two translational pulling stages. The fiber was then drawn to smaller dimensions by pulling the taper around a heated sapphire rod with a diameter of several tens of microns. [13] The losses associated with this method were much greater than those achieved with brush flame methods, however, demonstrating the ability to create submicrometer diameter optical wires renewed interest in the applications of these small scale optical devices. [3, 13]

Although the brushed flame method is popular, it is not flawless. Two major concerns with any flame-based tapering methods are the stability and turbulence associated with the flame. [14] The flame should be low-flow as to not break the fiber due to turbulence or convection, as well as stable to ensure even heating. The brushed approach does address the issue of even heating by

varying the position of the flame, but does not perfectly correct for the inherent instability of flames. Table 1 shows an experiment in which Brambilla et al. demonstrate the correlation between flame stability and transmission loss.

Table 1: Transmission loss in a 375nm diameter optical fiber produced in stable and unstable flames

Taper #	*Loss (dB/mm)*	*Flame*	*Average Loss (dB/mm)*
4	0.0245	Stable	0.0204
5	0.0169		
6	0.0168		
7	0.0236		
8	0.0363	Unstable	0.0407
9	0.0416		
10	0.0443		

To address the issues of random turbulence in flame-based tapering methods, alternative heat sources such as CO2 lasers and resistive electrical elements have been explored.

2.2.2 CO_2 Laser Heating

The use of carbon dioxide lasers to melt optical fibers is based on the fiber's absorption of the power emitted by the laser; the temperature of the fiber is proportional to the applied laser power. [17] Laser heat sources can be used in stationary and brushing setups, similar to flames. Scanning the laser along the length of the fiber results in a more even temperature distribution both along the axis and perpendicular to it, while focusing the laser at a fixed point only creates an even temperature distribution along the axis of the fiber. A fixed spot laser also introduces a strong temperature gradient perpendicular to the axis of the fiber, which results in asymmetry that induces propagation losses in the taper. [18]

In flame-based tapering methods, the process is stopped when the desired taper length or diameter is reached. Direct CO2 laser heating, however, is a "self-regulating" process. [12, 17] The power acquired from the laser is proportional to the volume of the fiber, given asV=r2h, whereas the power dissipated by the fiber is proportional to its surface area, given as A=2rh. [14] Since the volume decreases with the square of the radius while the surface area only decreases linearly with the radius, the fiber will reach a diameter where insufficient energy is absorbed and elongation stops. [17] Although sometimes convenient, this phenomenon prevents direct laser heating from producing fibers with diameters on the sub-micrometer scale.

A solution to the limitation of direct laser heating is indirect laser heating. Sumetsky et al. have demonstrated optical fiber tapering using a sapphire capillary tube heated by a CO2 laser. [14] In this approach, the laser heats a sapphire tube that acts as a microfurnace, as shown in Figure 6. Since the dimensions of the sapphire tube do not change, the temperature reaching the fiber is not affected by the variation in fiber radius. The microfurnace also provides an even temperature distribution along the axis of the fiber.

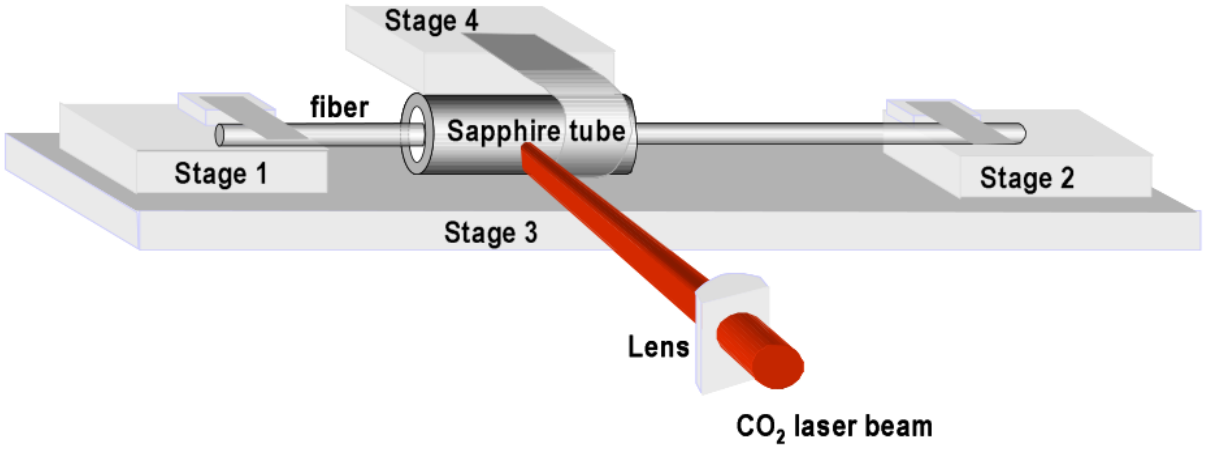

Figure 6: Indirect laser heating of optical fiber using sapphire tube microfurnace. The inner diameter of the tube is 0.6mm and the outer diameter is 0.9mm. [14]

The indirect heating method described above still suffers from a temperature gradient along the cross section of the fiber. The authors note that this effect is minimal for thin fibers and can also be reduced by introducing axially symmetric heating. [19] Another study presented a laser heating method for fiber tapering using a dual-spot laser that simultaneously heated two sides of the fiber. [18] A diffractive element was used to produce two laser beams that intercepted the fiber symmetrically about its axis. This application of even heating results in optical tapers with very low ellipticity.

CO2 laser methods for fabricating tapered optical fibers are a clean and effective heat source that offer consistent performance and control. Although issues involving temperature gradients and size limitations have been addressed, other fabrication methods may offer simpler and more robust solutions.

2.2.3 Electrical Heating

Electrical heating is a tapering method using a resistive material and running a controlled current through it to reach a certain temperature. These resistive materials are then used to create furnaces in which the fiber will be tapered. Electrical heating has some distinct advantages over laser and flame heating methods. First, electrical heaters are more stable and do not produce the turbulence that flame heating methods do. [12] In CO2 laser heating methods, as the diameter of the taper decreases, the rate that power is absorbed decreases and eventually equals the rate of power loss, so the fiber stops tapering. Electrical methods provides constant heat regardless of how small the tapered section becomes. [20]

One group of researchers used a resistive metal as both the heating element and the furnace enclosure. [21] The furnace was 30mm long and had an inside diameter of 2 mm. A slit extended along the side for the fiber to be placed in and removed from the furnace, as shown in Figure 7. The temperature was current controlled and the primary stable heating region of the furnace was the middle 12.4mm of the enclosure. The advantage of this approach is the wide, stable heating area, which is unlike flame methods that utilize a heat source approximately 2mm wide.

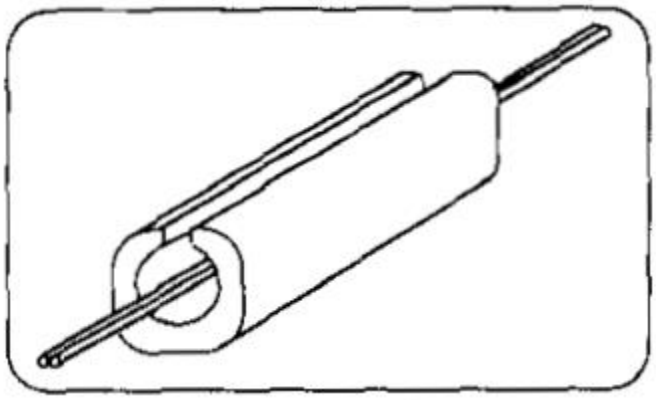

Figure 7: Illustration of heater with optical fibers [21]

This application was intended for the fabrication of fiber couplers, but its basic principles extend to the fabrication of tapered fibers. The continuous control of temperature allows for slow and precise pulling speeds, which contributed to producing smooth fibers with average losses of around 0.13 dB.

Electrical micro furnaces are beneficial to compound-glass optical nanowires, where fibers are made of materials other than pure silica. Brambilla et al. demonstrated the tapering process in various glass compounds using a graphite microheater. [22] These compound glasses, such as lead-silicate or bismuth-silicate have softening points around 500℃, whereas pure silica requires temperatures around 1600℃. [10, 22] The graphite microheater, however, was capable of providing temperatures between 200℃ and 1700℃. The fiber was set up like in most methods with two motorized stages drawing the fiber. This method produced fibers with lengths between 30mm and 100mm.

Another group of researchers set up an electrical heating rig in the form of an electrically resistive strip heater, shown in Figure 8. [20] The heater is 12cm long and has a distance of 0.5cm between the top and bottom plate, with the front face being open for the fiber to be easily placed and removed. By controlling the voltage through the resistive heater, the temperature can reach around 1600℃. This heater shows excellent temperature distribution and heat preservation. The drawing method used involves one stationary and one moving motorized stage. This method has yielded tapered fibers much longer than the flame or laser methods. The fibers usually have lengths on the order of tens of centimeters with the biconical sections of tens of centimeters and tapered sections of around 12 centimeters. The fibers also have waist diameters of around 900 nm and transmissions losses less than .1 dB/cm at 532 nm of light.

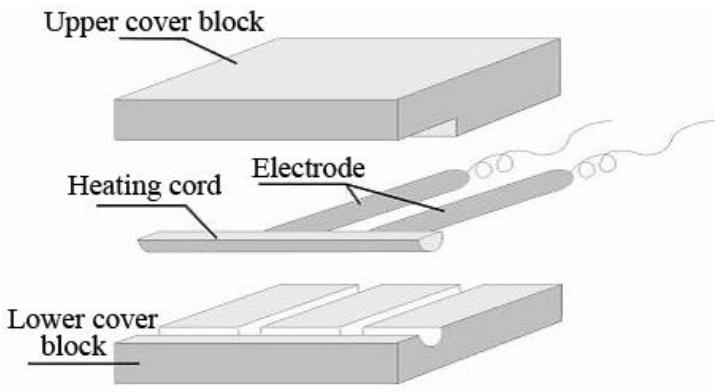

Figure 8: Electriclly resistive strip heater [20]

2.2.3 Properties of Tapered Optical Fibers

Several special properties develop as a result of the tapering process, including the presence of an evanescent field, transition regions and strong confinement. Primarily, these properties are used to interact with external media outside the physical boundary of the optical nanowire. [23] The transition regions of the taper are also used to convert and filter modes. [3]

The presence of an evanescent field arises from the phenomenon of total internal reflection. Although the cladding layer of an optical fiber has a lower index of refraction than the core, thus allowing total internal reflection to occur, a portion of the electromagnetic field extends beyond this boundary, depicted in Figure 9. [24] The small diameter of a tapered fiber increases the portion of light that propagates outside the boundary of the glass itself.

Figure 10 depicts three optical fibers with different diameters where light is propagating in its fundamental mode. In the largest fiber, the evanescent field is small, but still present. Most of the intensity of the light is propagating through the center of the fiber. In the smaller fibers, a larger fraction of the light intensity exists outside the glass as a result of the reduced diameter. Typically, the evanescent field would be confined to the cladding of an unaltered fiber and would not be able to interact with external media.

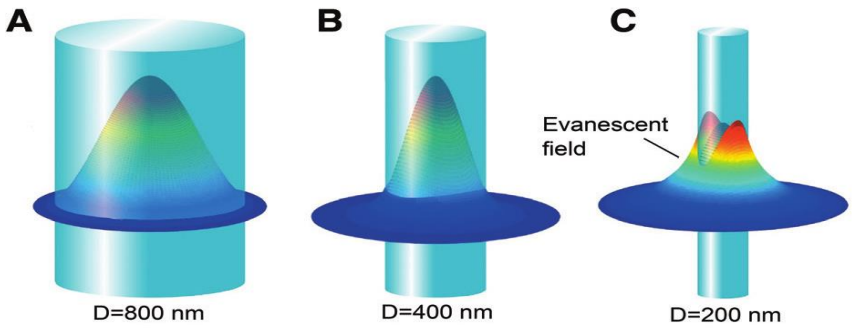

Figure 9: Evanescent field propagating outside fibers of various diameters. [12]

Tapering an optical fiber increases the strength of the evanescent field by removing the cladding, which is intended to prevent light from exiting the core, and by decreasing the diameter of the core. In the transition region, the entrance angle of light decreases, thus increasing the frequency of total internal reflection. [11] The evanescent field is also strongest in tapers with smaller waist diameters, and can even extend several micrometers into the surrounding medium. [3] The evanescent field is used in sensing and particle manipulation.

2.2.4 Applications of Tapered Optical Fibers

Standard optical fibers are used primarily in telecommunications, but also find applications in sensing, imaging, and other fields. The use of fiber optics in many applications is beneficial since they are not affected by external electromagnetic fields (electromagnetic interference) and exhibit little to no power loss. The range of applications of fiber optics is expanded by the use of tapered optical fibers; their properties suit applications that standard fibers may not.

Optical fiber nanowires can be coiled to form high-Q resonators, typically as multiple-turn coils or single loops, which are useful for cavity quantum electrodynamics, nonlinear optics, and sensing. [3, 5] Optical nanowires can be bent into coils and loops with small radii due to strong their property of strong confinement. [12] The coil or loop geometry allows modes in different sections of the fiber to couple, thus creating a microscale resonator. Since optical fiber tapers provide large evanescent fields and high Q-factors in resonators, they are ideal for sensing applications requiring high sensitivity and low detection limits. [5, 11] The small mass of optical fiber tapers also contributes to the high sensitivity of sensors, which often have piconewton resolution. [12]

In the realm of microfluidics, tapered optical fibers have been used for efficient, non-contact sensing of optical properties of ambient fluids, such as in the schematic shown in Figure 10. [12, 25]

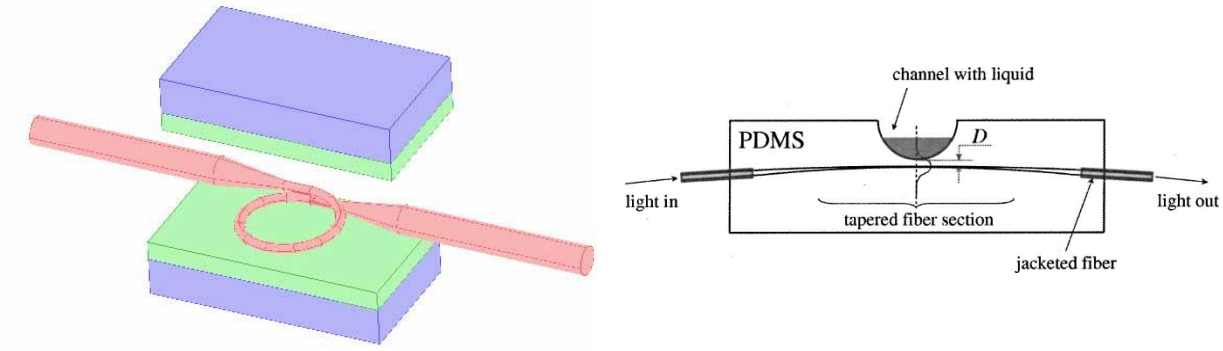

(a) (b)

Figure 10: Nanowire loop resonator for measuring indices of refraction (a) [5] and tapered fiber used for sensing optical properties near liquid (b) [25]

The evanescent field present outside tapered regions of optical nanowires is also beneficial to the application of particle trapping and manipulation. A large optical gradient force arises from the confinement of the evanescent field around the fiber, causing micro and nanoparticles to become trapped near the fiber. [3, 12] Simultaneously, particles are propelled along the length of the fiber

due to the axial forces associated with radiation pressures from the propagating light. [3] An example of this trapping and manipulation is shown in Figure 11.

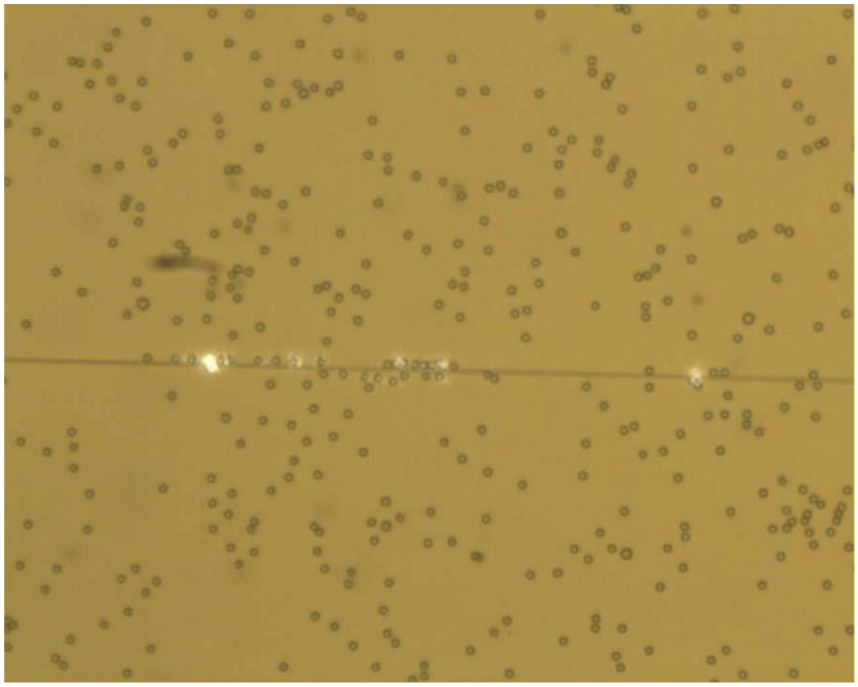

Figure 11: 3µm-diameter polystyrene particles propelled along optical fiber taper [3]

The applications of this gradient force are limited to particles of small masses due to the low magnitude of the gradient force. The limited scalability of this approach to particle manipulation is also impacted by power loss through the fiber tapers. It has been shown that the attenuation losses in tapered fibers can range between 2 and 5 dB when water is the surrounding medium, as opposed to 1 dB for the same fiber in air. [4] A similar exploitation of radiation pressure can be used for particle manipulation in planar waveguides that do not see significant losses in different mediums, however optical fiber tapers offer the advantages of having further extending evanescent fields and extending to 3D space. [3]

There are several applications of an optical conveyor belts for biology and physics. In biology these optical conveyor belts can be used in targeted drug delivery systems since they can push particles against flow and with a defect made in the fiber can act as a stopping point for the drugs. [26, 27] In physics optical conveyor belts are being tested to help with the isolation of cold atoms for research. [28]

2.3.5 WPI Lab Setup

The optomechanics laboratory at WPI previously fabricated tapered optical fibers using a stationary flame approach. Similar to other flame-based tapering methods, a portion of the buffer layer is stripped from the fiber and it is clamped onto translational stages. The setup is contained in an acrylic enclosure to minimize drafts and external disturbances.

The heat source used for tapering in this setup is a denatured alcohol candle. The fuel is delivered by a wick submerged in a glass container filled with the alcohol. To prevent depositing particulate matter, the length of the wick is minimized such that the flame burns in a low, clean,

and stable manner. The candle is placed on a 3-dimensional stage such that it can be positioned accurately beneath the fiber. The tapering setup is shown in Figure 12.

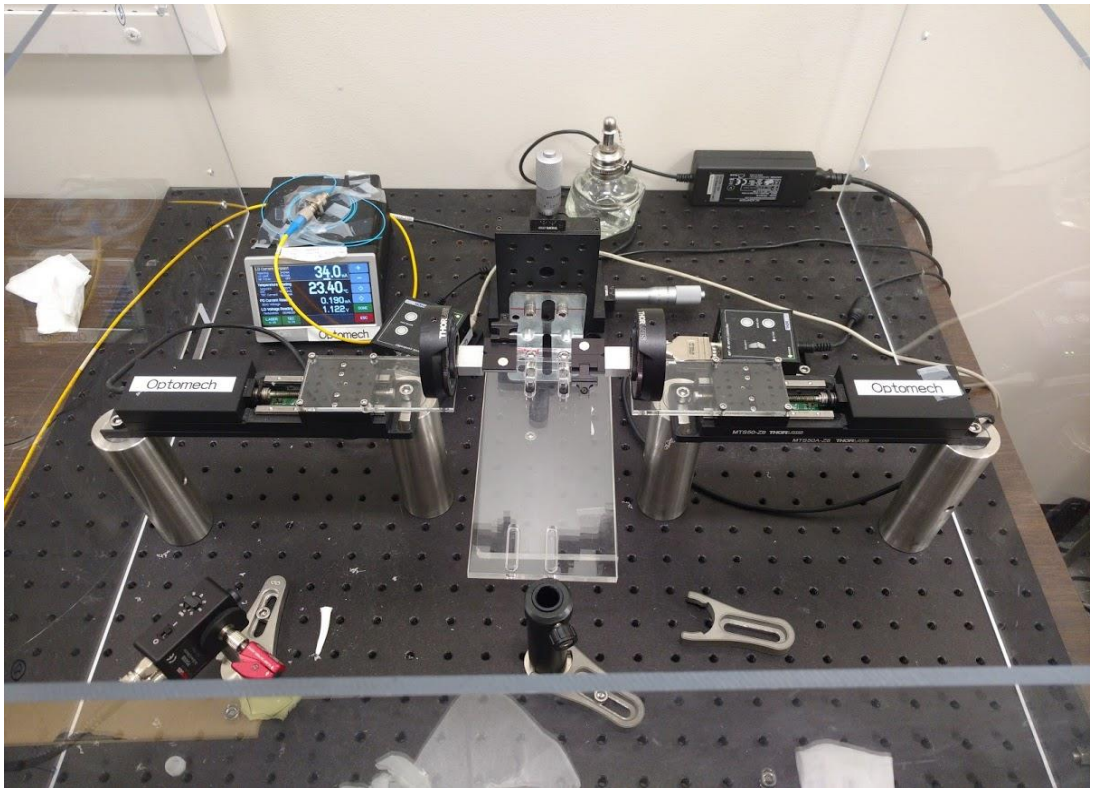

Figure 12: WPI optical fiber tapering setup

A laser is coupled to one end of the fiber such that transmission may be monitored in-situ. A LabVIEW program controls the translation of the two stages which pull the fiber as it is heated. This program also monitors the transmission received by a photodetector to indicate the progress and success of the tapering process. While the tapered fiber is drawn out, the transmission will fluctuate in a sinusoidal pattern. As the core and cladding diameters are reduced, the amount of light transmitted through the fiber will decrease. When light is "squeezed" out of the core and begins to propagate through the cladding, the effective radius of the fiber increases, thus increasing the amount of light transmitted. This process repeats until the light is successfully guided along the tapered fiber.

One of the largest issues with the tapering setup in this laboratory is the stability of the heat source. Although the setup is enclosed, the flame provided by the alcohol candle is still subject to turbulence from even the slightest drafts or movements. In addition, the presence of the wick introduces impurities in the flame that may result in an unclean optical fiber.

2.3 Challenges of Existing Methods

The variety of methods used to fabricate tapered optical fibers each offer various benefits and drawbacks. Since optical fiber tapers and nanowires are used for a breadth of applications, different methods are used to create tapers depending on the application. For example, a large coil used as a resonator will require a very long fiber, which must be created using a method that can produce tapers of long lengths, such as indirect laser heating.

Overall, the methods presented share the goal of producing low-loss optical fiber tapers. Many bottom-up fabrication methods produce fibers which exhibit irregular profiles or surface roughness, while top-down methods such as those discussed in the previous chapter pose many challenges that limit their potential. [3] These issues pertain to the special care required for fabricating tapers, such as maintaining a clean environment, a stable and uniform heat source, low turbulence, and developing a repeatable setup for the tapering process. The challenges presented by fabricating tapered optical fibers include:

(1) Maintaining a high optical transmission rate, particularly when the medium surrounding the fiber is water
(2) Creating a stable heating area
(3) Developing a repeatable and controllable tapering process

This project seeks to address these challenges by investigating several tapering methods to optimize an existing setup. Additional constraints include those associated with the lab space, budget, and timeline of this project.

2.4 Scope of Work

Since the optical and mechanical performance of a tapered optical fiber, e.g. transmission, can be traced to the process by which is was made, implementing a consistent and quality tapering setup is critical to repeatedly producing low-loss optical tapers. This project will investigate several promising methods for fabricating tapered optical fibers in order to improve the performance of the setup in the WPI laboratory space. The success of these methods will be determined by the measured transmission through the tapered fiber for surrounding mediums of air and water and validated through particle trapping experiments.

2.5 Organization of the Report

The remainder of this paper will discuss the design methodology we used to create a repeatable process for fabricating tapered optical fibers and the results of water and optical trapping testing. Chapter 3 will discuss the iterative design process used to create and modify our tapering apparatus. Chapter 4 will present the results of various tests used to demonstrate the effectiveness of our work in creating tapered optical fibers. A discussion of the project and its results is provided in Chapter 5. Concluding remarks are provided in Chapter 6.

Chapter 3: Design and Fabrication

As discussed in our background chapter, there are multiple methods of creating tapered optical fibers. However, since the details of each of these methods is not provided, they are, to a certain extent, just concepts. In order to fully develop a process that satisfies the objectives of this project, an iterative design process was used to continuously modify and improve a given concept. This iterative methodology is summarized by the chart in Figure 13.

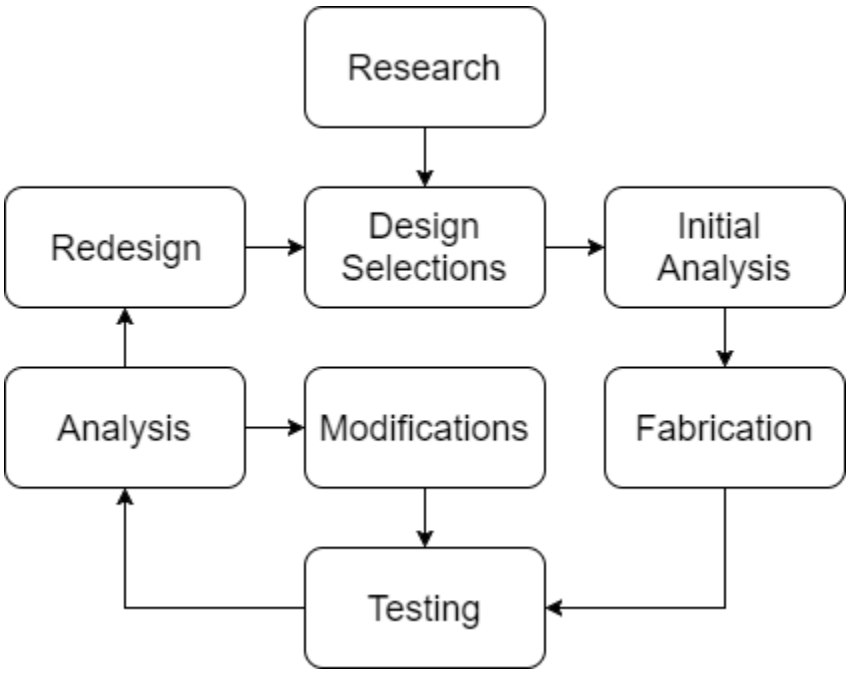

Figure 13: Iterative design loop methodology

In this design loop, a collection of concepts were taken from literature, e.g. the brushed flame method, laser heating, and electrical heating. For each selected concept, a prototype was built and tested after an initial analysis to determine the necessary parameters of its design. Modifications were made based on the results of testing in an attempt to improve the design. If an analysis of the results indicates the design is unsuccessful, a new concept is selected for development. Chapter 3 is organized following this design process, and each section (3.1, 3.2, and 3.3) is a complete loop of the design process. The subsections of sections 3.1 and 3.2 follow inner loop involving the modification of selected designs after testing and analysis.

3.1 Flame Shield Approach

The concept of a flame shield was developed to address the issue of turbulence when using a flame, in the form of a blowtorch, to heat the fiber during the tapering process. A blowtorch produces a more stable temperature distribution than a candle due to the forced flow of air, but may also break tapered fibers. A metallic shield was placed between the flame heat source and the fiber such that it would block any turbulence but still conduct heat through to soften the fiber, as shown in Figure 14.

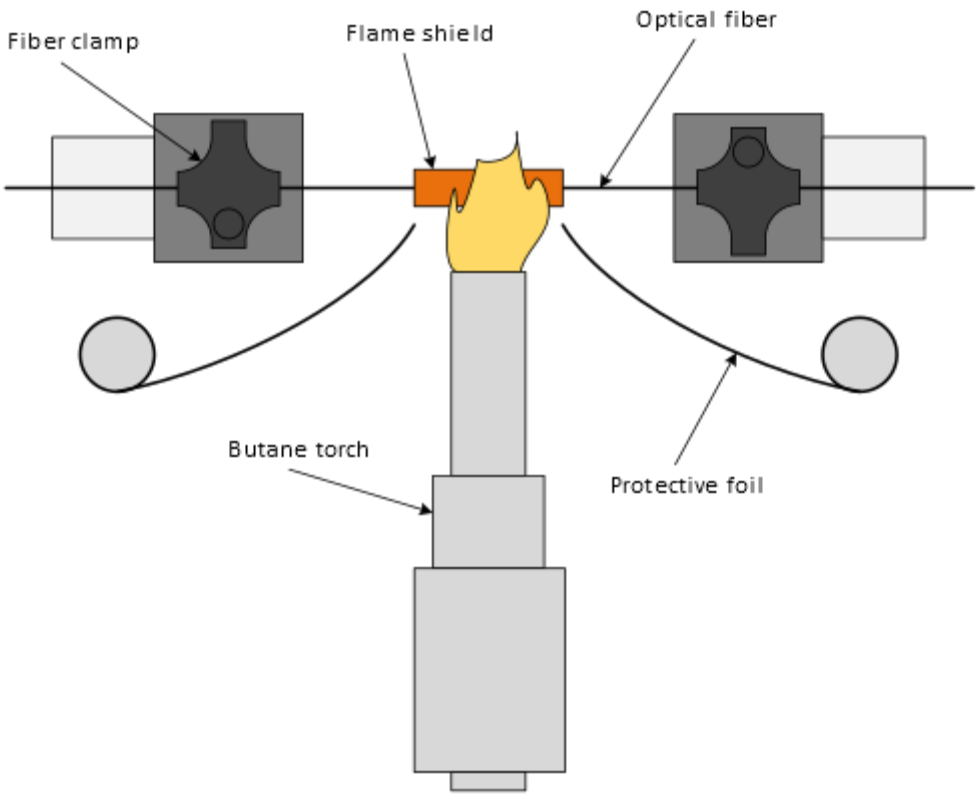

Figure 14: Top-down schematic drawing of flame shield test setup

In this setup, a butane torch is used to supply heat to the fiber. Although the torch produces a steady temperature around 1200°C, the air-butane mixture exits the nozzle at a high velocity.

3.1.1 Bowtie Flame Shield Design

3.1.1.1 Bowtie Shield Design and Fabrication

The first shield design used in testing, shown in Figure 16, was developed by another student's previous research. A thin piece of stainless steel approximately 1 inch long and 0.03 inches thick was formed into a bowtie shape. A side-view of the shield is shown in Figure 15.

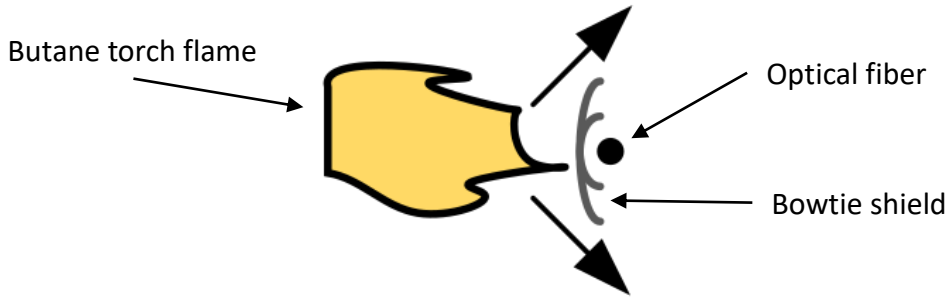

Figure 15: Profile of the bowtie flame shield deflecting flame from fiber

The flared ends deflected heat away from the fiber while the cylindrical center portion closely surrounded the fiber. The shield surrounds the fiber such that any air flow is diverted around the fiber while heat is still conducted through the thin metal to the fiber. Aluminum foil shields were placed adjacent to the fiber shield to protect the clamps from the heat produced by the torch.

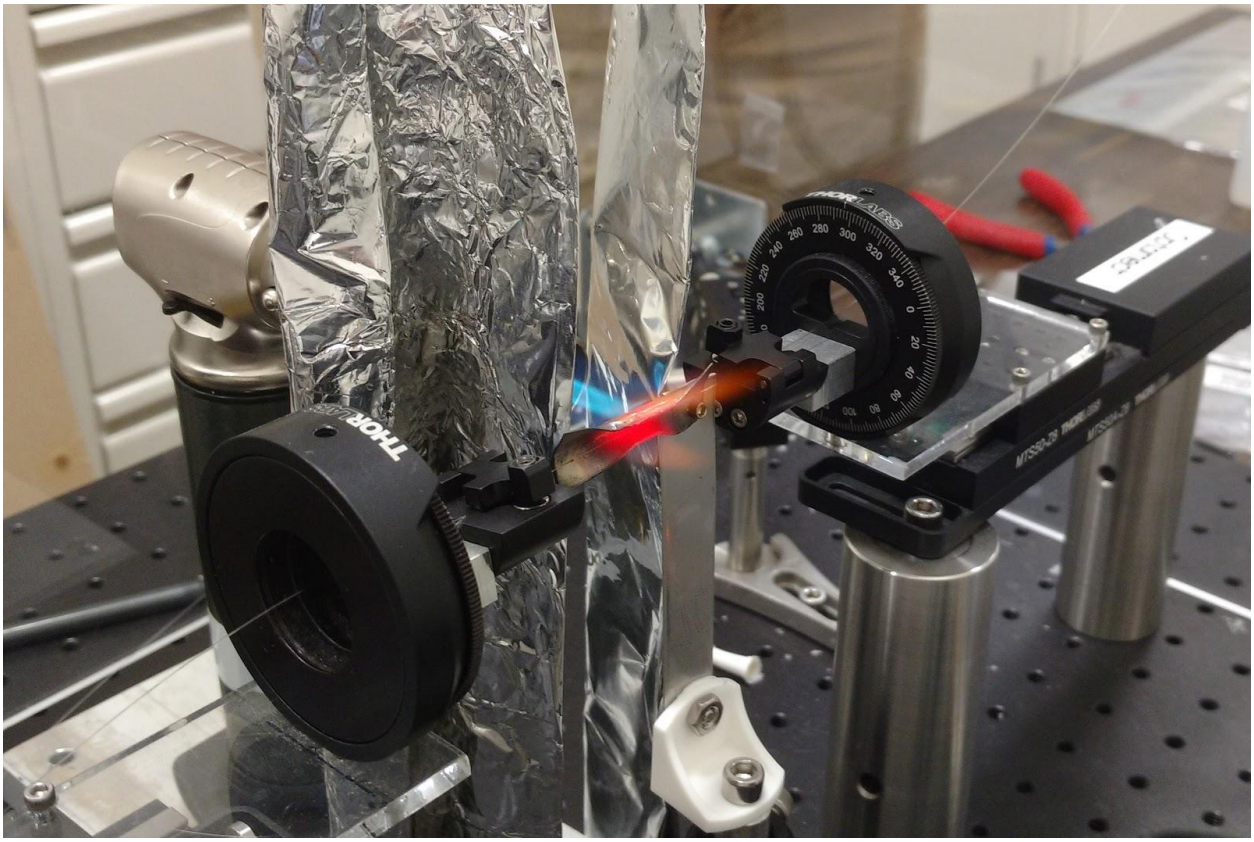

Figure 16: Original flame shield design in position

3.1.1.2 Bowtie Shield Testing and Analysis

In testing, the shield was aligned such that it was as close as possible to the fiber without making any physical contact to avoid contamination of the fiber, any particles deposited on the tapered fiber produce large losses of optical power.

During the first trial, the flame shield was heated by the blowtorch for two minutes to reach a steady-state condition before the motorized stages began to pull the fiber. In subsequent trials, the shield was heated for five minutes before the motorized stages began to pull.

For all trials the clamps stripped the outer buffer layer of the fiber shown in Figure 17. When the stages pull the clamped ends of the fiber, the fiber can draw out and become tapered, slip or strip at the clamps, or simply break. Since the buffer was being stripped off it means the fiber wasn't hot enough to taper. Some of the flaw with the design include its inability to align properly with the fiber and the material not being conductive or thin enough to conduct the required heat.

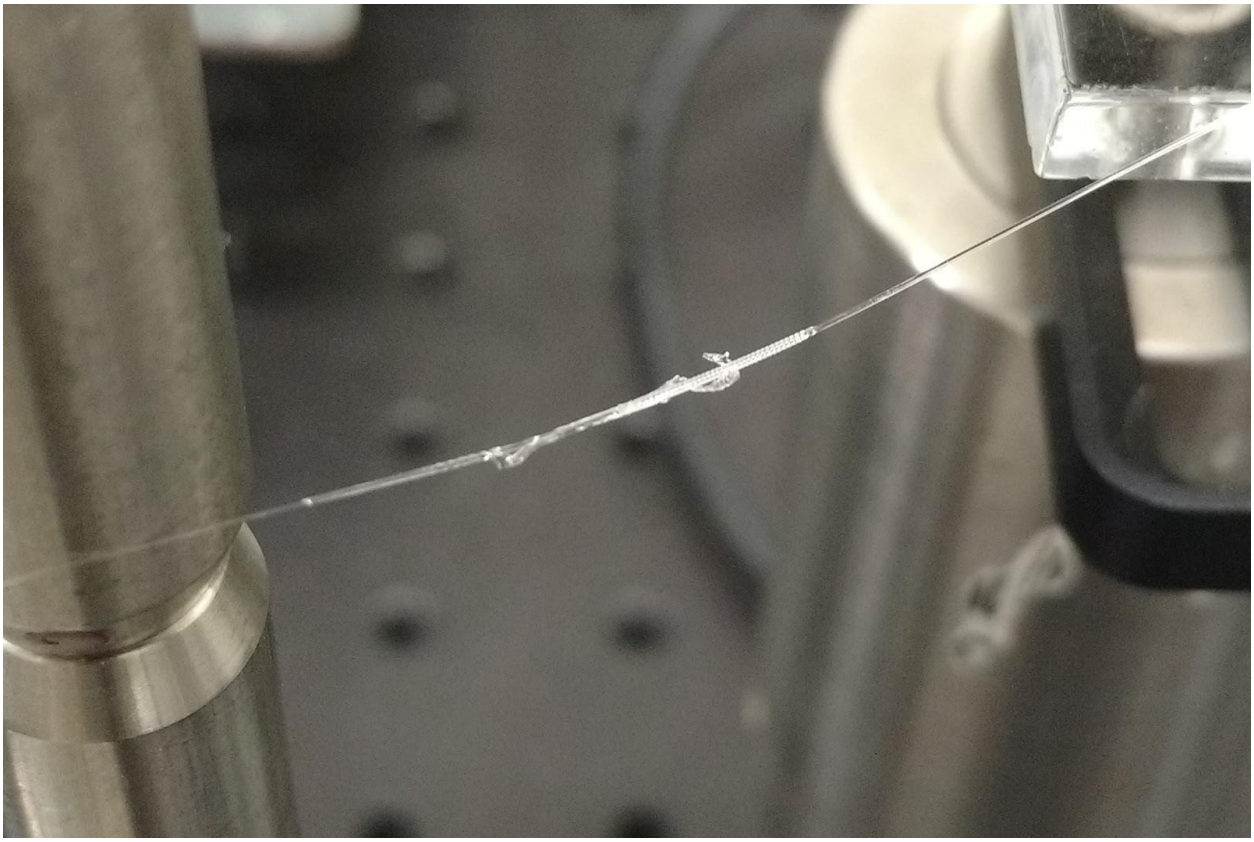

Figure 17: Result of fiber stripping at clamp. The thicker white area is the buffer plastic building up as the inner layers of the fiber are pulled through the clamp. This stripping occurs rather than tapering due to insufficient temperatures.

3.1.2 Corner Flame Shield Design

3.1.2.1 Corner Shield Design and Fabrication

The bowtie-shaped shield was replaced with a new stainless steel shield that was thinner (approximately 0.018 inches thick) and shaped to form a corner angle of about 45°, as shown in Figure 18 and Figure 19. The thinner material was intended to conduct more heat through to the fiber, and the interior angle would allow the fiber to be more closely surrounded than with the bowtie-shaped shield.

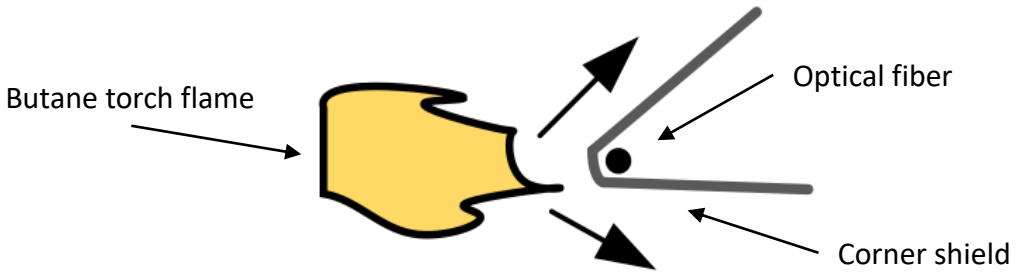

Figure 18: Profile of corner shield deflecting flame from fiber

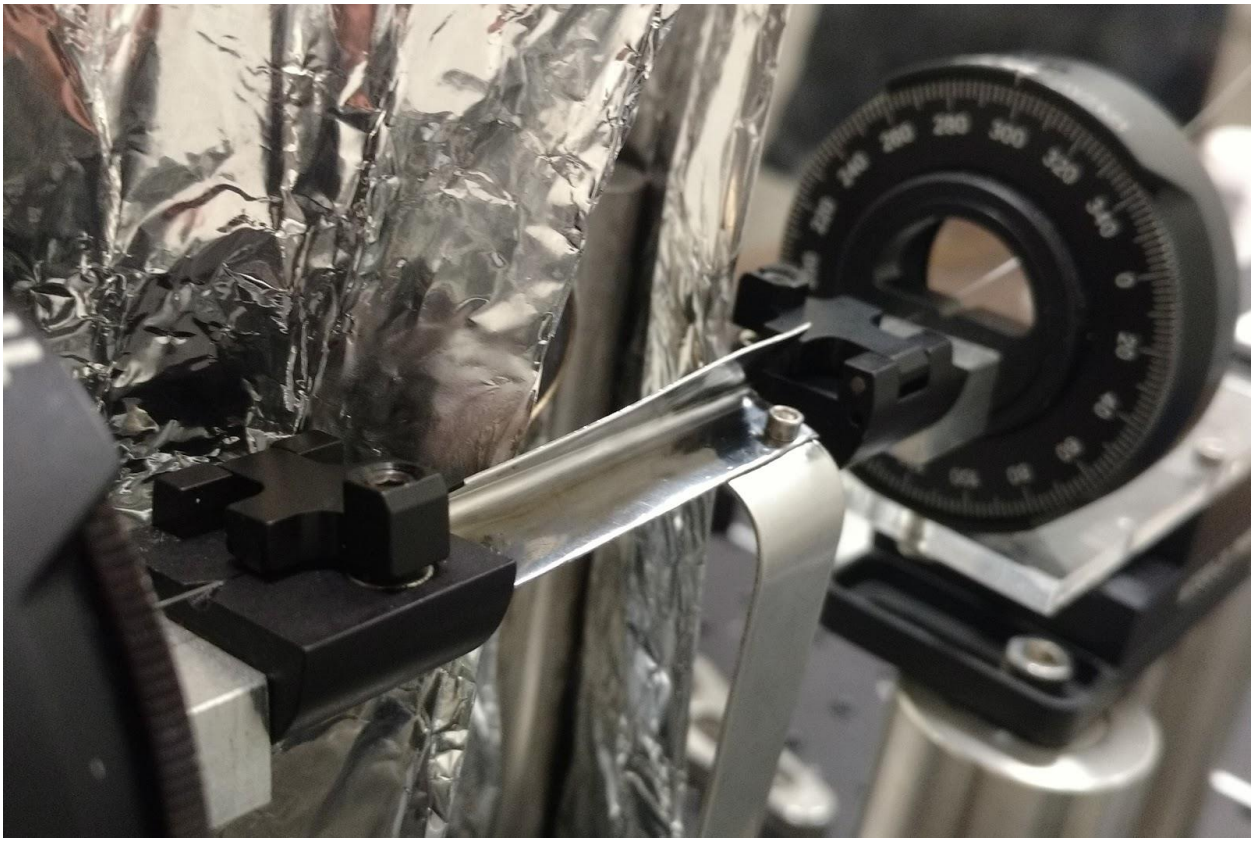

Figure 19: Angled flame shield around fiber

3.1.2.2 Corner Shield Testing and Analysis

Similarly to the previous trials, the new shield was heated prior to pulling the fiber. The fiber did not taper as the stages moved and the buffer layer began to strip again, as shown in Figure 20. Several flaws with the angled shield were attributed to the failure of the design. The material was not perfectly straight, so the fiber was not uniformly spaced from the shield, which would lead to inconsistent heating and therefore failure to produce a taper. More importantly, the geometry of the shield exposed a lot of the fiber and shield material to the ambient air, which meant heat was transferred away from the glass in the fiber. To reduce these effects of heat loss, the shield would need to surround the fiber closely such that most of the heat transferred through the shield would be directed at the fiber as well as being contained.

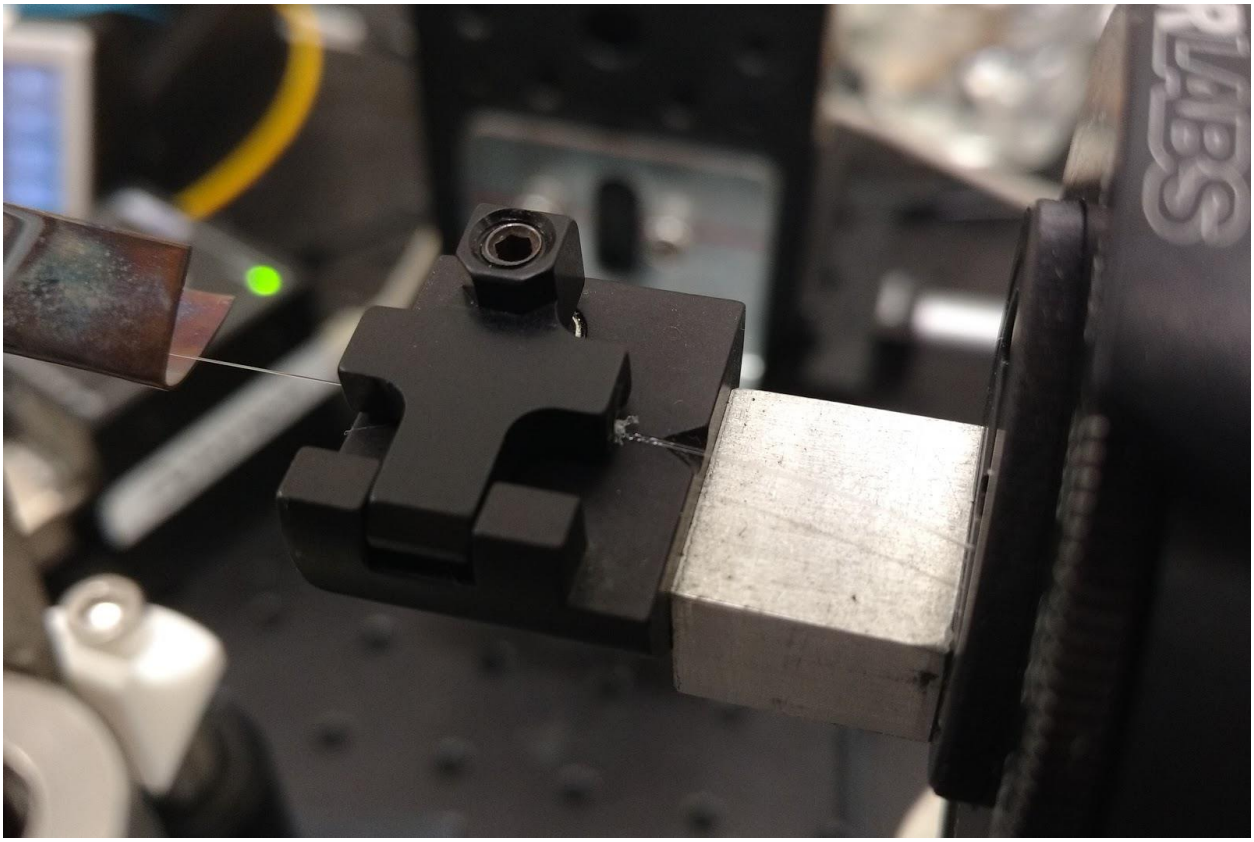

Figure 20: Build-up of fiber buffer material at clamp face due to stripping

3.1.3 Concentric Flame Shield Design

3.1.3.1 Concentric Shield Design and Fabrication

The next attempt to use a flame-shield, shown in Figure 22, in the fiber tapering process involved a cylindrical shield made of copper. This design used a 1 inch-wide, 0.016 inch-thick copper sheet that was formed into a circular fashion, such that the fiber would be mostly surrounded concentrically by the copper shield shown in Figure 21. Therefore, more heat radiating from the shield would be directed towards the glass fiber than previously.

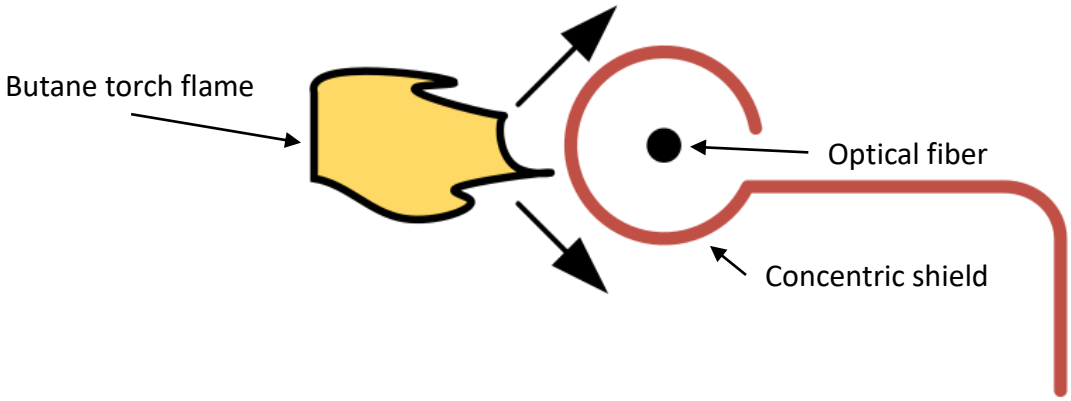

Figure 21: Profile of concentric shield deflecting flame from fiber

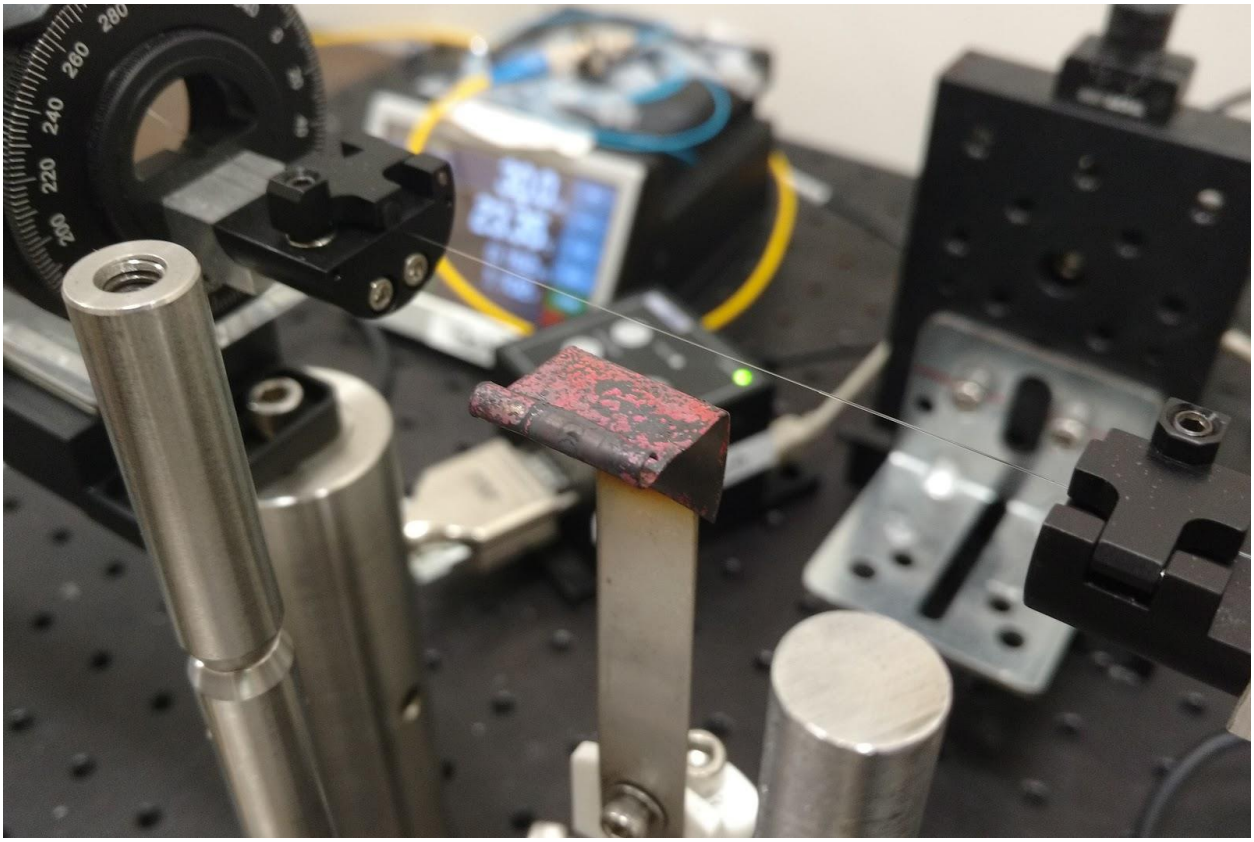

Figure 22: Copper flame shield near fiber setup

3.1.3.2 Concentric Shield Testing and Analysis

The testing procedure remained the same as the previous two designs and no trials were successful in producing a tapered fiber; the fiber would simply slip or strip at the clamps. The several unsuccessful attempts at heating the fiber through a shield indicated it was necessary to investigate the cause of failure.

To verify the temperature of the torch was high enough to soften the fiber for the tapering process, optical fibers were held by hand in the flame of the torch. With a small amount of tension, the fibers quickly softened and stretched until they broke. As theorized, the shield was not allowing enough heat to reach the fiber. Although the butane torch was evidently hot enough to soften the fiber, the temperature of the shield was unknown. By heating the shield in the flame and observing its color, the temperature of the shield material could be estimated due to the incandescence of the metal. Figure 23 shows the shield glowing to a cherry red color, which indicates a temperature of approximately 800°C according reference [29] (see Appendix A). This temperature alone is not in the melting range for the glass fiber, and since the shield is not in direct contact with the fiber, the glass is not hot enough to soften.

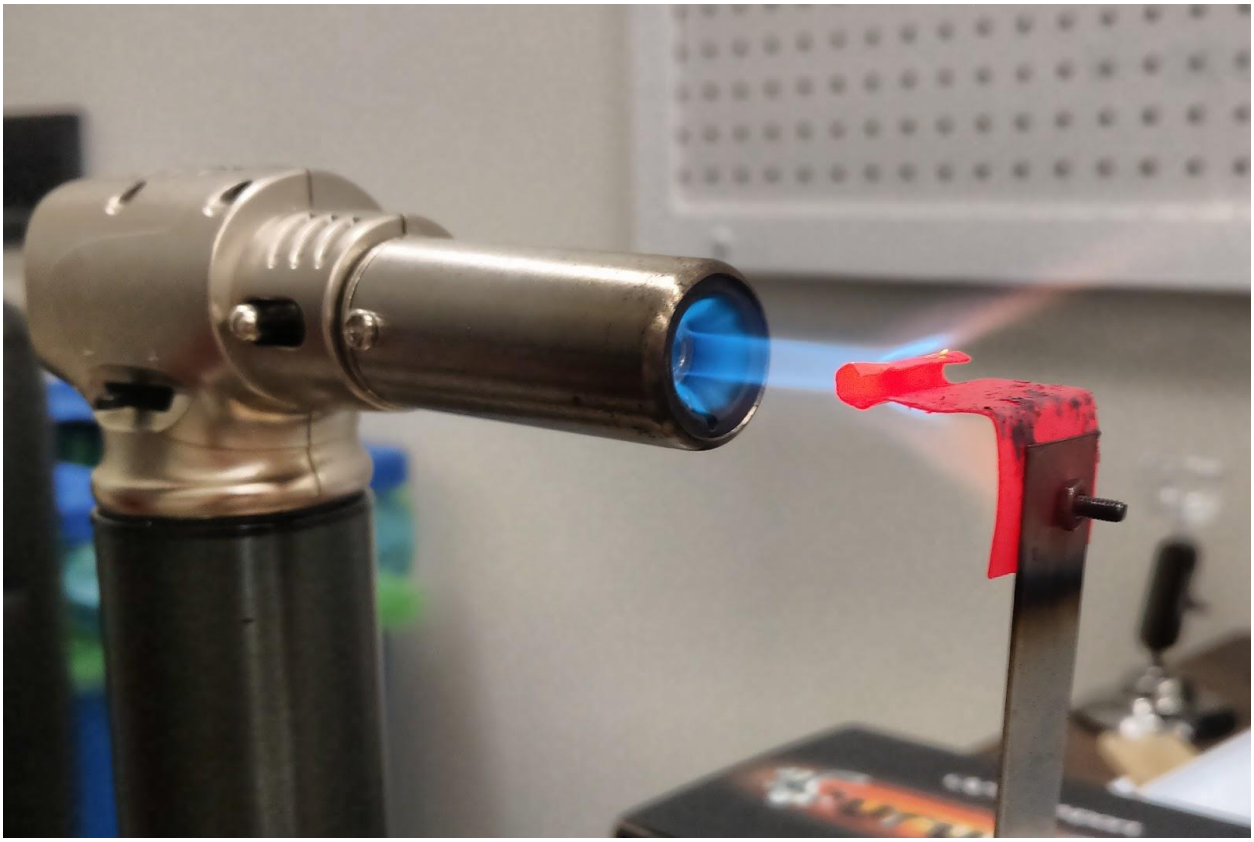

Figure 23: Copper shield in the direct flame of the butane torch showing color corresponding to temperature through incandescence

The flame shield was clearly preventing the fiber from heating up to the necessary temperature for the tapering process. Even when the fiber was in contact with the shield (which is generally avoided in order to keep the fiber clean), it did not soften enough to create a tapered geometry. It was evidently necessary to explore alternative heating methods since the flame shield was unlikely to produce any acceptable results. Several alternatives to flame-based heating elements are proposed and investigated in other publications, including electrical resistance wire, CO2 lasers, or electrical arcs. An electrical resistance heater was selected as the next design attempt.

3.2 Electrical Microfurnace

Several publications discuss the implementation of electrical resistance heating in the tapering process. If an electrical current is passed through a resistive wire, power is dissipated in the form of heat. This principle is seen in common household appliances such as toasters, electric ranges, and even incandescent light bulbs.

The concept of the microfurnace could be implemented in a variety of configurations, including different sizes, wire patterns, and power levels. A power supply was also necessary to supply the appropriate current through the wire in order to generate heat. The basic configuration of these parts is shown in Figure 24.

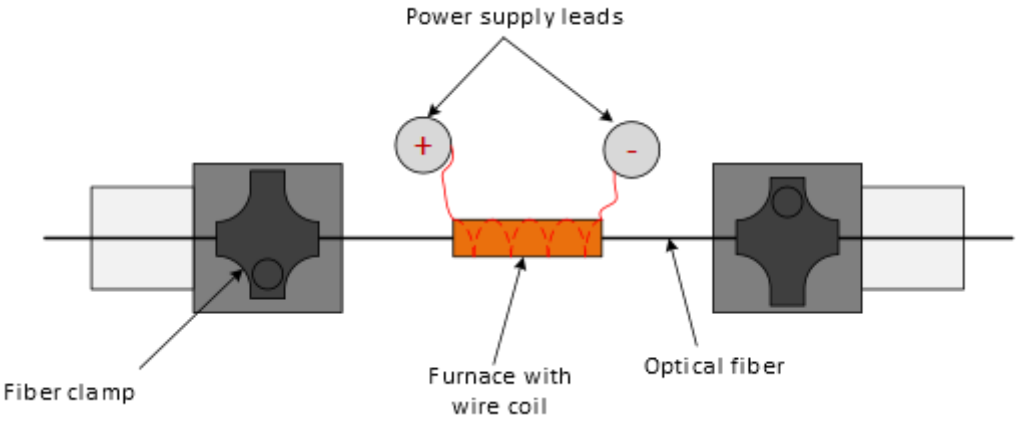

Figure 24: Top-down schematic drawing of the microfurnace test setup

The power dissipated by the wire was calculated as the product of the applied voltage and current, which were displayed on the power supply. The temperature of the wire is proportional to the electrical current through it. According to the experimental data found, the current should be around 3.15 Amperes to reach the appropriate temperature for the tapering process. [30] The resistivity of the wire was provided by the manufacturer in Ohms per unit length, so the maximum length of wire that could be used was calculated using Ohm's law. Since the power supply can provide a maximum of 30 Volts and 3.15 Amperes are required, the wire can have a resistance of at most approximately 9.5 Ohms. At 13.1 Ohms per foot, this equates to about 8.7 inches of wire. [31]

3.2.1 ¾" Length ¼" Diameter Furnace

3.2.1.1 Design and Fabrication

To test the viability of this approach, a microfurnace was created using an alumina ceramic tube measuring ¾" in length and ⅛" inner diameter. A coil of resistance wire was formed and placed within the ceramic, which was held in place by the stainless steel handles of a binder clip.

For this application, Kanthal A1 resistance wire was selected based on cost, size availability, and temperature data. [30] The experimental temperature data provided by Pelican Wire Company, Inc. indicated that a 32 AWG wire (0.008 inch diameter) can reach 1200°C when 3.15 Amperes of current is supplied. This wire size was suitable for the scale of the microfurnace, and the power requirement was within the limits of the power supply available in the laboratory, which can supply up to 6 Amperes at 32 Volts.

The resistive wire was coiled around a small drill bit such that it would fit the inner diameter of the ceramic tube. The ends of the resistive wire were connected to the power supply through two ¼" diameter bolts resting in teflon standoffs that electrically insulated the setup. The bolts provided a convenient attachment point for the power supply leads (alligator clips). This setup is shown in Figure 25.

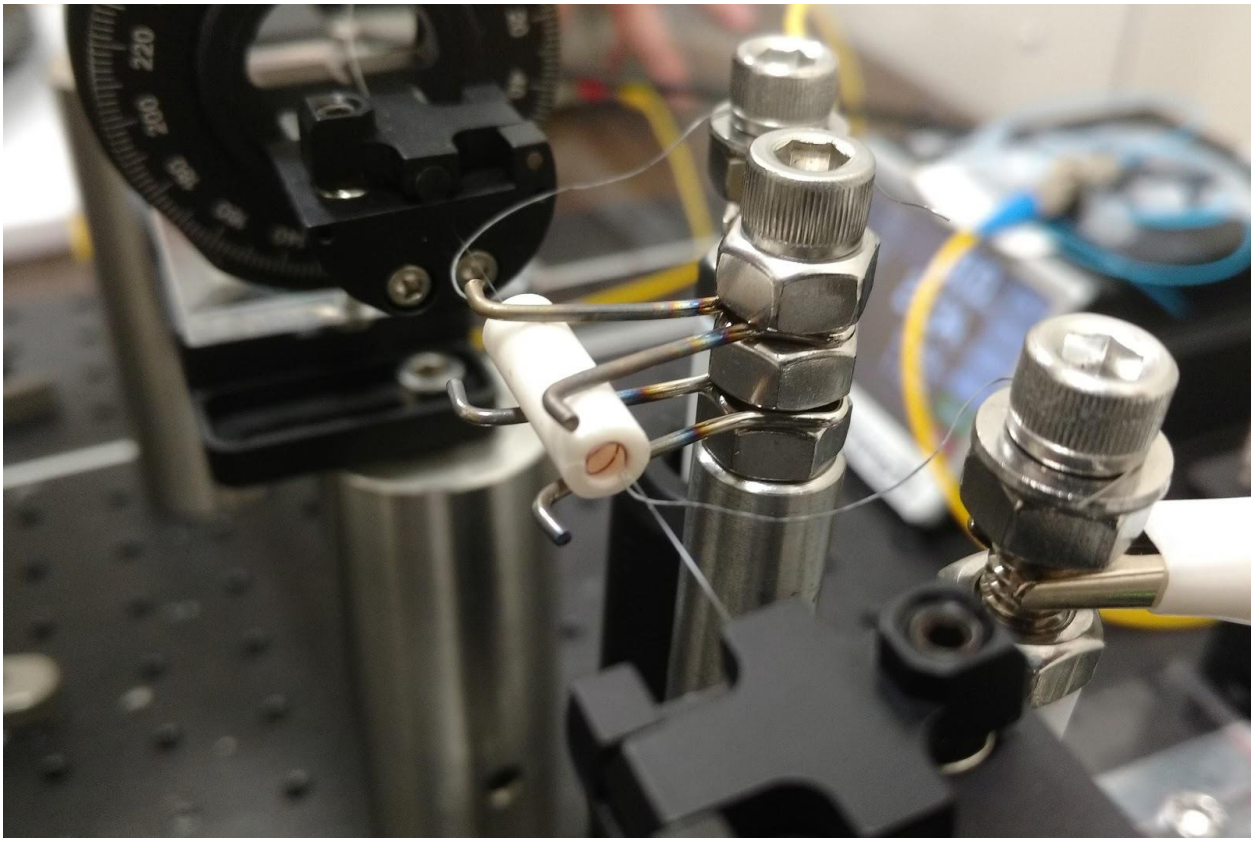

Figure 25: Microfurnace with fiber and resistive wire connected to power supply

3.2.1.2 Parametric Study of Electrical Input

With an initial set of physical dimensions of the furnace apparatus now selected, a series of tests were completed to study the effect of input electrical power on the performance of the furnace. The DC power supply was used to control the amperage drawn by the resistance wire, and therefore the power dissipated as heat. Power inputs ranging from 50 W to 100 W were tested.

The microfurnace was positioned within the tapering setup so that the motorized stages would pull the fiber. The fiber was prepared in the same manner as with any flame-based tapering method we used and held in place by the fiber holders as power was supplied to the coil. After 30 seconds of heating, the fiber easily stretched. The transmission through the optical fiber was monitored using the LabVIEW program. In previous tapering methods using an alcohol flame, the progress of the tapering process was determined by fluctuations in the transmission as monitored by the LabVIEW program. When the fiber began to soften and form a tapered profile, a sinusoidal pattern would emerge in the transmission readout. According to Eqs.3-6 and reference [9], when the fiber taper diameter is above a certain threshold, more than one optical modes is allowed. Larger waveguide diameters support more modes. The fluctuation observed in the Figure 26 shows the optical power fluctuation due to varying number of optical modes in the taper, the latter of which resulted from the changing taper diameter during the tapering process. This pattern would collapse to an approximate straight line when the tapering process was complete. This same process was used for the microfurnace setup. Figure 26 illustrates the first success at trying to create a working tapered optical fiber.

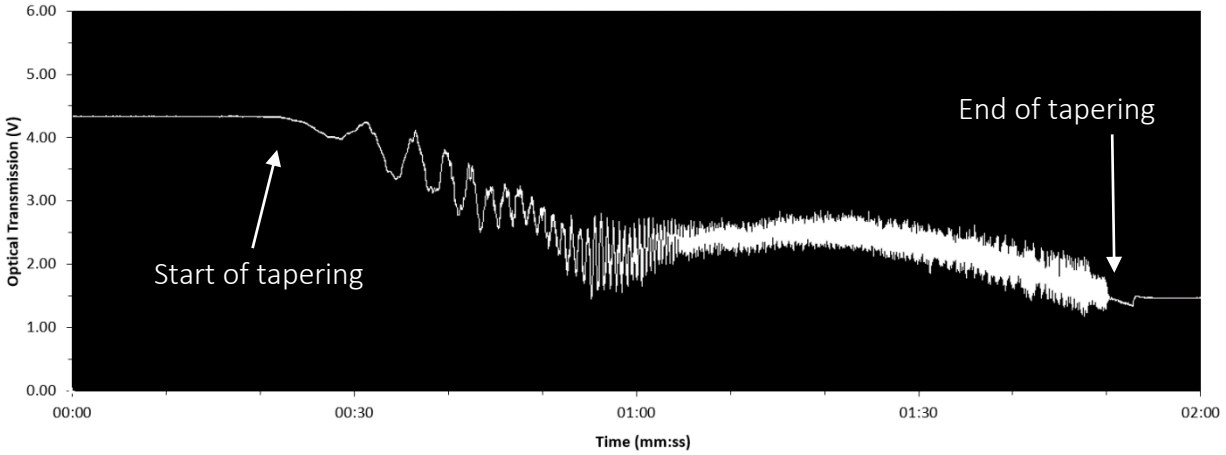

Figure 26: Transmission data for an initial microfurnace tapering trial (32 V, 2.8 A, ~90 Watts). These plots were generated by a LabVIEW program recording the voltage produced by the photodetector during the tapering process, which is linearly proportional to the optical power transmitted through the fiber.

Although the transmission pattern seen in Figure 26 is representative of a successfully tapered fiber, it does also show significant losses. The amplitude of the graph is a measure of transmission; it is a measure of the power read by the photodetector. In this trial, the final transmission is approximately 38% of the starting transmission. Existing background literature indicates that in order for tapered optical fibers to have high transmission, they need to be smooth and uniform tapers with little to no surface defects. Therefore, it was important to understand how variables such as coil length and power input affect the physical characteristics of the tapered fibers produced.

Figure 27 shows microscope images of the tapered fiber corresponding to the transmission data in Figure 26. The low transmission for this trial was likely caused by the defects and roughness seen in this particular fiber under the microscope. The cause of these defects, however, was unknown. We ran multiple trials varying the input power to see how it affected transmission.

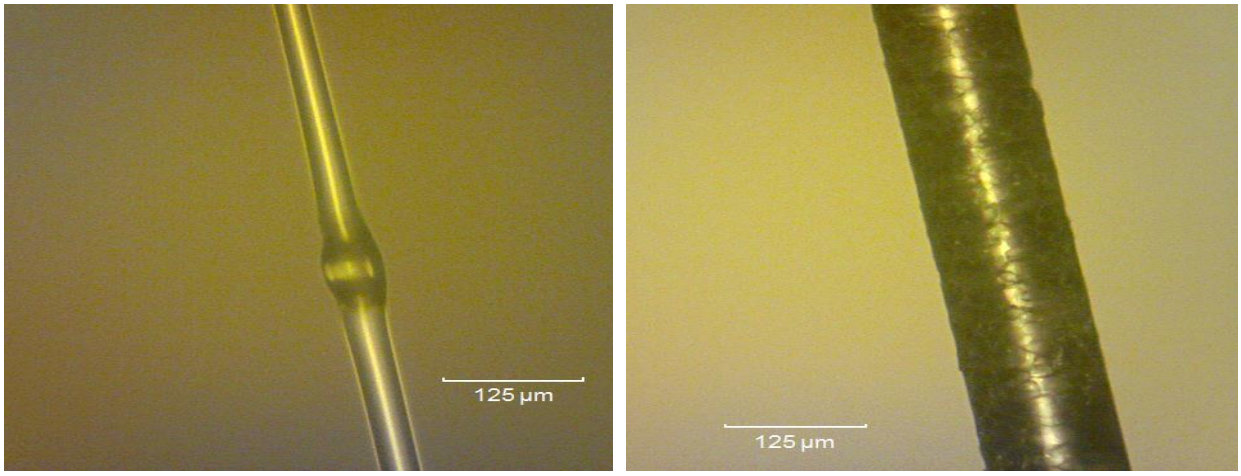

Figure 27: Bubble defect in tapered section of optical fiber (left) and high surface roughness (right)

Figure 28 shows a highly successful trial in which the tapered fiber demonstrated only a 20% transmission loss meaning it has a transmission of 80%. We examined the fiber again under a light microscope in order to see why the transmission dropped. We found that there were zero imperfections in the tapered section of the fiber. According to our research, loss in transmission can also come from a steep slope of the conical section of the taper. Since we did not find any imperfections, the cause of transmission loss must have been a rapidly-transitioning tapered section. This result also shows that lowering the input power could help increase transmission.

Although the results were varied, one pattern that began to emerge from the failures was the effect of input power on the resulting transmission loss. Lower power levels typically produced more promising transmission data that showed the appropriate fluctuations and low losses. Figure 29 shows the transmission during a trial that used approximately 86 Watts of power. Similar or higher input powers caused transmissions to decline rapidly without showing the signature sinusoidal fluctuations indicative of tapering.

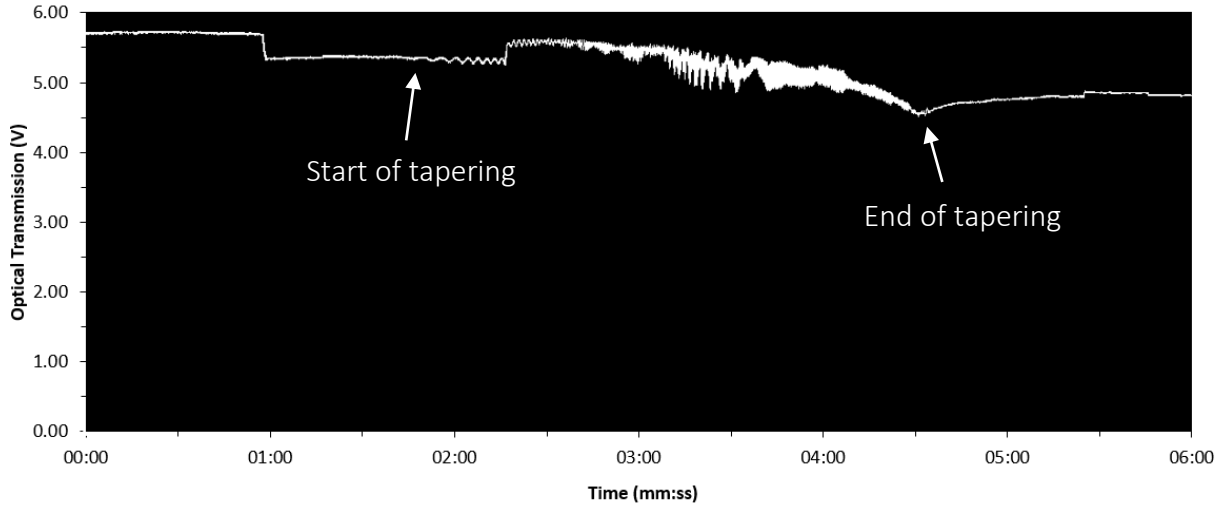

Figure 28: Transmission data for a successful trial with ¾" furnace at 29.7 V, 2.8 A (~83 Watts)

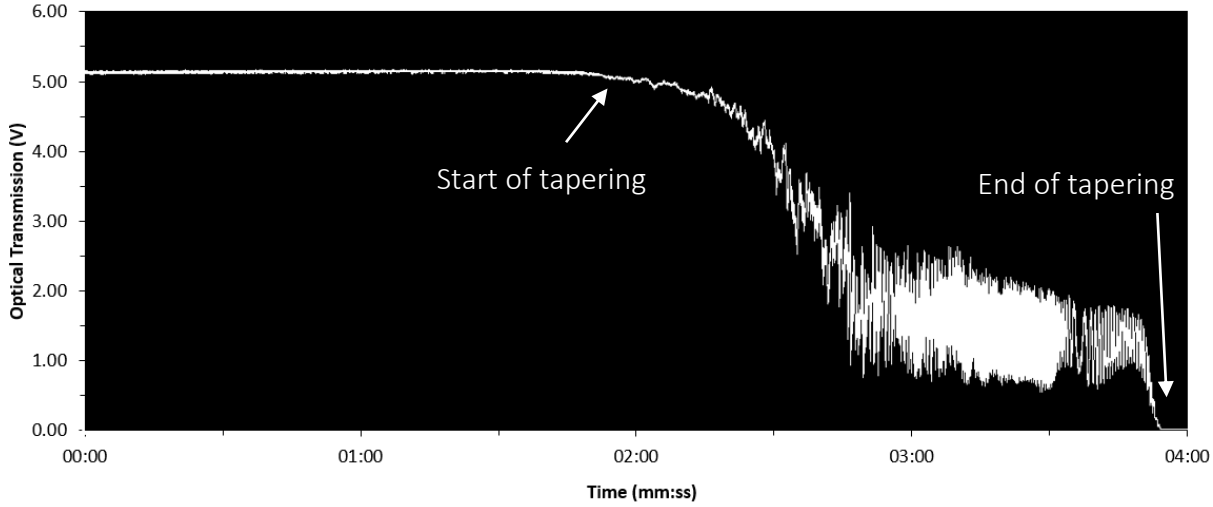

Figure 29: Transmission data for typical failed tapering attempts. ¾" coil at 27 V, 3.2 A (~86 Watts)

The transmission data shown in Figure 29 represents a common profile that emerged during tapering trials; the transmission dropped heavily early on then fluctuated more steadily before declining to zero. Microscope images of the fiber used in Figure 29 are shown in Figure 30. These captures show another commonality among trials: small bubbles and indentations.

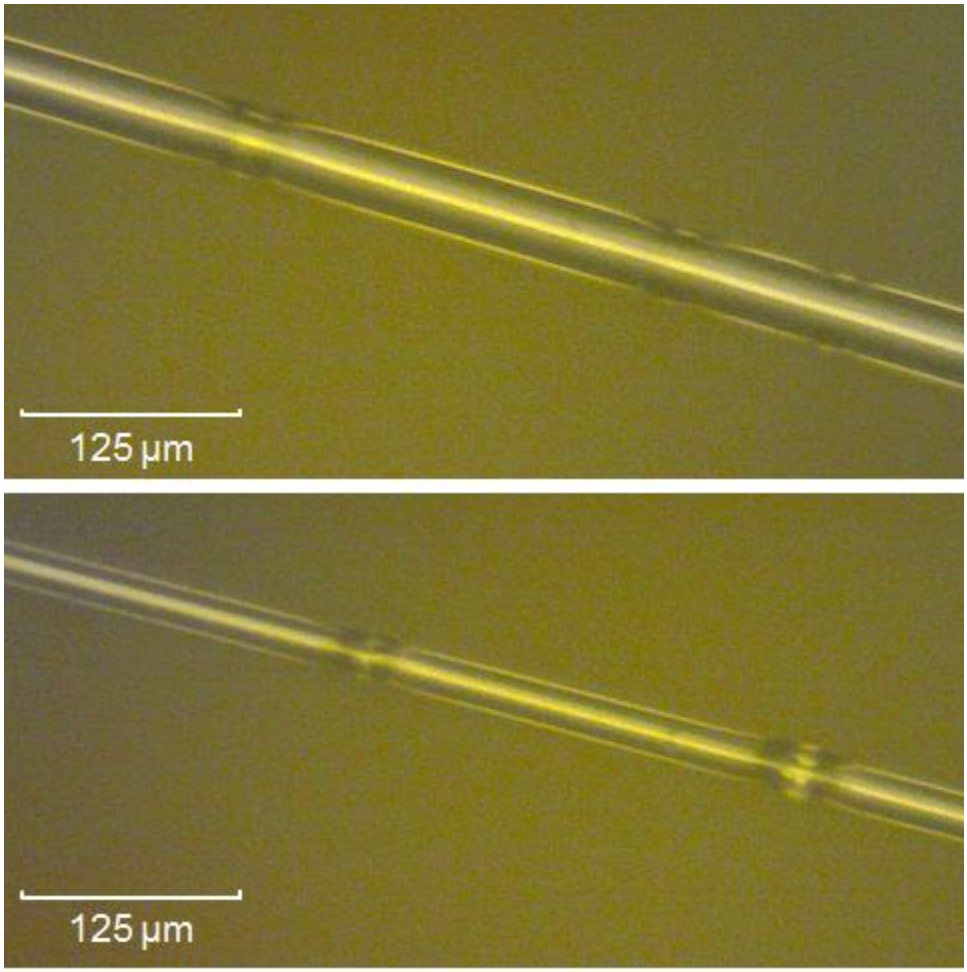

Figure 30: Microscope images showing indentations (top) and bubbles (bottom) along fiber after tapering. These types of imperfections are largely responsible for optical power losses through tapered fibers.

Many of the fibers with low final transmission contained bubbles and indentations along their surface. Although it was unclear exactly why these defects formed, we theorized that the length of the heating area and the resulting temperature distribution was responsible. Whereas the flame-based methods used a flame with a heating area of approximately 5mm in length, this microfurnace was approximately 20mm in length. As a result, there is no "peak" temperature like a flame produces, but rather a "plateau" where temperatures are high enough to soften the fiber along a length of the microfurnace. As a result, there is a wider range in which the fiber could start tapering. Random spots along the fiber may begin to form a waist simultaneously before moving out of the heating zone, which results in the indentations or "micro tapers." Likewise, areas along the fiber subject to high temperatures for too long may begin to melt and cause bubbles to form.

SolidWorks simulations shown in Figure 31 were used to quickly investigate how the length of the microfurnace and heating coil affected the temperature distribution. Identical conditions for two different lengths of coils were simulated. A ¾" furnace was compared to a ½" furnace, where both lengths had coils of with the same spacing and 65 Watts of power dissipation.

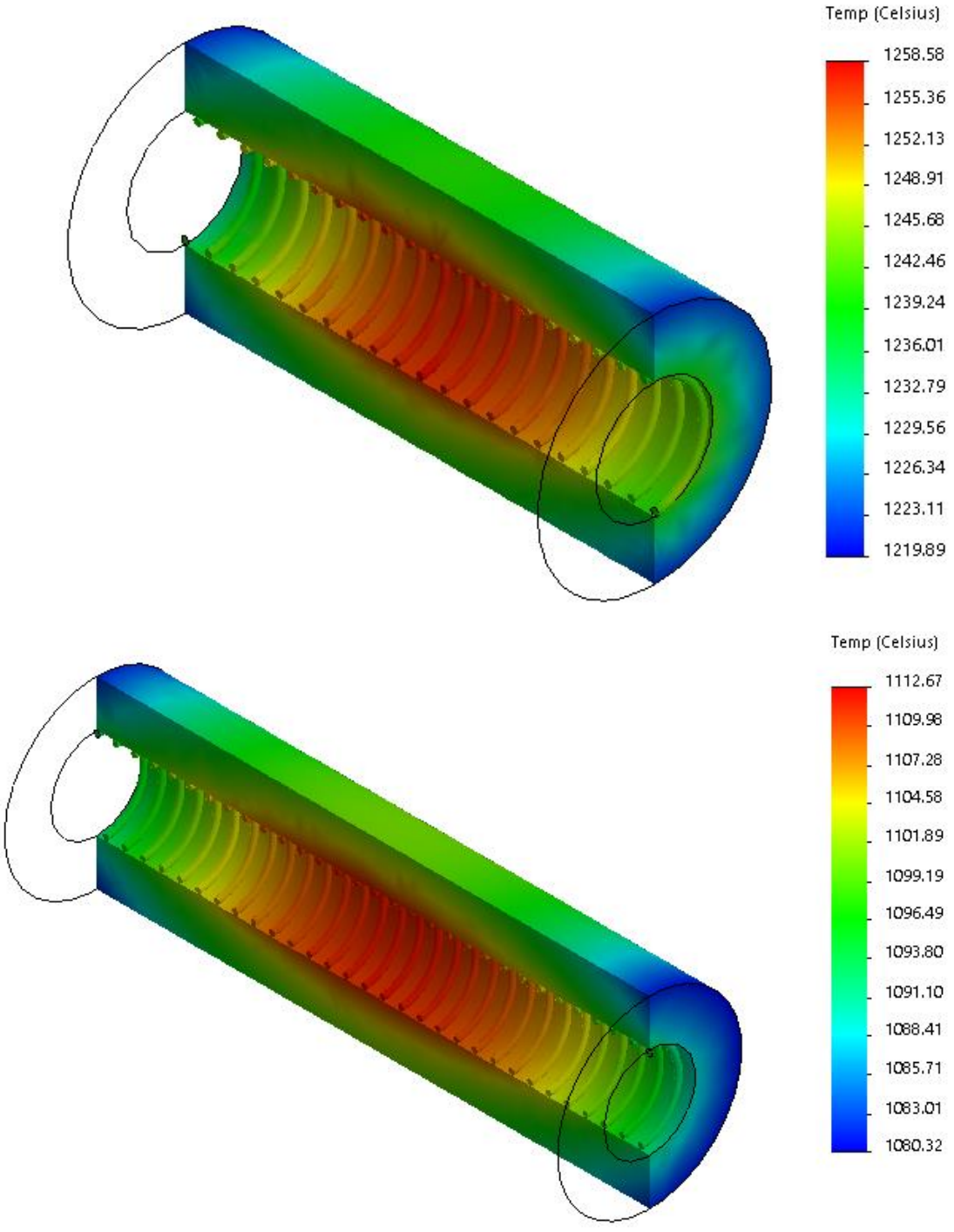

Figure 31: Thermal simulation results for ½" (top) and ¾" (bottom) coils with 65 Watts of heat input from the resistance wire.

Both coils show a similar temperature differential (between 20°C and 30°C) within the interior of the ceramic furnace. For the ¾" length furnace, a larger portion of the interior is near the maximum temperature and the transition to cooler regions is more gradual than in the ½" length furnace. The shorter furnace more accurately represents the single-peak temperature distribution found in a flame, whereas the long furnace shows a high-temperature plateau near the center of its length. Therefore, using a shorter microfurnace in practice should prevent the defects from forming since it is more representative of a flame.

3.2.2 ½" Length ¼" Diameter Furnace

3.2.2.1 Fabrication

The same ceramic tube was used as before but cut to a length of ½". It was held in place by the same clips and a resistive wire coil was inserted into the tube.

3.2.2.2 Testing and Analysis

The new microfurnace was used at a lower power input of approximately 75 Watts. The resulting transmission plot is shown in Figure 32. The transmission showed tapering behavior at very low losses, maintaining nearly 95% of its original transmission.

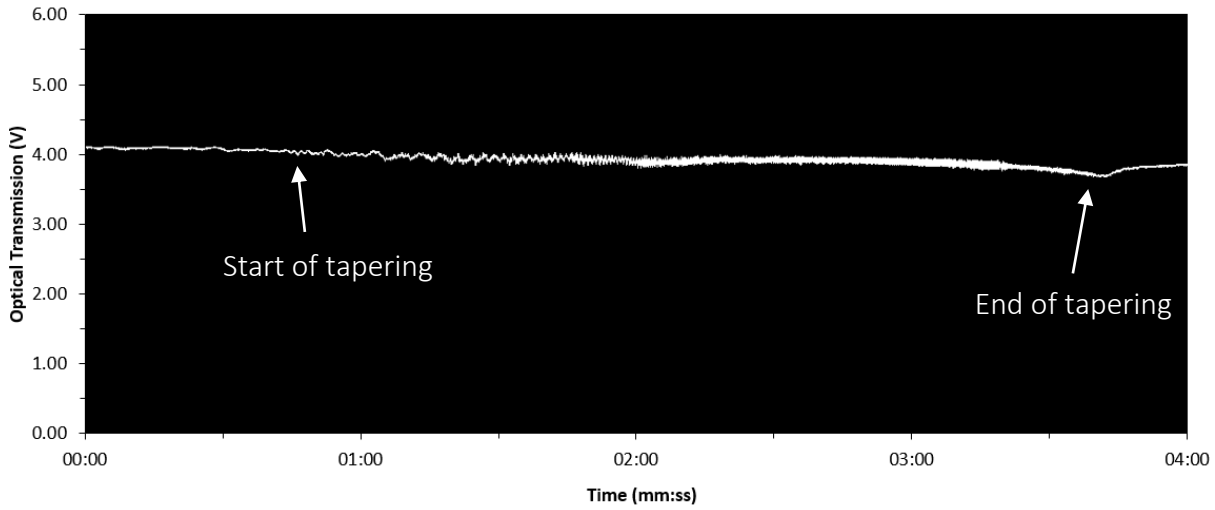

Figure 32: Transmission data for the initial test using a ½" coil at 32 V, 2.4 A (~77 Watts)

Several additional trials were conducted, resulting in transmissions ranging from 80% to 95%. The length of tapered fibers produced ranged from approximately 40mm to 55mm. The microscope image in Figure 33 shows only minor surface imperfections along the fiber.

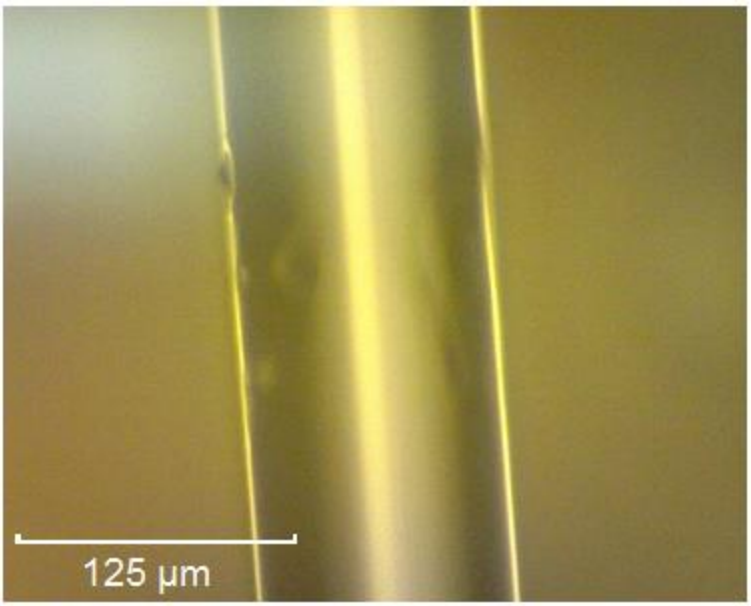

Figure 33: 10x magnification microscope image of fiber from ½" coil

These results show a significant improvement in the consistency and performance of tapered fibers produced compared to the previous flame technique. Unfortunately, over time the setup that held the microfurnace slowly began to warp due to temperature fluctuations, thus misaligning the fiber concentrically in the furnace. This misalignment caused the fibers produced to have poor transmission. A more stable furnace fixture that would not warp was required.

3.2.3 Aluminum Holder 1

3.2.3.1 Design and Fabrication

The new holder was made out of an aluminum block measuring 3" in length by ½ " in width by ½" in height, shown in Figure 34. A ¼" hole was drilled horizontally in the front face to hold the ceramic tube while also maintaining partial visibility of the tube, which we used to see the hot glow and gauge when the tube is fully heated and ready for us to start the tapering process. At the top of the ¼" hole was a 6-32 tapped hole for a set screw to hold the ceramic tube firmly in place. A ¼" hole was drilled on the opposite end of the holder to secure it to our 3D stage for precise alignment with the optical fiber.

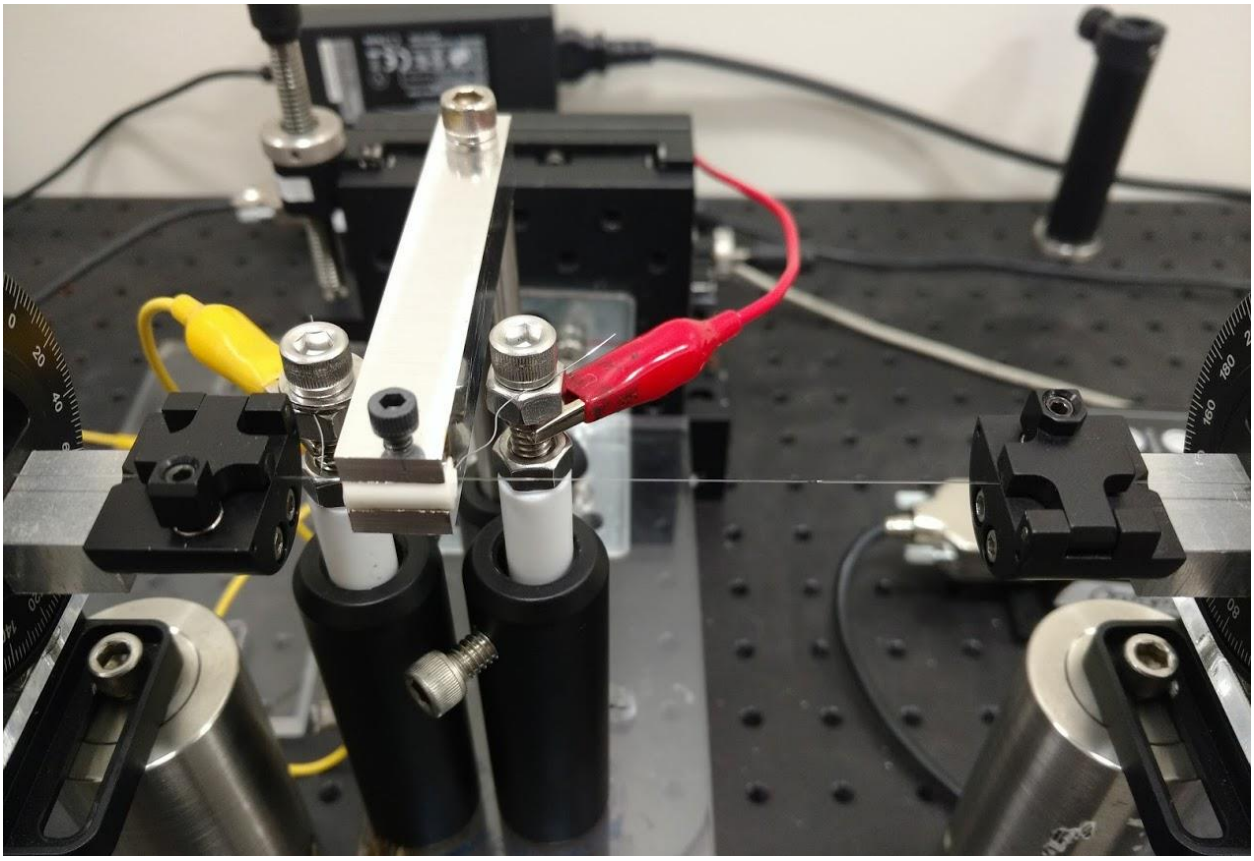

Figure 34: New holder for the ceramic furnace

3.2.3.2 Testing and Analysis

When we tested this new holder, it held up to the constant heat and cooling cycles without warping, but we found ourselves waiting around 5-10 minutes before the tube reached equilibrium. We also tested it with a wide range of power inputs from 60 to 100 Watts. Most of trials resulted in either no tapering from the setup or unfinished tapering. The few tests that actually worked produced tapers with poor transmission, such as the test shown in Figure 35.

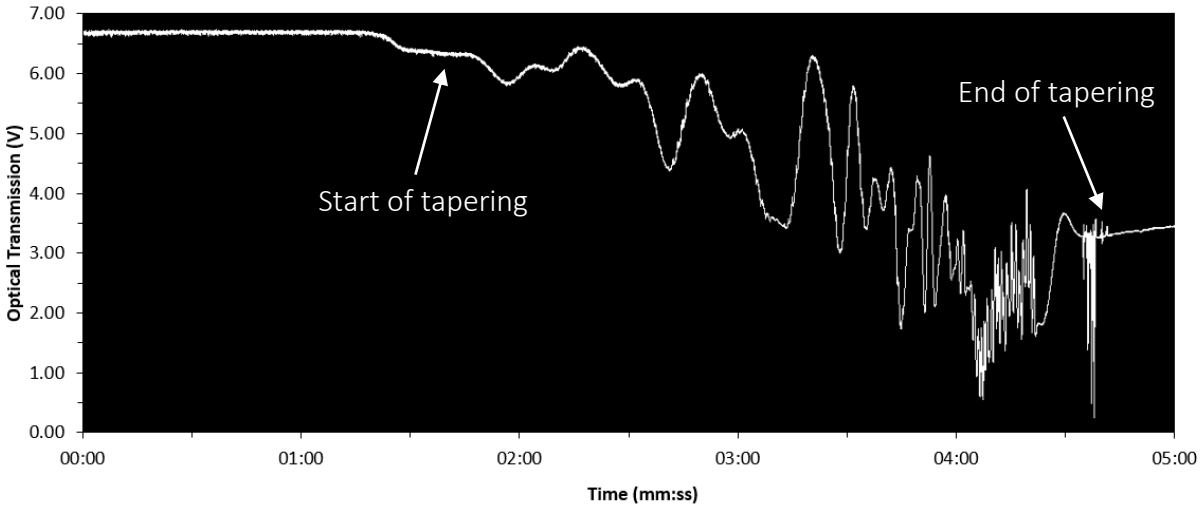

Figure 35: Transmission data from ½" furnace and new aluminum holder, which preformed poorly

Since aluminum is a thermally conductive material, the holder was conducting too much heat away from the microfurnace, which explained the need for higher power inputs. The longer waiting times were the caused by the fact that a larger mass needed to reach thermal equilibrium.

3.2.4 Aluminum Holder 2

3.2.4.1 Design and Fabrication

As a result of the excessive heat loss due to the high conductivity and contact area of the aluminum holder, we attempted to better insulate the microfurnace by adding more ceramic between the resistive coil and the holder. Rather than insert the ¼" diameter microfurnace into a ¼" hole in the aluminum holder, the microfurnace was placed inside another piece of alumina ceramic with an inner diameter of ¼" inch and an outer diameter of ½ inch, shown in Figure 36. This larger ceramic piece was then secured inside the aluminum holder.

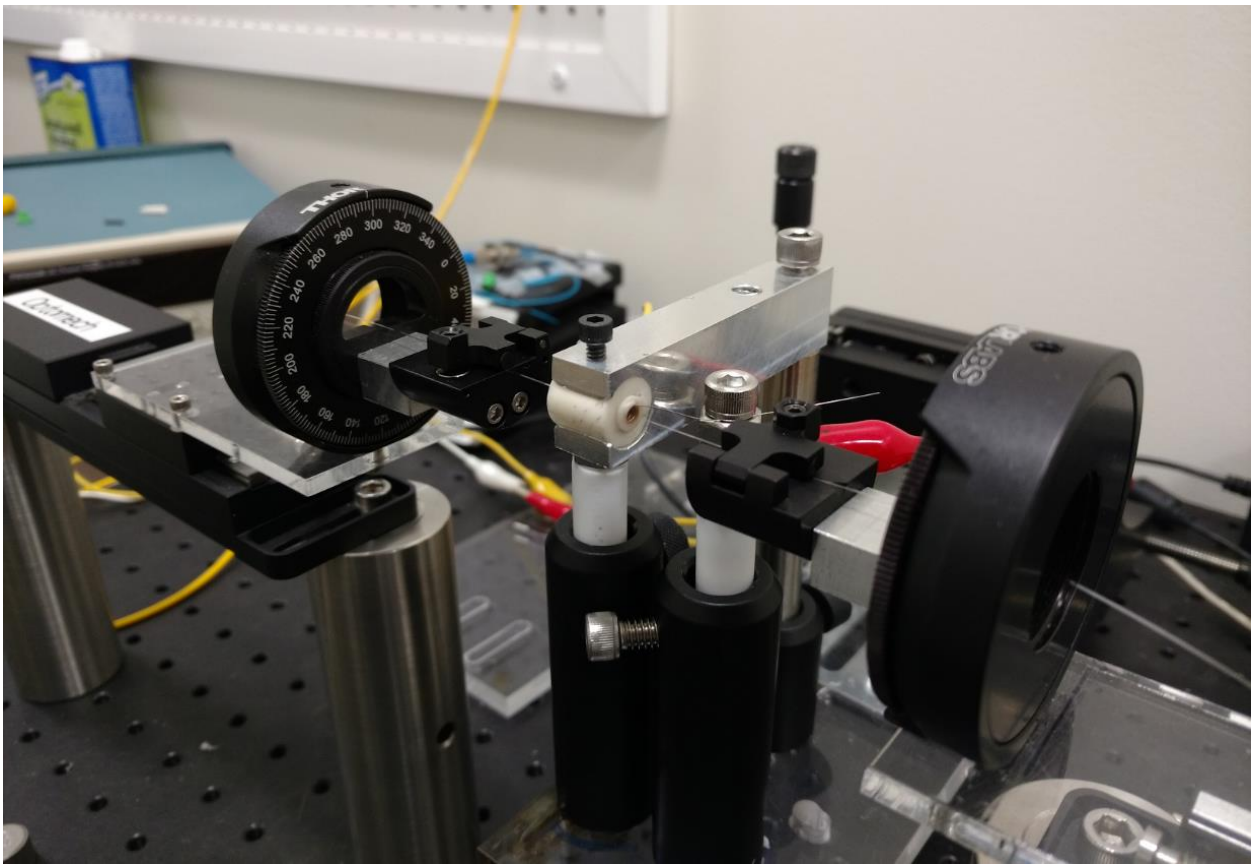

Figure 36: Double-insulated microfurnace in aluminum holder

3.2.4.2 Testing and Analysis

Although theoretically the additional insulation should keep more heat inside the furnace for heating the fiber, it did not improve performance as expected. With the highest transmission being 17.5%.

When considering only the heat conduction through the walls of the ceramic tubes, additional thickness decreases heat transfer according to Fourier's Law. However, since the outer surface also transfers heat to the ambient air and aluminum, the additional insulation also decreases thermal resistance to conduction and convection heat transfer because of the increase in surface area. As such, a critical radius exists where maximum heat transfer can be achieved. The farther a given radius is from this critical value, the larger insulating effect it will have. In the case of the microfurnace, the additional material brought the radius closer to this critical value, thus increasing the heat transfer through the walls of the ceramic tubes. In order to insulate the furnace by adding material, a several inches of wall thickness is required. Therefore, it was optimal to simply use the nominal wall thickness of the ¼" diameter tube alone.

3.2.5 Aluminum Holder 3

3.2.5.1 Design and Fabrication

Despite the outcome of varying the thickness of the ceramic tubes used in the microfurnace, the aluminum holder alone maintained a larger contact area with the outer surface of the furnace

than the binder clips had. As a result, it was still taking several minutes from startup before the tapering process began and the fibers were not tapering as well as previously.

To reduce the effects of the highly thermally conductive aluminum holder, we removed some material from the width of the holder such that the furnace was resting on only a small portion of the device, held in place from the top by the set screw, as shown in Figure 37.

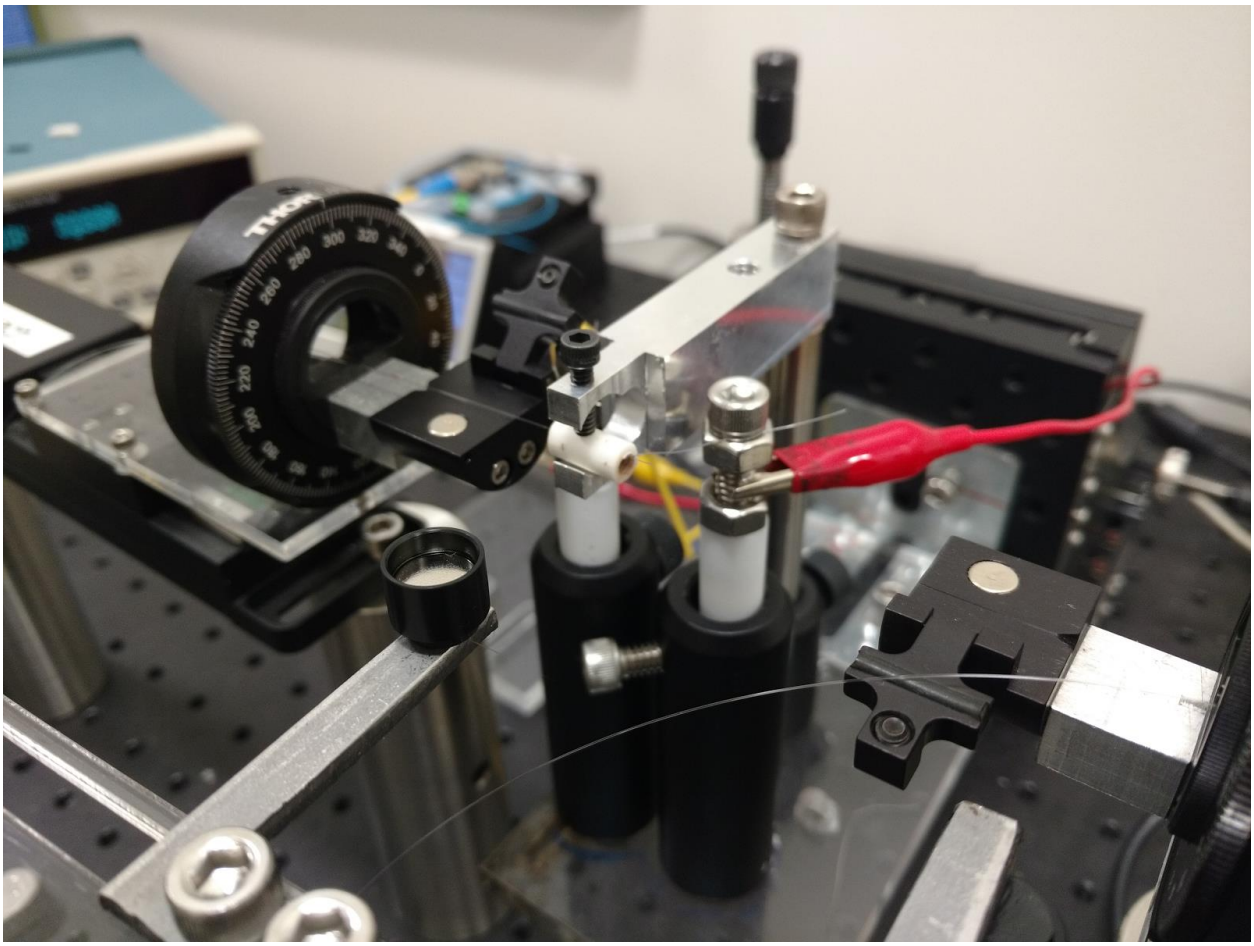

Figure 37: Aluminum holder having minimal contact with ceramic furnace

3.2.5.2 Testing and Analysis

Although some of the tapered fibers produced were of relatively high transmission, the tapering process did not noticeably begin until several minutes after the coil heated and the stages began pulling. The inconsistency of this device along with the delayed tapering process led us to believe even with a considerably reduced contact area, the aluminum was dissipating too much heat. Therefore, the small clips were reintroduced to the system to maintain minimal contact area.

3.2.6 Final Design

Since we were unable to get high transmission results from the aluminum holder, we decided to return to the consistency of the ½" diameter ¾" length ceramic furnace held by steel clips shown in Figure 38. We rearranged the components to reduce the overall size of the apparatus.

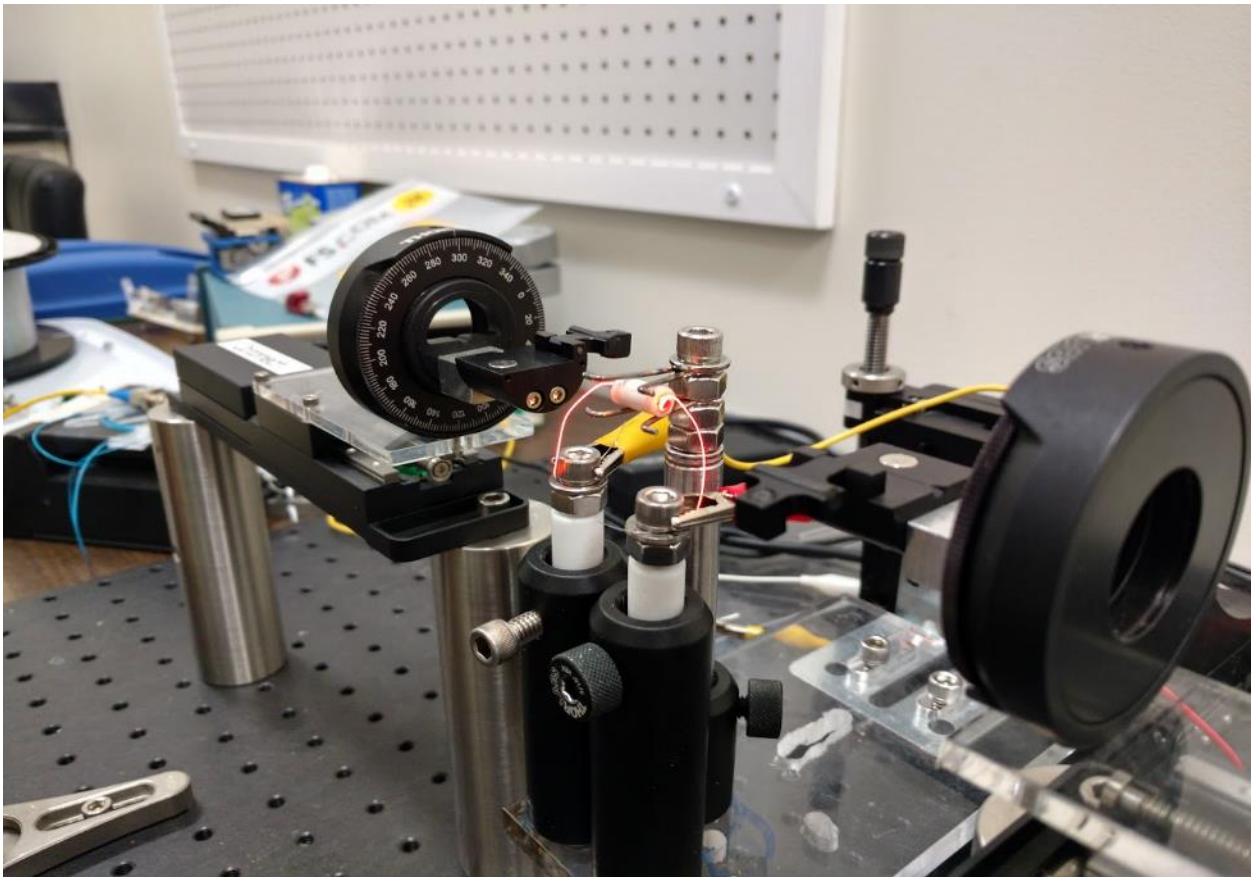

Figure 38: Final design using ceramic furnace with steel clips

The performance of the microfurnace design can be assessed by the consistency of transmission measured through the tapers it produces. Although some testing is required to determine the optimal inputs each time the furnace heating wire coil or holder is replaced, the device performs consistently once these parameters are found. Table 2 shows that for identical inputs, the apparatus produces tapered fibers with similar optical power transmission. This is a major improvement over the previous flame based method of tapering used in the lab, where even though the same flame was always, it never would produce consistent tapers.

Table 2: Repeatbility of fiber transmission

Input Parameter (Amperage)	Transmission After Tapering
2.4	95%
2.4	83%
2.4	76%
2.1	82%
2.1	91%
2.1	72%
2.3	76%
2.3	71%
2.3	71%
2.3	69%
2.8	46%
2.8	57%
2.8	57%

In Table 2, each shaded or unshaded region refers to a set of tapering trials with the same input current. For a given input, the resulting transmission varied by no more than ±10%. Attempting to duplicate a flame between trials could result in tapers with transmissions with much higher variability.

3.3 Fiber Holder

In addition to the tapering system, we designed and fabricated a fiber holder to transport the tapered fibers between the fabrication setup and experiments. The previous holder used by the lab used two acrylic arms that the fiber was taped onto. The distance between the arms was adjustable by loosening a couple of screws and sliding the arms along a slot. The acrylic arms could also rotate in order to bend the optical fiber into a U-shape.

In the new design of the fiber holder, we maintained the adjustability of the width and rotation of the arms. The acrylic arms were replaced with steel arms, which utilized magnets to clamp the fiber more securely and temporarily than tape.

A comparison between the original fiber holder and the new fiber holder is shown in Figure 39 and Figure 40.

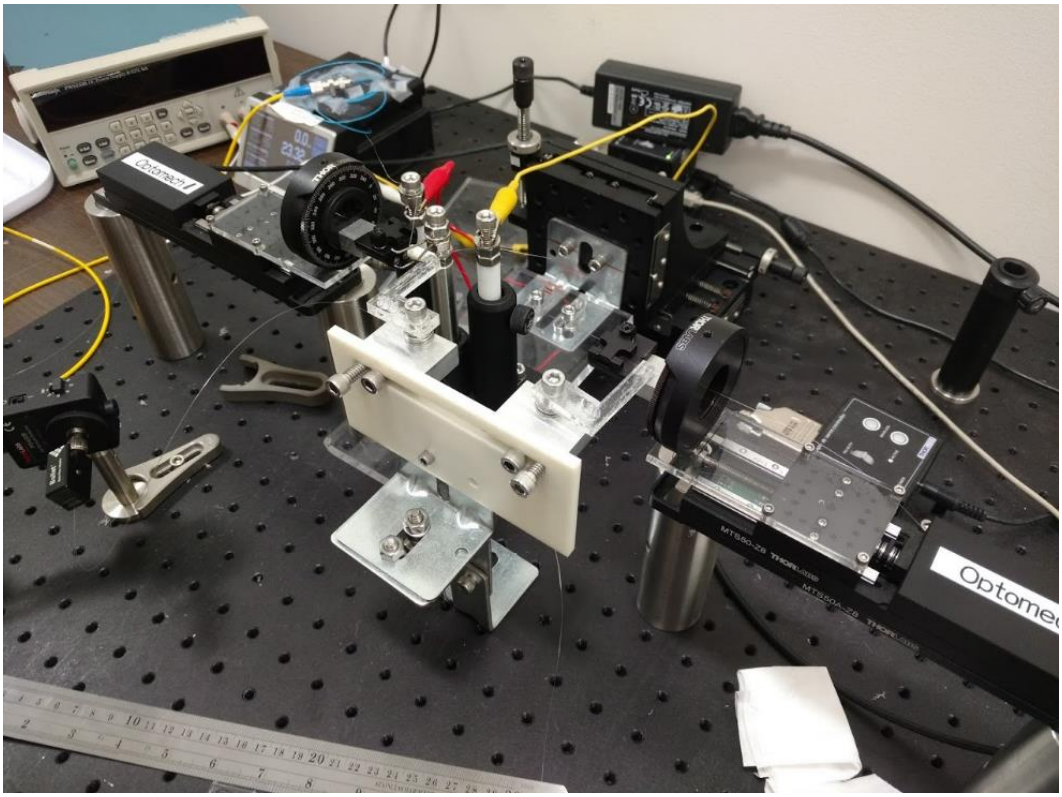

Figure 39: Original fiber holder

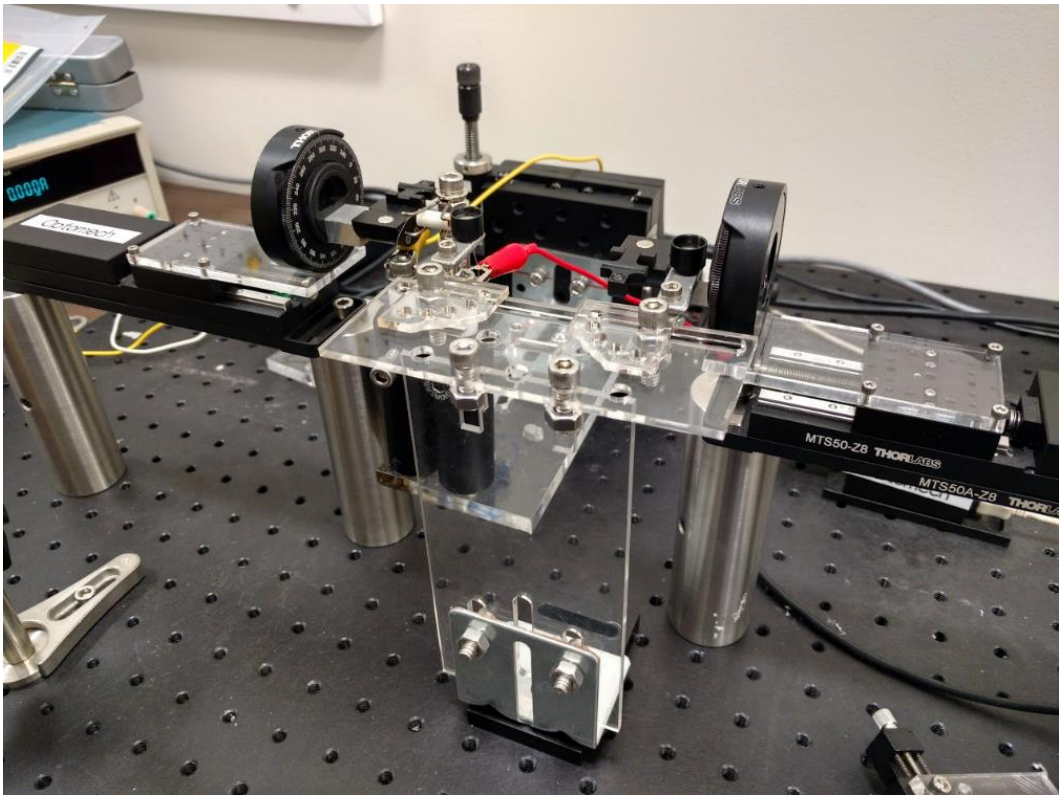

Figure 40: New fiber holder

3.4 Taper Fabrication Procedure

Fabricating tapered optical fibers using the microfurnace setup is similar to the previously-used flame method. The polymer buffer is stripped off the fiber along the heated area and the fiber is pulled in tension while heat is applied. Transmission through the fiber is monitored through LabVIEW throughout the tapering process. The DC power supply supplies a current through the wire coil to generate heat. The current is slowly increased from zero to gradually heat the resistance wire, thus increasing the lifespan of the coil. After the tapering process is complete, the fiber is removed using the fiber holder. A detailed procedure for this fabrication process is described in Appendix B.

Chapter 4: Optical Trapping Tests

The transmission data presented in the previous chapter was used to alter and improve the design of the tapering setup, namely the parameters associated with the microfurnace. While these results indicated the relative success of various design modifications, they were not truly representative of how well the fibers performed in terms of our objective: to reduce transmission loss when water is the surrounding medium for the purposes of particle trapping and manipulation.

The performance of the fibers produced by the tapering process we developed can be measured by testing their transmission in water as well as demonstrating their ability to trap particles. Due to the effects of the evanescent field present in tapered optical fibers, it can be reasoned that, for a given input power, lower optical power losses will produce larger forces due to radiation pressure in the evanescent field. Therefore, when tapered fibers are placed in water, smaller transmission losses will correspond to stronger particle trapping effects.

In section 4.1, the transmission of fabricated fiber tapers was tested in water instead of air. Particle trapping results are presented in section 4.2 and a discussion is provided in section 4.3.

4.1 Transmission in Water

Testing the performance of the tapered optical fibers in water required removing the fibers from the tapering setup and submerging them into a bowl of water while monitoring transmission for any changes, as shown in Figure 41. Regular tap water was used for testing, since the purpose of these tests was simply to see the relative change in transmission from after the tapering process to submersion in water.

Due to the high surface tension of water, the clamped fiber was inserted at an angle, such that the holder and magnets would break the tension first. Each fiber tested in this manner was held under water momentarily to allow for any changes to become apparent. The fibers were then removed similarly to how they were submerged.

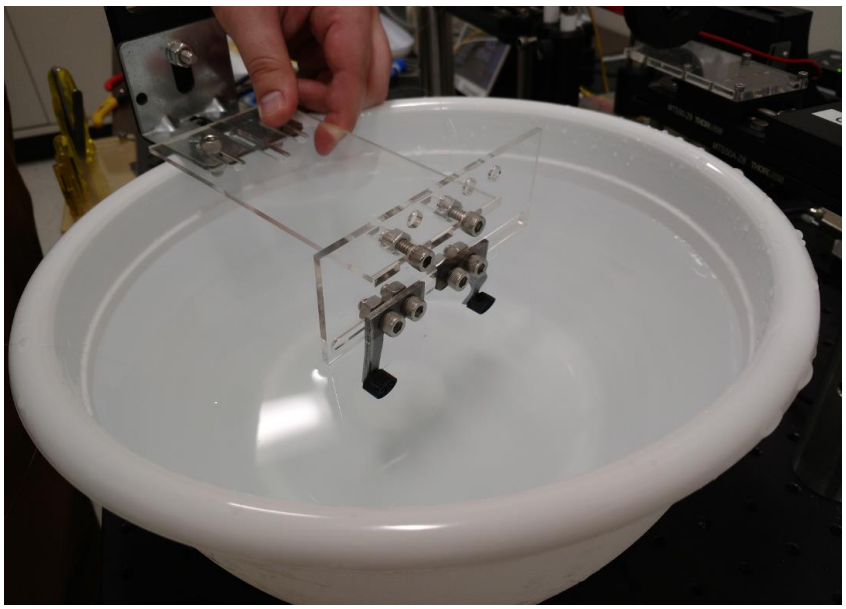

Figure 41: Tapered fiber submerged in water

Several fibers were tested in water, each of which had a different magnitude of loss due to the tapering process. No clear trend emerged showing any correlation between transmission loss during the tapering process and transmission loss when submerged in water. In other words, low-loss tapered fibers would not necessarily perform better in water than high-loss fibers. However, the appropriate comparison is not between fibers of high and low loss, but rather between tapered fibers produced with the electrical microfurnace and fibers produced with the flame method.

Figure 42 shows the transmission through a tapered fiber during testing in water. This particular fiber maintained approximately 92% transmission after the tapering process. The graph shows the transmission in air before submerging (up to approximately 28 seconds), the transmission with water surrounding the tapered fiber, and the transmission when the fiber is removed from water (after 1:26).

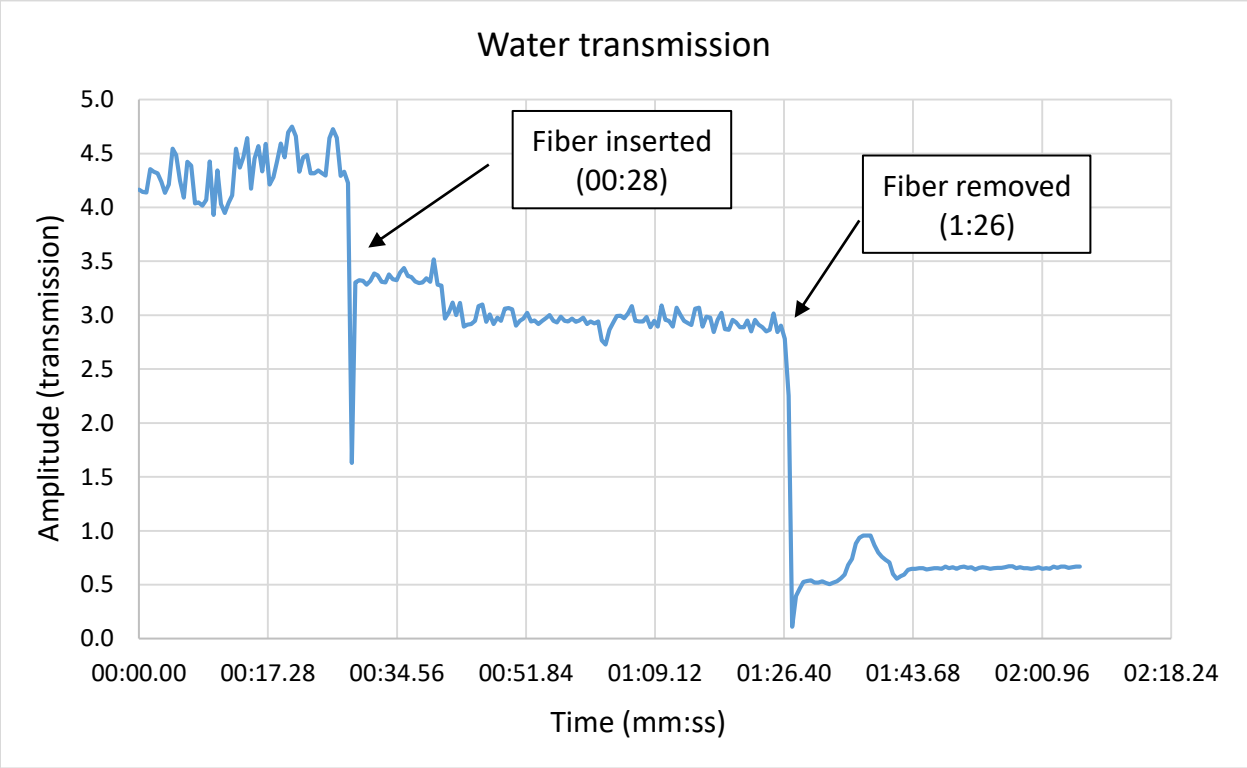

Figure 42: Fiber transmission change during water test

Many of the transmission plots for fibers tested in water look similar to the graph in Figure 42. Occasionally, a distinct but temporary drop would occur after the fiber has been submerged momentarily. We hypothesized that these drops may have been due to particle trapping effects for small amounts of dust or debris in the water.

Although submerging tapered fibers in water typically resulted in additional losses, the transmission through some of the tapered fibers actually increased. These results may be inconclusive since the increase can be explained by factors not having to do with the change in refractive index of the surrounding medium. For example, particles of dust attached to the tapered regions may cause a loss in transmission. In water, such particles are washed away and the transmission will therefore increase.

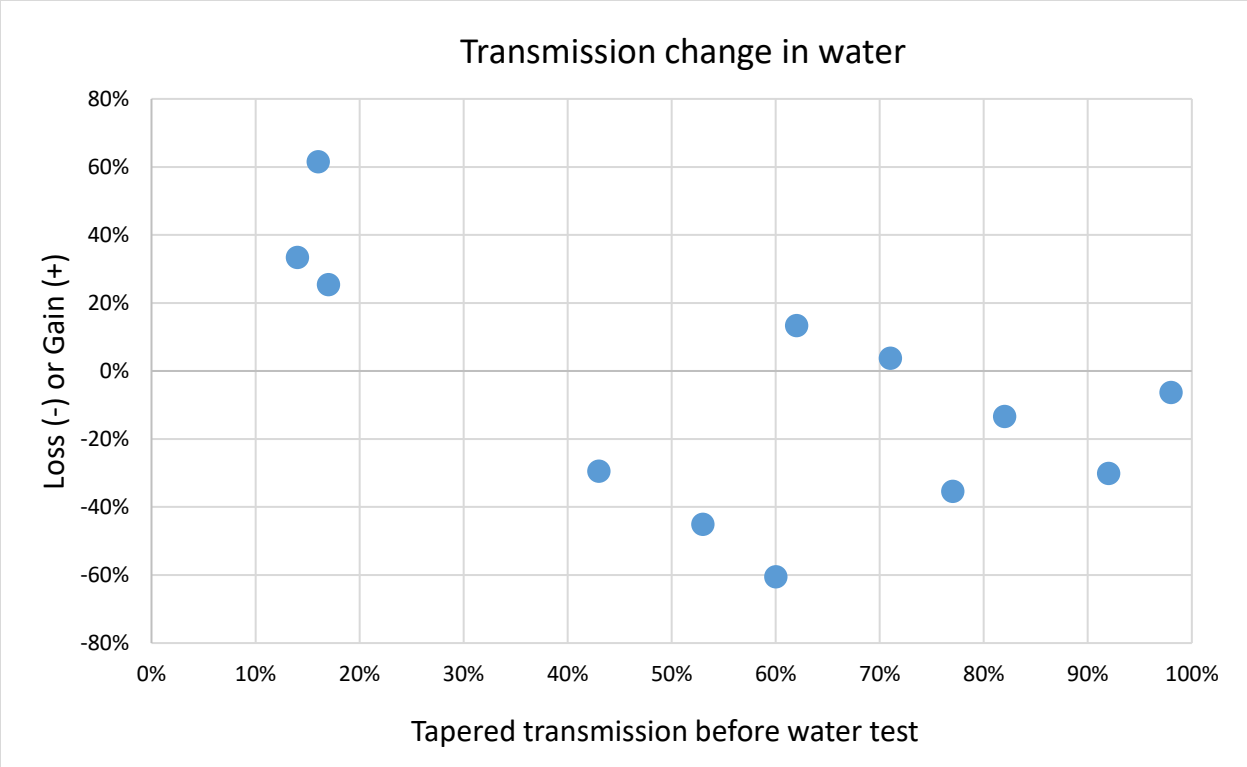

Figure 43: Relative change in transmission through fibers submerged in water for 12 selected tapered fibers. Each data point corresponds to a different fiber. The horizontal axis plots the optical transmission through the tapered fiber after the fabrication process; the vertical axis indicates additional losses (or gain) that occurred when submerged in water.

In addition to the changes that occur due to submerging the fibers in water, various behaviors were displayed in the fibers after removing them from water. A few fibers broke on removal, but most remained intact. Some of the surviving fibers were restored to their transmission before submersion, while others showed a significant loss. Losses may be the result of small droplets of water that remain attached along the tapered region after it is removed from water.

As seen in Figure 43, the water tests yielded a variety of results. Neglecting fibers with starting transmissions below 60%, the fibers performed relatively well when submerged in water, losing an average of approximately 21% and no more than 40% of their transmission when surrounded by water.

4.2 Particle Trapping

To test the tapered fibers for their optical trapping capabilities, we transferred the fibers to our testing setup, which consisted of two 3D stages (one to hold the tapered fiber and the other to hold a cover slide on which the water was placed), an optical microscope and laser. First, a bead solution had to be prepared by mixing a concentrated mixture of 4.63 micrometer silica beads and approximately 3 mL of deionized water using a ultrasonic vibration tank. To prepare the fiber for testing, it first had to be made into a U-shape with the taper waist being the bottom of the U. We transferred the fiber onto another holder that was compatible with our testing setup and we used the fiber fusion splicer to attach the taper to a laser for power. Then, using the 3D

stages, we moved the fiber close to the surface of the cover glass and added the bead solution on top of the taper.

After placing several drops of the bead solution on the cover slide, the tapered fiber was surrounded by beads floating in the droplet. Several beads near the fiber were attracted to the fiber and propelled along its length, as shown in Figure 44. Many different beads were propelled along the fiber during the test.

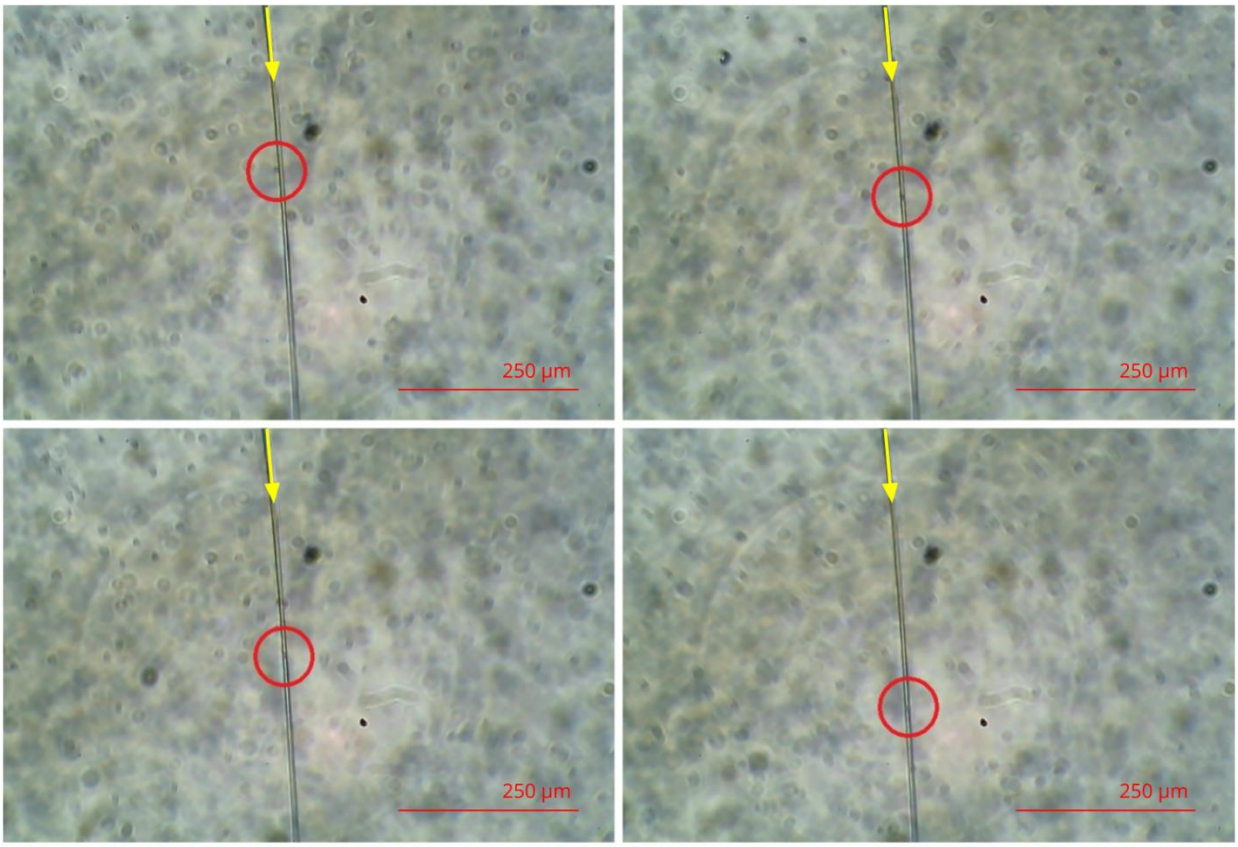

Figure 44: Optical Trapping of a 4.63 micrometer silica bead.

The bead circled in red in Figure 44 travels along the tapered fiber due to the radiation pressure of light propagating outside the fiber in the water. The top left image shows the bead approaching the fiber and attaching to the fiber. The bead then travels along the fiber, shown in the top right, bottom left, and bottom right images, sequentially.

We calculated the velocities of the beads by viewing the microscope images on a large television screen and using an image of an untampered fiber for scale. Since we took four pictures per second, we also knew the time scale of the images. We then flipped through hundreds of photos and found the trapped beads. We measured the distance and divided by time between photos to determine the velocities. The bead velocities as a function of input power are shown in Figure 45. The input powers used for particle trapping were 265mW, 325mW, and 365mW.

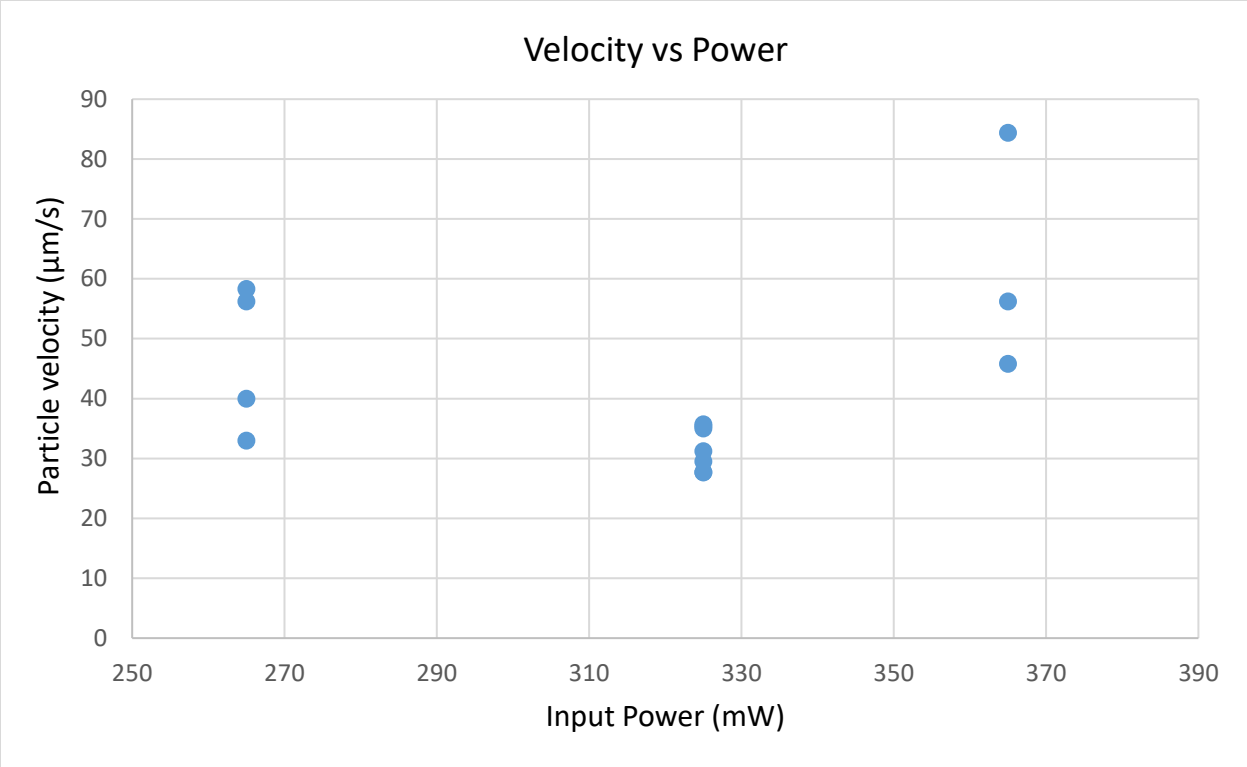

Figure 45: Graph of optical power vs velocity of bead

Figure 45 shows that an input power of 365mW produces, on average, larger particle velocities than an input power of 265mW and 325mW. However, the sample size is not very large and our measurements are subject to human error.

Possible explanations for the nonlinear relationship seen in Figure 45 include friction between the beads and surroundings, trapping of particles upstream (before the measured bead) causing light to scatter, and potential scattering from the proximity of the cover glass to the fiber. If light is scattered before the measured bead, the optical power will be much lower than originally measured, thus introducing error into our data. These reasons could cause the measurements to be less repeatable.

4.3 Comparison with Published Work

We found two different studies with measures of bead velocity versus input power for comparison. The graph shown in Figure 46 plots our data along with the data from "Targeted Delivery And Controllable Release Of Nanoparticles Using A Defect-Decorated Optical Nanofiber" [27] and the data from "Backward Transport Of Nanoparticles In Fluidic Flow." [26]

The fibers tested by the other researchers were approximately 1µm in diameter and produced by a flame-based method of fabrication, whereas our tapers were also approximately 1 micrometer in diameter, but produced with the microfurnace. Both of the studies were performed in the same research laboratory and the tapers tested from the best of our knowledge were of same diameter, so we know that the production method is not always consistent. Since the graph below shows that our data is within the trend lines for the two publications, we can predict that with more testing and a larger sample size, our method could reveal a linear trend. A strong linear trend

validates that the process is controllable, and therefore useful in producing tapered optical fibers for applications in biological cell sorting.

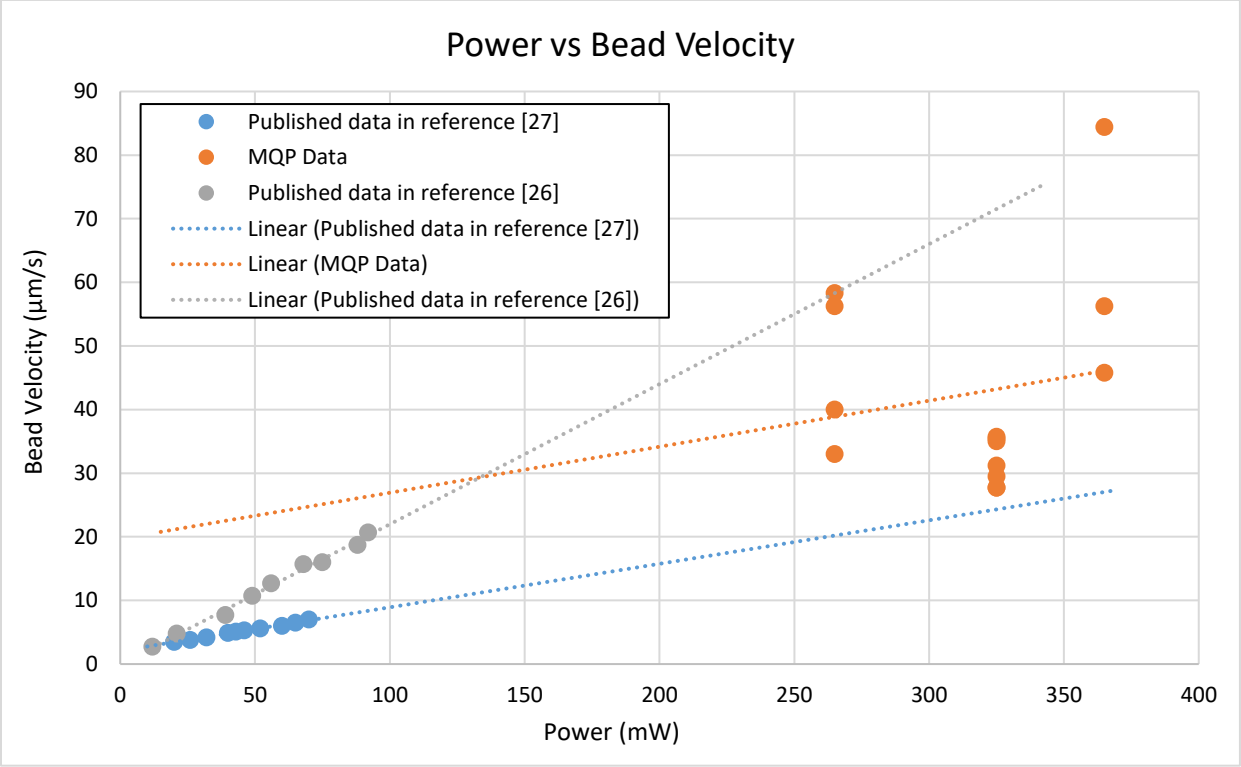

Figure 46: MQP data compared with outside research data

The graphs in Figure 47 are the original graphs with the error bars for the data used in Figure 46. One pattern that emerges from both graphs is the error bar increasing with increasing power. This explains why we have such varied results at higher power. If we were to conduct additional tests, we predict that our data would narrow down to a better fitting linear trend line with lower power. In addition, it is clear there is a tradeoff between controllability of speed and power.

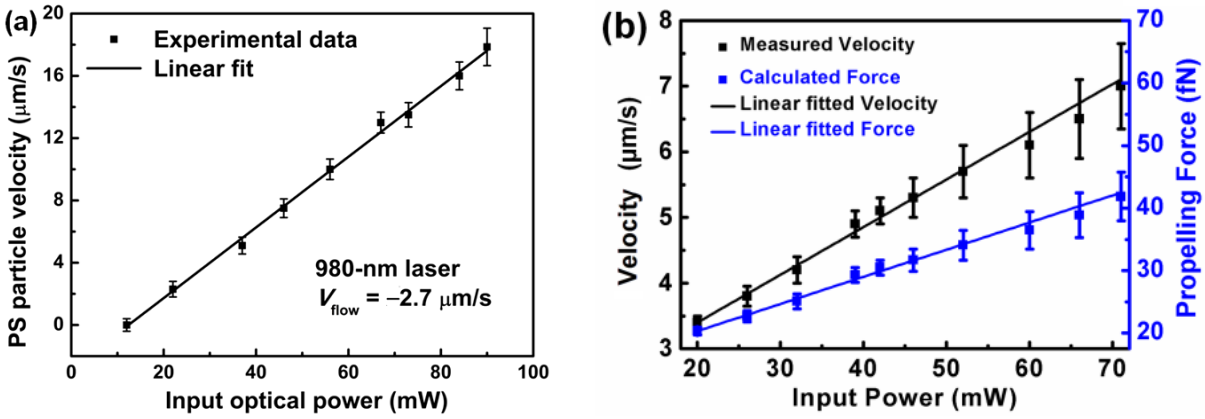

Figure 47: Published data in reference [26] (left) and those in reference [27] (right)

Another study at WPI also researched particle trapping using the previous setup in the WPI optomechanics lab. [32] The fiber tested had only approximately 20% transmission in water and the bead was propelled at 5μm/s with 500mW of input power. The fiber we tested was around 70% transmission in water and at we had velocities of around 35μm/s at 265mW input power. From this, we can see that our method of producing optical fiber tapers has greatly increased the ability of the lab's setup to produce high quality tapers.

Chapter 5: Challenges, Outlook, and Potential Societal Impact

The results obtained from the tests described in Chapter 3 and 4 indicate that we have accomplished our project objectives. However, due to the potential applications and future developments of this work we must reflect on the remaining challenges and the relative significance of our work in a broader sense.

5.1 Challenges and Improvements

Working with delicate fibers and particles on the microscale is inherently challenging. Additional challenges arose from technical issues involving the safe and effective fabrication and layout of components, including electrical connections and small ceramic pieces. The final configuration, although effective, is not flawless.

The primary issue with the microfurnace apparatus is the lifetime of its operation. Since the diameter of the furnace was intentionally small, it required a small (32 AWG), and therefore weak, wire. We found that in order to increase the lifespan of the resistance wire coil, the applied current should be gradually increased to working conditions and then gradually decreased to power down the system. The nut-and-bolt clamp used to connect the resistance wire with the power supply leads also needed to be used gently as to not introduce any unnecessary torsion or bending in the wire. Even with these precautions, the coil will break from the cyclic thermal load after nearly a dozen cycles. Similarly, the metal clips used to hold the ceramic piece in place eventually warped and needed to be replaced. As previously discussed, we attempted to combat this by implementing a larger holder, but the minimal contact area of the clips are what made them effective. Fortunately, the clips survive many more cycles than the resistance wire coil does.

Another challenge that has been addressed to a certain degree is the removal process after tapering. Since the furnace and coil fully surround the fiber, the taper can only be removed by carefully pulling it out from the end of the furnace. We have repeatedly accomplished this, but the process requires patience and finesse. If the initial setup is not done properly, the fiber may be clamped by the exposed cladding and can easily break during removal. To simplify and expedite this process, it may be worthwhile to investigate the fabrication of a furnace that is hinged along its length, such that it can open after the tapering process and the fiber can be removed radially rather than axially. In this configuration, the coil will need to be replaced by a comparable resistance wire layout that accommodates opening and closing at the hinged.

5.2 Potential Societal Impact

The particle trapping demonstrated by our research can be used in lab-on-chip devices for flow based cytometry. By implementing tapered optical fibers into flow based cytometry, medical diagnostic equipment can be made smaller and more portable for remote point of care. By making smaller and more portable devices, more advanced medical care can be brought to remote areas of the world. These types of devices are also inexpensive and therefore can deliver affordable health care to those in need. The development of these devices relies on people continuing research in this field.

Chapter 6: Conclusion

This MQP developed an electrical microfurnace for repeatedly fabricating tapered optical fibers with low losses. Through an iterative design process, various parameters of the design were refined such that the final system operated in a manner consistent with our objectives. The microfurnace design improves upon the deficiencies of many static flame-based fabrication methods by removing unpredictable behavior and increasing user control over the fabrication process. Tapered fibers produced with the microfurnace apparatus showed lower losses as a result of the tapering process and significantly lower losses when placed in water. The particle trapping effects of the tapered fibers produced were tested and successfully demonstrated, indicated great potential for biological applications such as cell manipulation and sorting. The data collected from particle trapping experiments suggests that the microfurnace is a unique and alternative tapering process that performs equally as well as methods used in leading research.

In addition to serving as meaningful research experience, this MQP helped us better understand the design process used to solve scientific and engineering problems by providing an opportunity to work on a system-level multidisciplinary problem involving topics of optics, heat transfer, mechanical design, material science, and engineering experimentation.

References

[1] "Optic fiber for recording the temperature in extreme industrial environments," Phys.org, 2015. [Online]. Available: https://phys.org/news/2015-01-optic-fiber-temperature-extreme-industrial.html.

[2] A. Felipe, G. Espíndola, J. Kalinowski, J. Lima and A. Paterno, "Stepwise fabrication of arbitrary fiber optic tapers," *Opt. Express,* vol. 20, no. 18, p. 19893, 2012.

[3] G. Brambilla, F. Xu, P. Horak, Y. Jung, F. Koizumi, N. Sessions, E. Koukharenko, X. Feng, G. Murugan, J. Wilkinson and D. Richardson, "Optical fiber nanowires and microwires: fabrication and applications," *Advances in Optics and Photonics,* vol. 1, no. 1, p. 107, 2009.

[4] O. Svitelskiy, Y. Li, M. Sumetsky, D. Carnegie, E. Rafailov and V. Astratov, "A microfluidic platform integrated with tapered optical fiber for studying resonant properties of compact high index microspheres," in *13th International Conference on Transparent Optical Networks,* Stockholm, 2011.

[5] F. Xu, V. Pruneri, V. Finazzi and G. Brambilla, "An embedded optical nanowire loop resonator refractometric sensor," *Opt. Express,* vol. 16, no. 2, p. 1062, 2008.

[6] G. Brambilla, F. Xu and X. Feng, "Fabrication of optical fibre nanowires and their optical and mechanical characterisation," *Electronics Letters,* vol. 42, no. 9, p. 517, 2006.

[7] A. Ghatak, "The Optical Fiber," *Transactions of the Indian Ceramic Society,* vol. 73, no. 4, pp. 256-257, 2014.

[8] Y. Liu, *Fiber Optics,* Worcester Polytechnic Institute, 2015.

[9] K. Okamoto, Fundamentals of Optical Waveguides (2nd ed.), 1st ed. Academic Press, 2006.

[10] H. Yu, Q. Huang and J. Zhao, "Fabrication of an Optical Fiber Micro-Sphere with a Diameter of Several Tens of Micrometers," *Materials,* vol. 7, no. 7, pp. 4878-4895, 2014.

[11] Z. Qiang, L. Junyang, Y. Yanling, G. Libo and X. Chenyang, "Micro double tapered optical fiber sensors based on the evanescent field-effect and surface modification," *Optik - International Journal for Light and Electron Optics*, vol. 125, no. 17, pp. 4614-4617, 2014.

[12] X. Wu and L. Tong, "Optical microfibers and nanofibers," *Nanophotonics,* vol. 2, pp. 5-6, 2013.

[13] G. Brambilla, V. Finazzi and D. Richardson, "Ultra-low-loss optical fiber nanotapers," *Opt. Express,* vol. 12, no. 10, p. 2258, 2004.

[14] M. Sumetsky, Y. Dulashko and A. Hale, "Fabrication and study of bent and coiled free silica nanowires: Self-coupling microloop optical interferometer," *Opt. Express,* vol. 12, no. 15, p. 3521, 2004.

[15] F. Bilodeau, K. Hill, S. Fraucher and D. Johnson, "Low-loss highly overcoupled fused couplers: fabrication and sensitivity to external pressure," *Journal of Lightwave Technology,* vol. 6, no. 10, pp. 1476-1482, 1988.

[16] C. Baker and M. Rochette, "A generalized heat-brush approach for precise control of the waist profile in fiber tapers," *Optical Materials Express,* vol. 1, no. 6, p. 1065, 2011.

[17] A. Grellier, N. Zayer and C. Pannell, "Heat transfer modelling in CO2 laser processing of optical fibres," *Optics Communications,* vol. 152, no. 4-6, pp. 324-328, 1998.

[18] L. Ozcan, V. Treanton, F. Guay and R. Kashyap, "Highly Symmetric Optical Fiber Tapers Fabricated With a CO2 Laser," *IEEE Photonics Technology Letters,* vol. 19, no. 9, pp. 656-658, 2007.

[19] S. Oh, W. Han, U. Paek and Y. Chung, "Azimuthally symmetric long-period fiber gratings fabricated with CO2 laser," *Microwave and Optical Technology Letters,* vol. 41, no. 3, pp. 188-190, 2004.

[20] L. Shi, X. Chen, H. Liu, Y. Chen, Z. Ye, W. Liao and Y. Xia, "Fabrication of submicron-diameter silica fibers using electric strip heater," *Opt. Express,* vol. 14, no. 12, p. 5055, 2006.

[21] Y. Takeuchi and J. Noda, "Novel fiber coupler tapering process using a microheater," *IEEE Photonics Technology Letters,* vol. 4, no. 5, pp. 465-467, 1992.

[22] G. Brambilla, F. Koizumi, X. Feng and D. Richardson, "Compound-glass optical nanowires," *Electronics Letters,* vol. 41, no. 7, p. 400, 2005.

[23] G. Kakarantzas, "TPCI - Photonics for Nano-applications," National Hellenic Research Foundation, [Online]. Available: http://www.eie.gr/nhrf/institutes/tpci/researchteams/pn/pn-fiber-en.html.

[24] E. Marin, "Optical fiber sensors - Evanescent field," Optique pour l'ingénieur, [Online]. Available: http://www.optique-ingenieur.org/en/courses/OPI_ang_M06_C04/co/Contenu_02.html.

[25] P. Polynkin, A. Polynkin, N. Peyghambarian and M. Mansuripur, "Evanescent field-based optical fiber sensing device for measuring the refractive index of liquids in microfluidic channels," *Optics Letters,* vol. 30, no. 11, p. 1273, 2005.

[26] C. Xu, H. Lei, Y. Zhang and B. Li, "Backward Transport Of Nanoparticles In Fluidic Flow," *Optics Express,* vol. 20, no. 3, p. 1930, 2012.

[27] H. Xin and B. Li, "Targeted Delivery And Controllable Release Of Nanoparticles Using A Defect-Decorated Optical Nanofiber," *Optics Express,* vol. 19, no. 14, p. 13285, 2011.

[28] P. Schneeweiss, S. Dawkins, R. Mitsch, D. Reitz, E. Vetsch and A. Rauschenbeutel, "A Nanofiber-Based Optical Conveyor Belt For Cold Atoms," *Applied Physics B,* vol. 110, no. 3, pp. 279-283, 2012.

[29] "Color and Temperature," Phys 251, 2001. [Online]. Available: http://webphysics.iupui.edu/webscience/physics_archive/colorandtemperature.html.

[30] "Alloy 875," Pelican Wire Company, [Online]. Available: http://www.pelicanwire.com/resistance-wire-alloys/alloy-875/.

[31] "Kanthal A1 Resistance Wire," TEMCo Industrial, [Online]. Available: https://www.temcoindustrial.com/kanthal-a1-resistance-wire.html.

[32] Y. Ren, R. Zhang, C. Ti and Y. Liu, "Tapered optical fiber loops and helices for integrated photonic device characterization and microfluidic roller coasters," *Optica,* vol. 3, no. 11, p. 1205, 2016.

Appendix A: Metal Temperature by Color

color	approximate temperature °F	°C	K
faint red	930	500	770
blood red	1075	580	855
dark cherry	1175	635	910
medium cherry	1275	0690	0965
cherry	1375	0745	1020
bright cherry	1450	0790	1060
salmon	1550	0845	1115
dark orange	1630	0890	1160
orange	1725	0940	1215
lemon	1830	1000	1270
light yellow	1975	1080	1355
white	2200	1205	1480

Figure 48: Temperature of metals according to color

Appendix B: Microfurnace Tapering Instructions

Setup

Step 1. Configure the LabVIEW program as shown in the image. First run the program and wait for the motor controls to connect. Stop the program and change the values as.

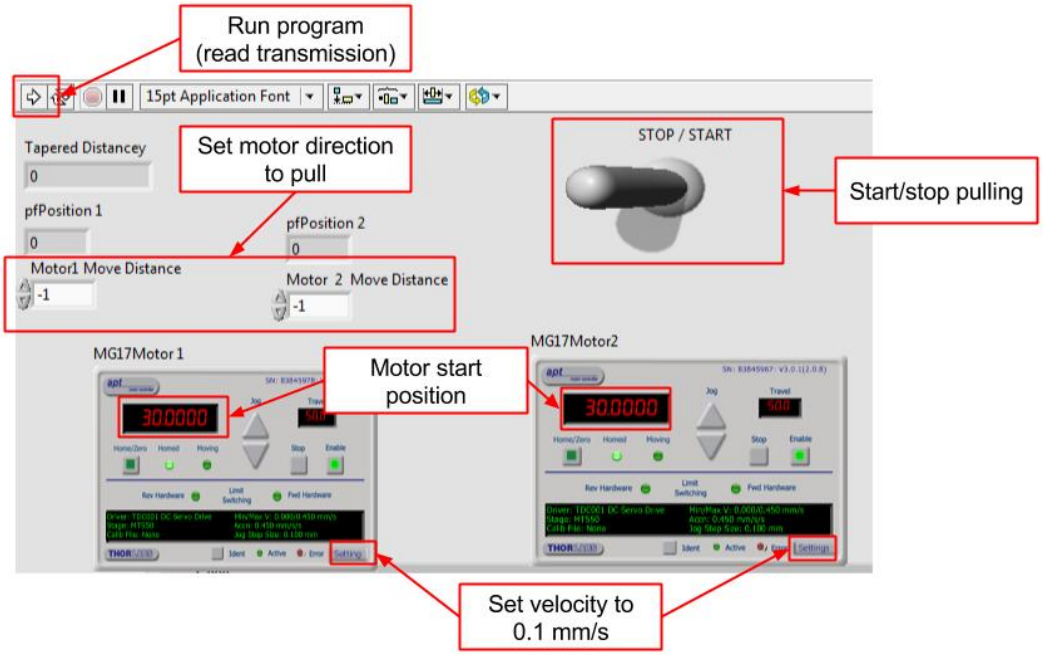

Step 2. Feed the optical fiber through the fiber clams and microfurnace. Be careful not to weave the fiber through the turns of the coil (the fiber should be concentric with the furnace).

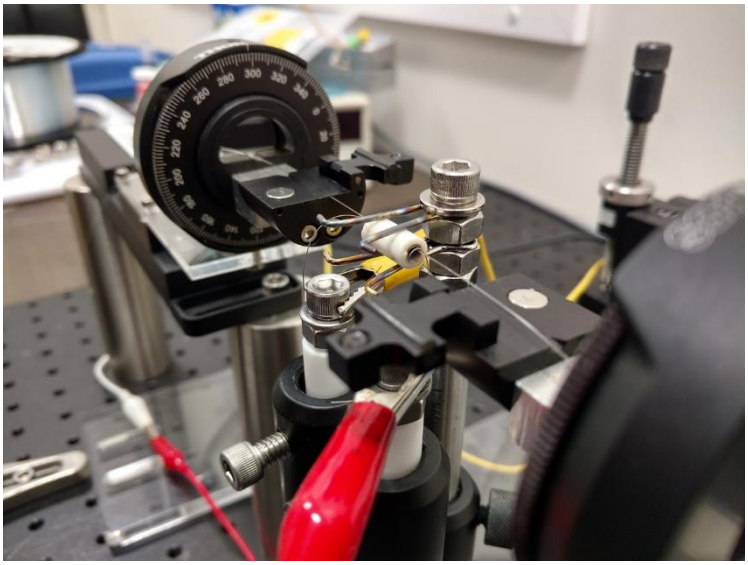

Step 3. Strip the end of the fiber using fiber strippers.

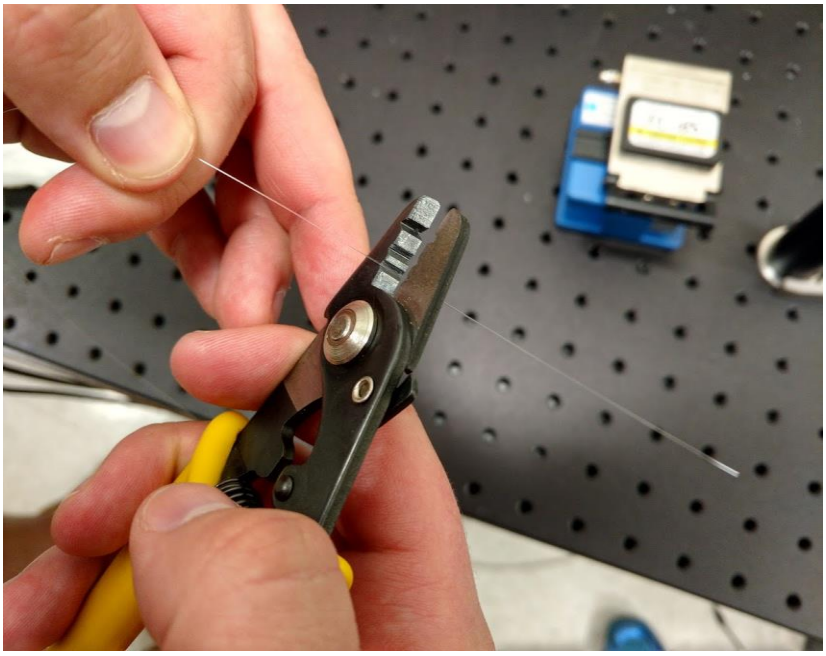

Step 4. Clean the stripped region of the fiber using Kimtech wipes and alcohol.

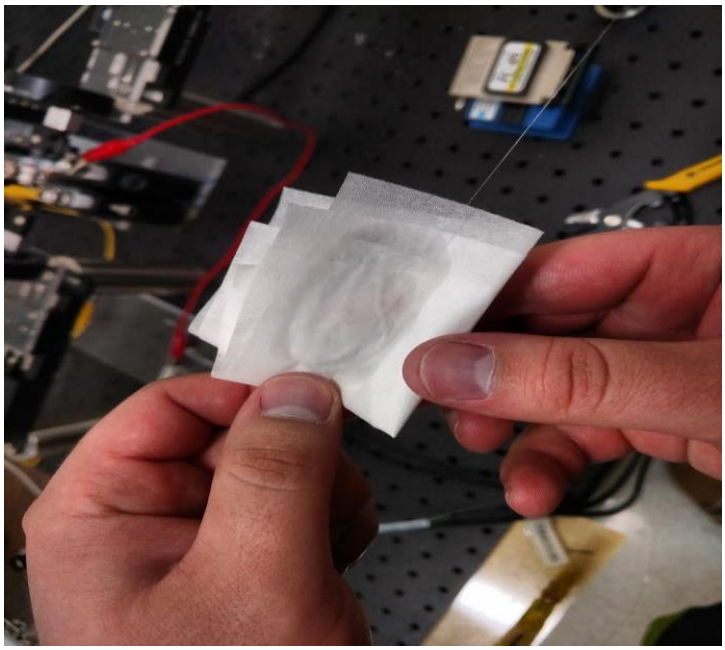

Step 5. Cleave the end of the stripped fiber.

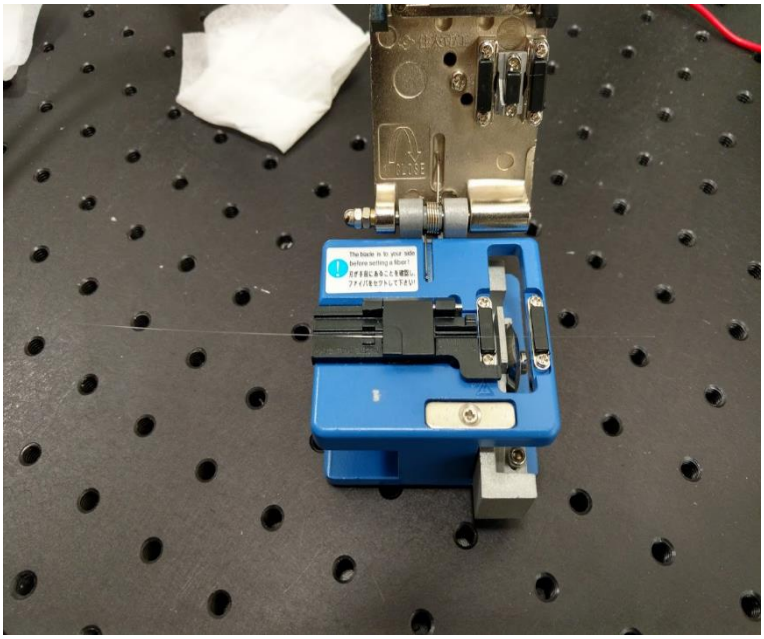

Step 6. Insert the stripped and cleaved fiber into the fiber bullet

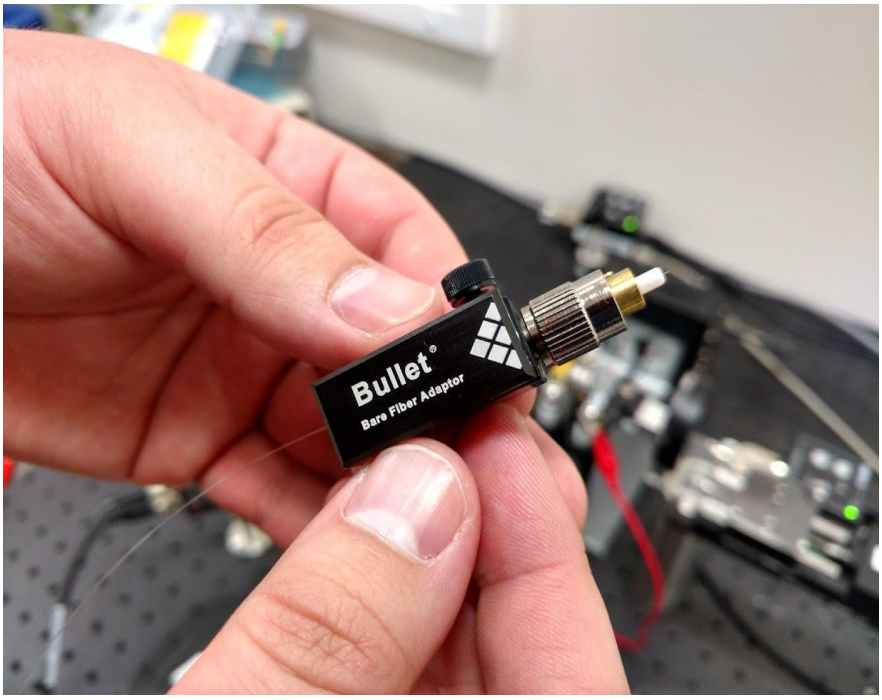

Step 7. Insert the fiber bullet connector into the photodiode for transmission monitoring.

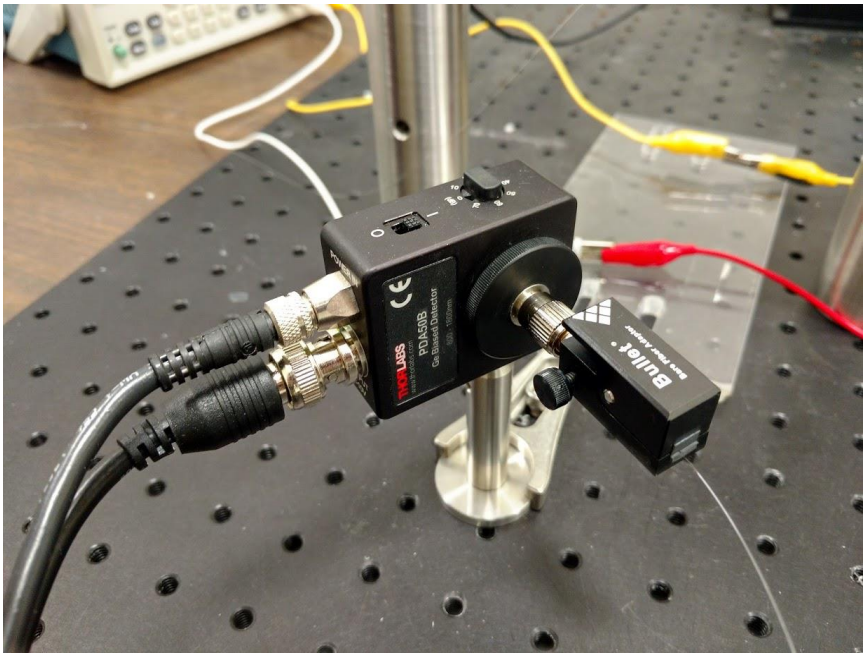

Step 8. Strip approximately 1.5 inches of the fiber in the middle to be inserted into the heating area. Clean the area with alcohol and Kimtech wipes.

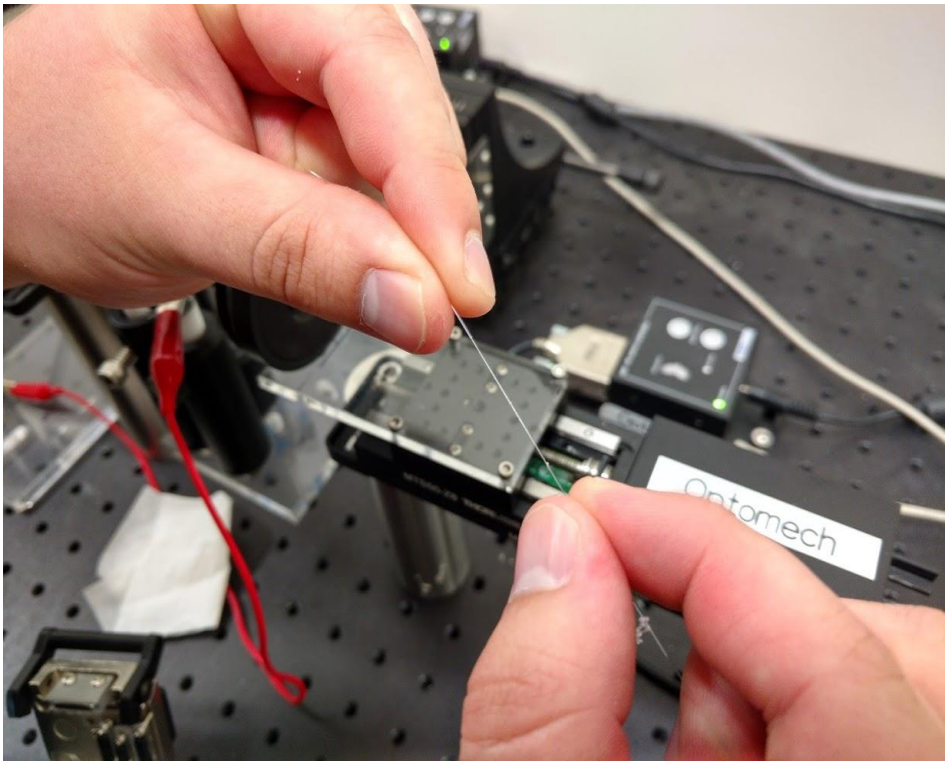

Step 9. Secure the fiber with the striped region between the two fiber clamps. The striped region should begin and end as indicated by the arrows in the picture. Make sure the unstripped fiber sits in the grooves of the fiber holder when the clamps are closed.

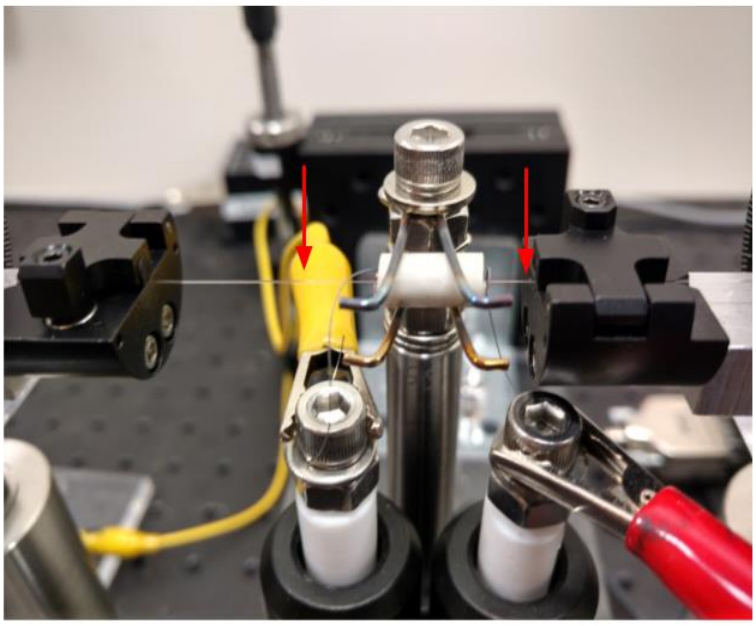

Tapering Process

Step 1. Connect the leads to the screw heads on the microfurnace as shown in the picture. Plug in and turn on the DC power supply by pressing the green button.

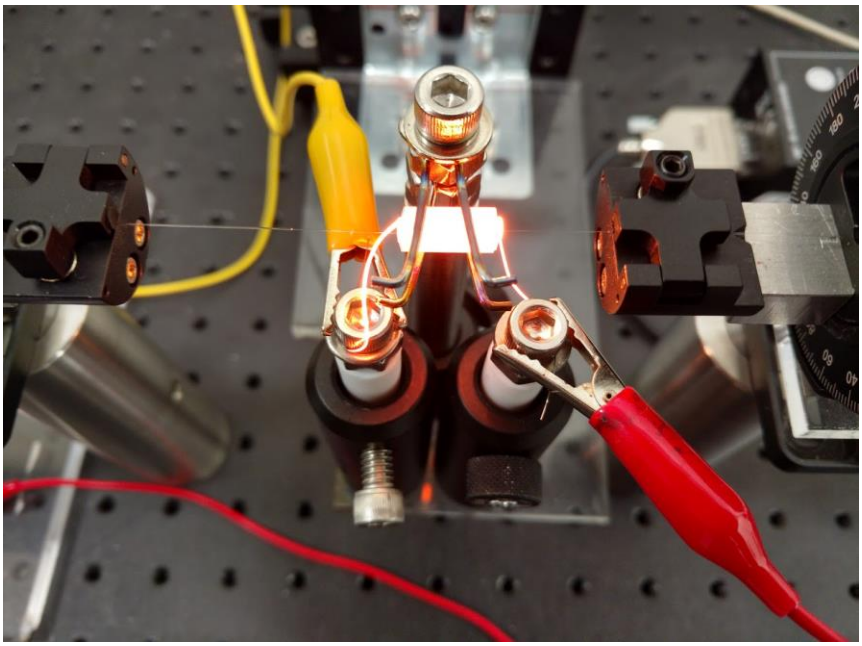

The leads are made of two wires connected by alligator clips. Make sure that the wires are not touching each other and that the connection is isolated from any conductive or metal surroundings. We used a piece of acrylic to rest the connection on. The nuts and bolts are held by teflon standoffs to electrically and thermally isolate them. This assembly is used to easily and safely connect and disconnect the alligator clips from the hot wire.

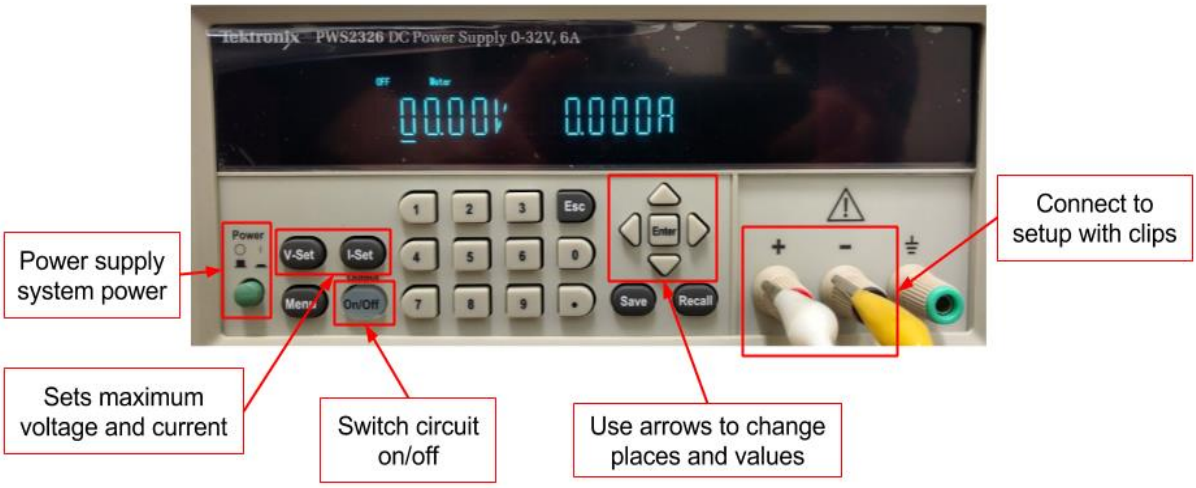

Step 2. Set the voltage to 32 V by pressing the V-Set button and entering a value of 32 then press enter.

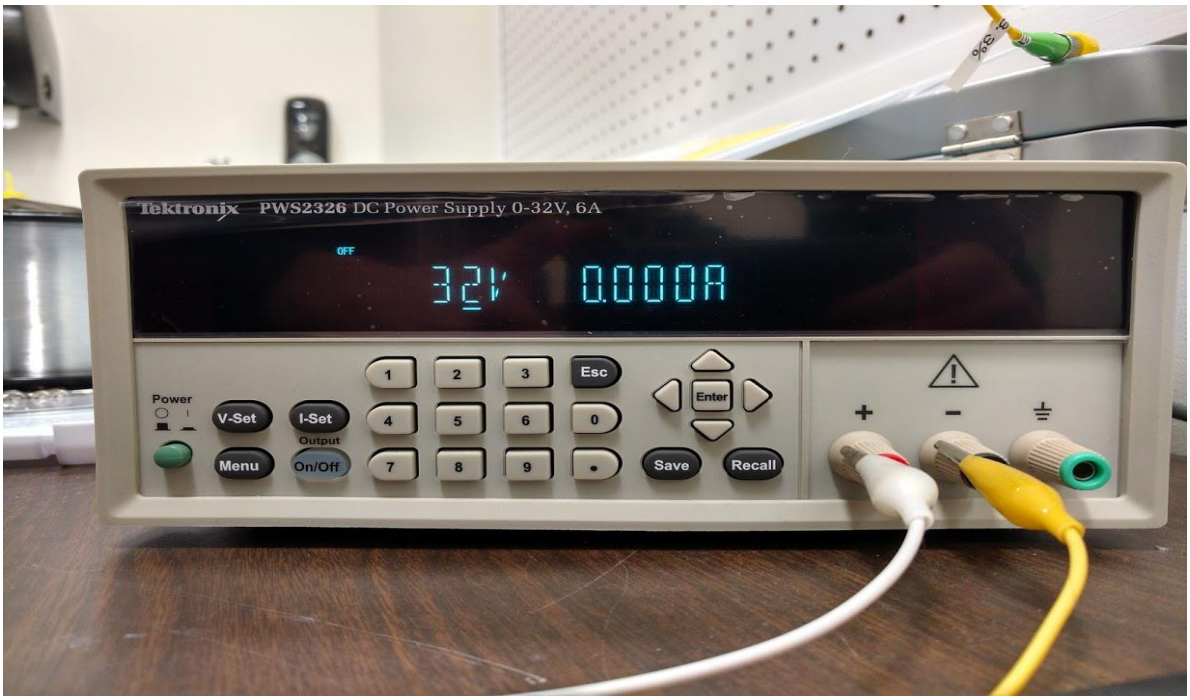

Step 3. Press the I-Set button and enter 0. Use the arrow keys to move the cursor to the 10ths place. Then press the on/off button so it illuminates green and use the up arrow to slowly bring the microfurnace online. By gradually increasing the current, the resistance wire coil will last longer. The ideal power range for the tapering process is between 55 and 75 Watts. The power is calculated by multiplying the voltage and current displayed on the power supply.

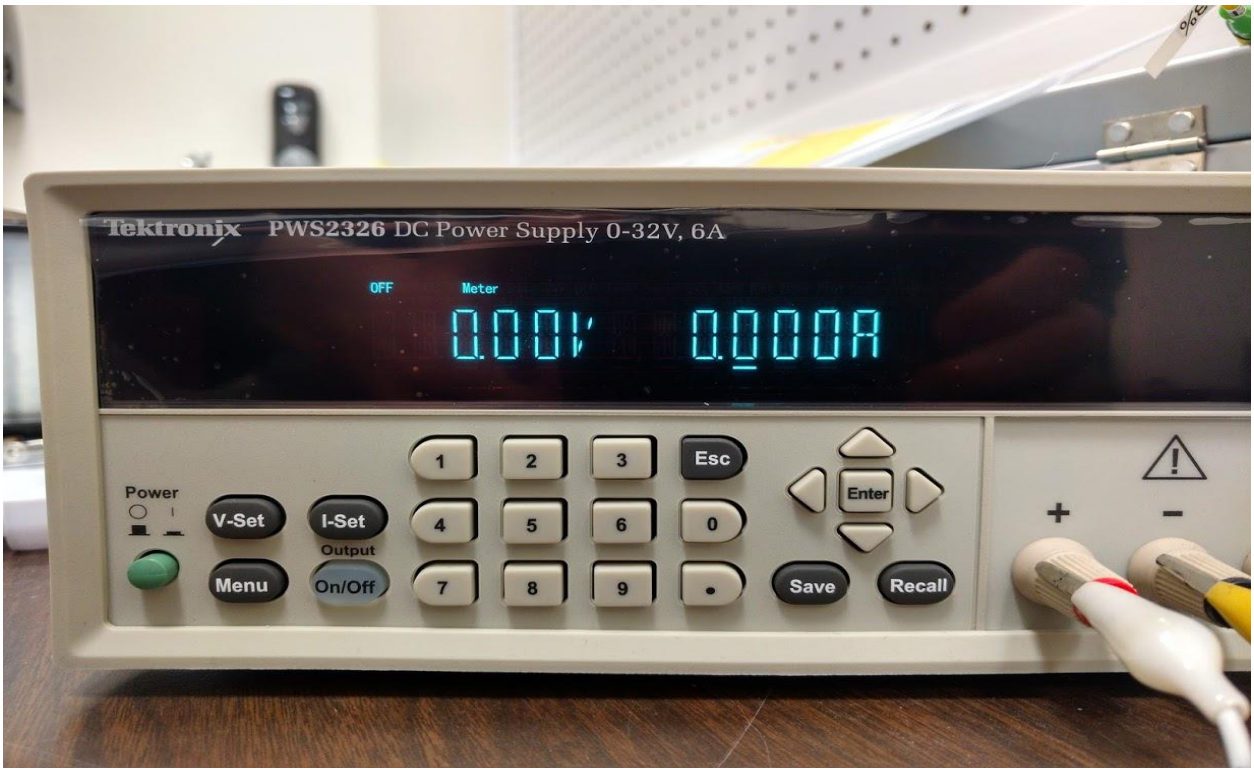

Typically, supplying between 2.3 A and 2.7 A will result in the appropriate power. The voltage will display less than 32 V because you are limiting the current and the resistance is fixed by the length of the wire.

Step 4. Allow the microfurnace to heat up for 30-60 seconds before starting the tapering process.

Step 5. Press the start/stop switch on the LabVIEW program to start tapering (motors will begin pulling)

Step 6. Look for a pattern similar to the one shown in the image below while tapering to know that the process is done and successful. Press the start/stop switch to stop the motors and stop the program from running by pressing the red stop button next to the program stop button.

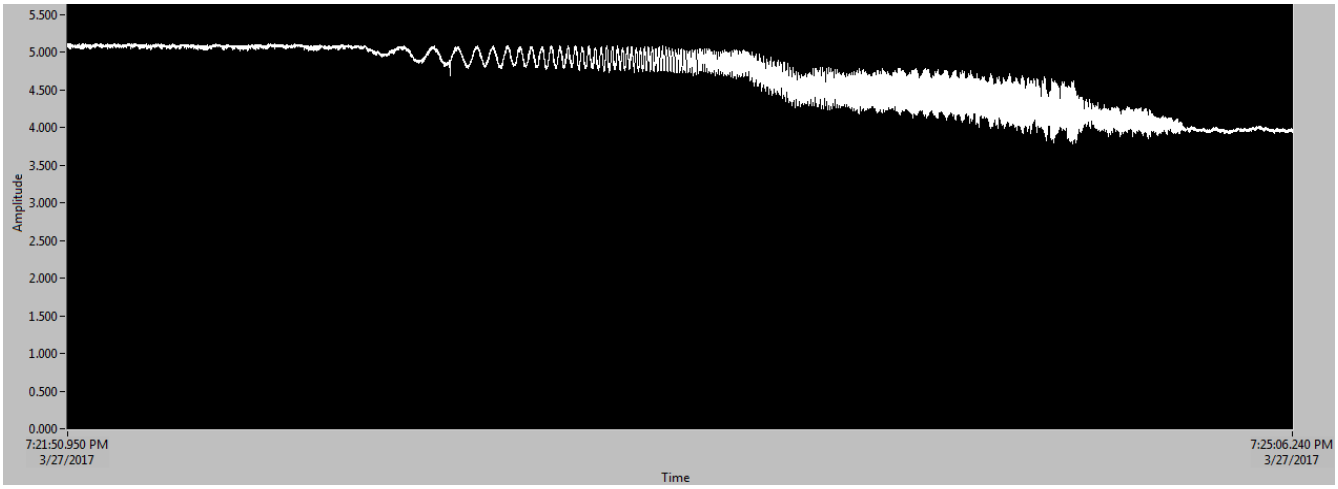

Here are some general troubleshooting guidelines:

- If the signal drops off right away, you waited too long for furnace to heat up
- If the signal doesn't look like a sin curve you don't have the right power
- If the signal consistently drops off sharply at any point due to the fiber touching the side of the furnace then the holder needs to be replaced (look in below sections for instructions) or the setup needs to be realigned

Step 7. Slowly lower the current limit of the microfurnace with the down arrow key, just as it was heated. For example, bring the amps from 2.3 to 2.2 to 2.1 and so on until 0. Press the green output on/off button for safety.

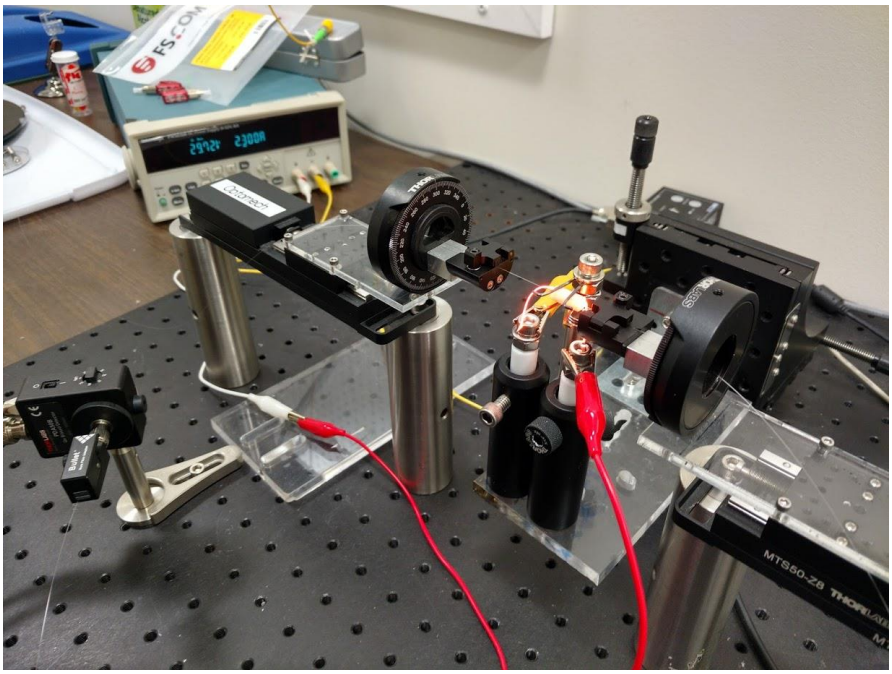

Image: Fiber tapering in process (This is what it should generally look like while you are tapering)

Removal of The Fiber

Step 1: Wait for the microfurnace to cool usually 2-3 mins so it does not burn the buffer on the optical fiber (smells kind of fruity). Move the furnace all the way to the left using the horizontal stage adjustment, as shown below. Unhook the right side of the fiber from the fiber bullet and cut a foot of excess fiber on the left.

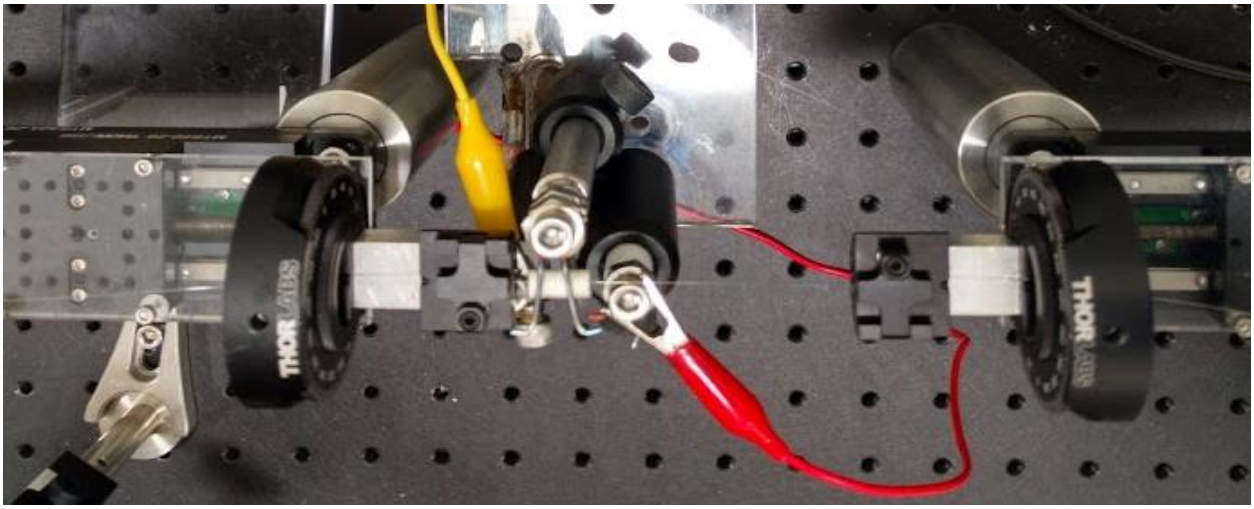

Step 2: Insert the fiber holder like the image below. Make sure you adjust the height and width to fit your specific taper length.

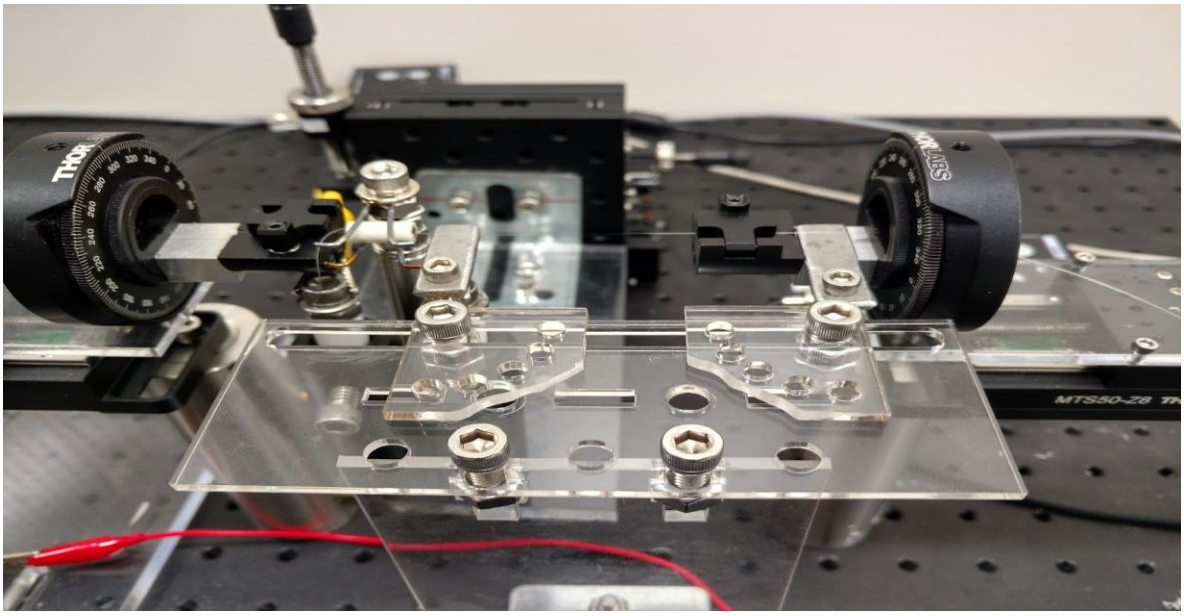

Step 3: Place the magnets over the fiber to secure the fiber to the fiber holder. Make sure that on the left arm of the holder that part of the unstripped fiber is held by the magnet or else the fiber will break during removal.

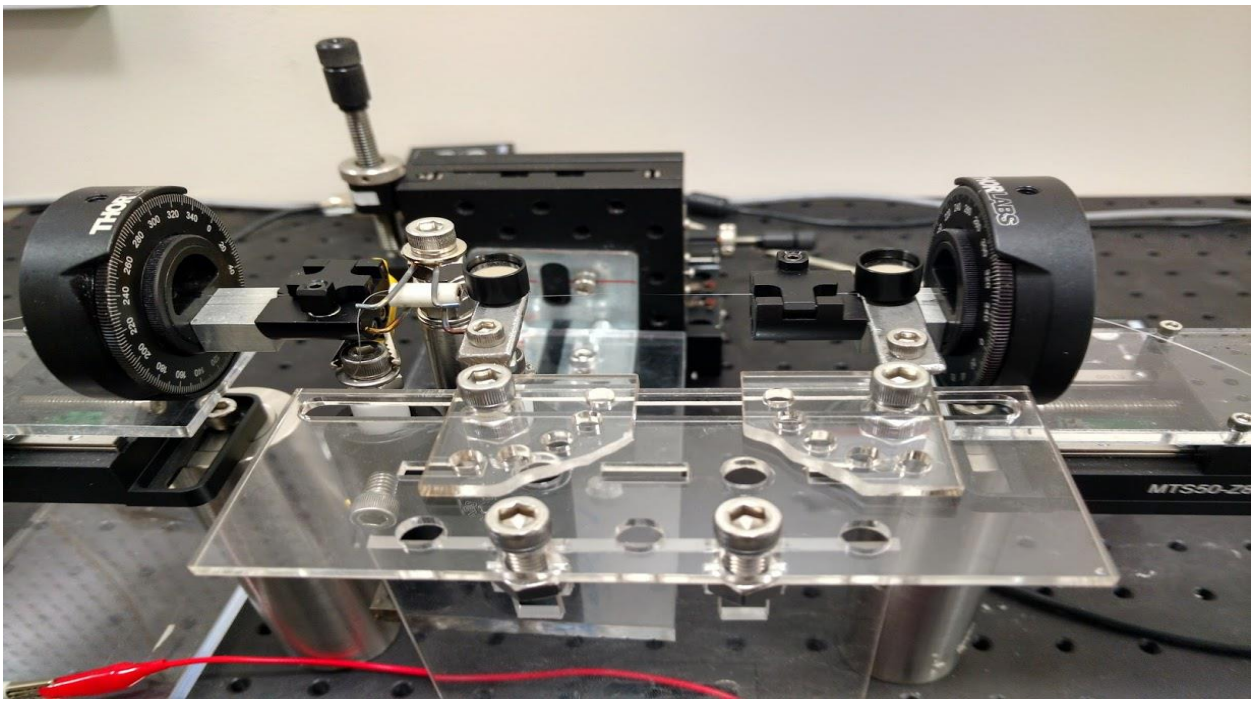

Step 4: Unclamp the optical fiber from the original clamps and use the velocity switch on the motor controller to manually move the left motor to position ~1mm for additional space.

Step 5: Move the microfurnace all the way over again using the horizontal stage adjustment so you are left with a space between the furnace and the left arm of the fiber holder, shown in the image below.

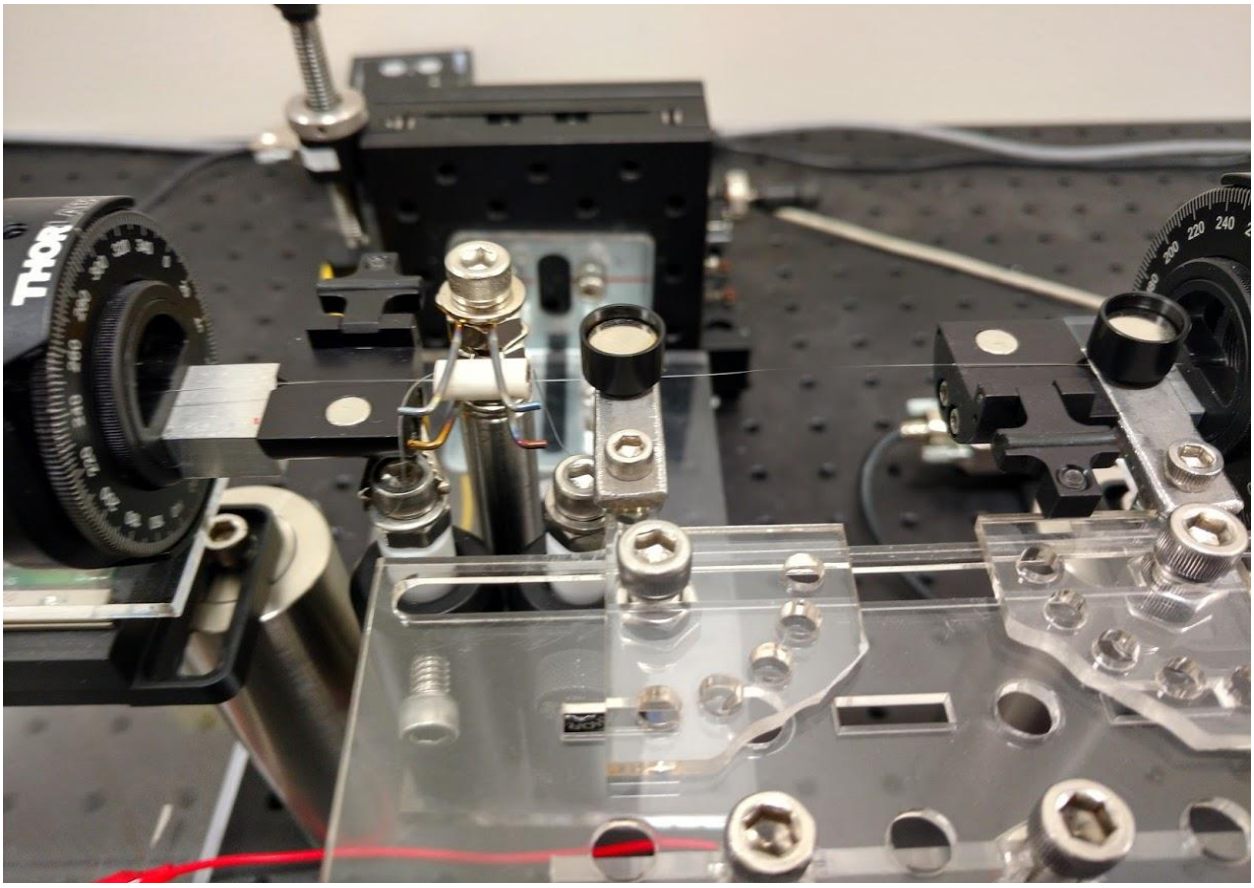

Step 6: Start by lifting up the right side of the fiber holder to get it over the fiber clamp.

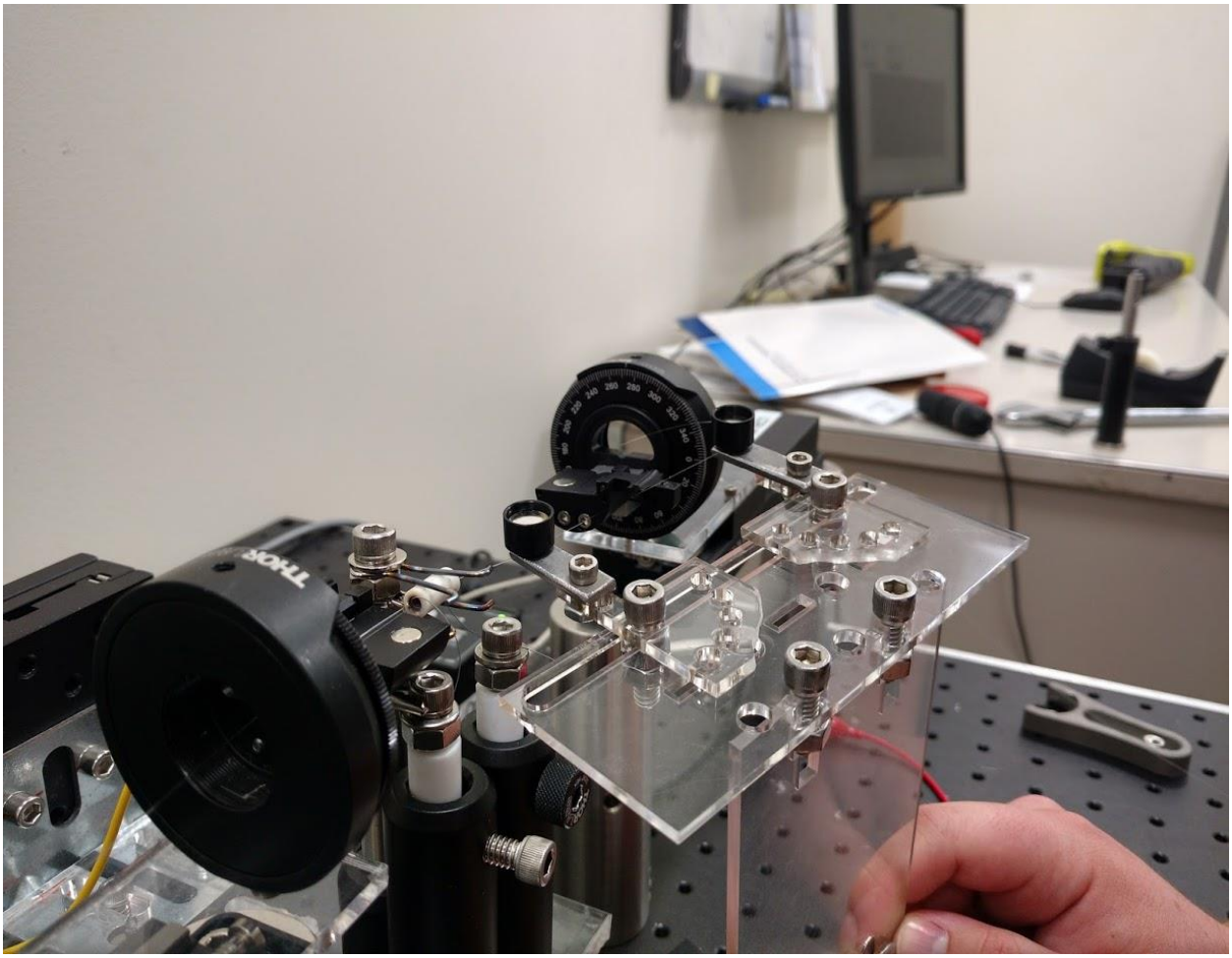

Step 7: Slowly start pulling the fiber holder away from the setup until the ends of the fiber are pulled completely through the big circles.

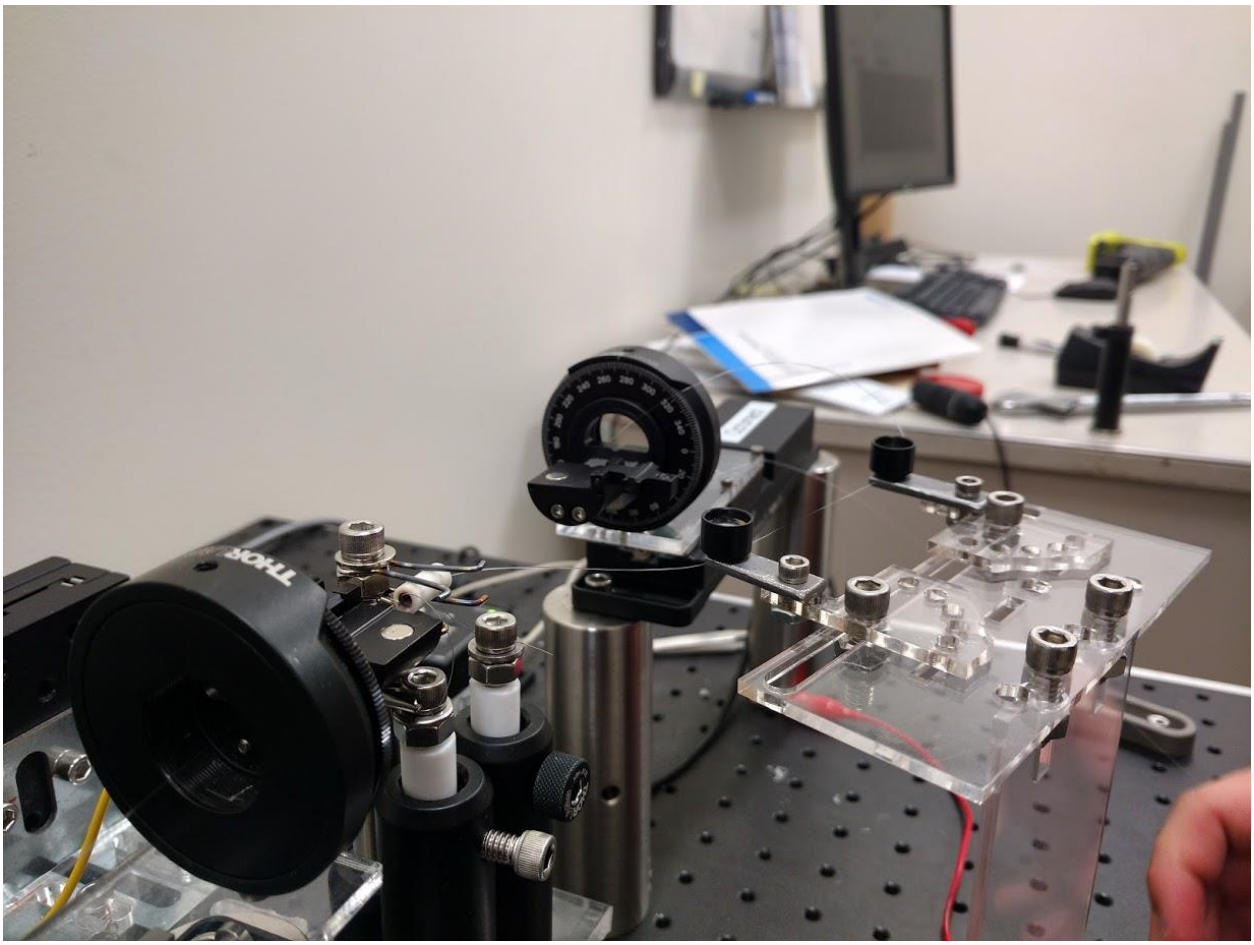

Once the fiber is removed from the furnace, it can rotated in the current holder to be transferred to other holders as needed.

Procedure for Replacing The Resistance Wire Coil

Step 1: Put a 3/32 inch drill bit backwards into the drill. Then mark with a red dry erase marker ½ inch from where the bit is held. Then wrap the resistance wire (32 AWG Kanthal A-1 resistive wire) around the bit and tape the end onto the drill.

Step 2: Slowly start turning the drill bit to make the coil.

Step 3: Stop the coiling when you get the the edge of the red spot since the coil tends to spring out a little. You want to make the coil about as dense as the one shown below. Then you want to cut about 3 inches of excess wire at the end of the coil.

Step 4: Use the vertical stage adjustment to move the microfurnace to the highest position.

Step 5: Remove the coil from the drill bit and put it on the 5/64 inch screw driver. Insert the end of the screwdriver into one end of the microfurnace and pull the coil through.

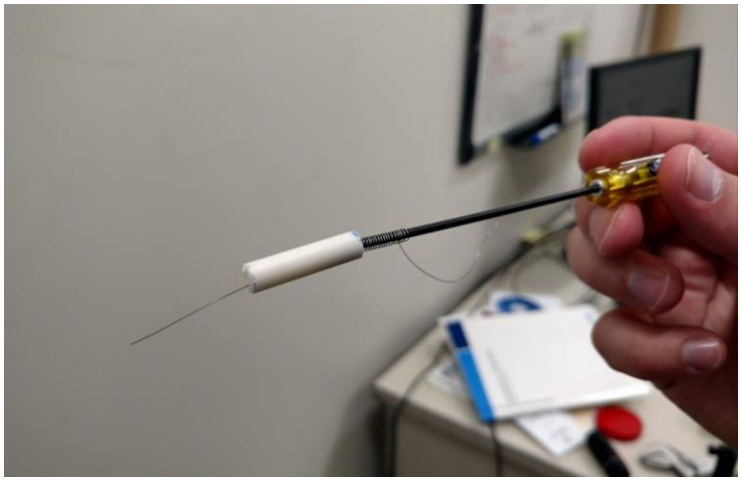

Step 6: You should now have the coil evenly in the microfurnace. You then want to attach each end of the coil to the screws. Make sure that the coil does not block your optical fiber from getting through the furnace, which usually requires a bit of finagling and experience.

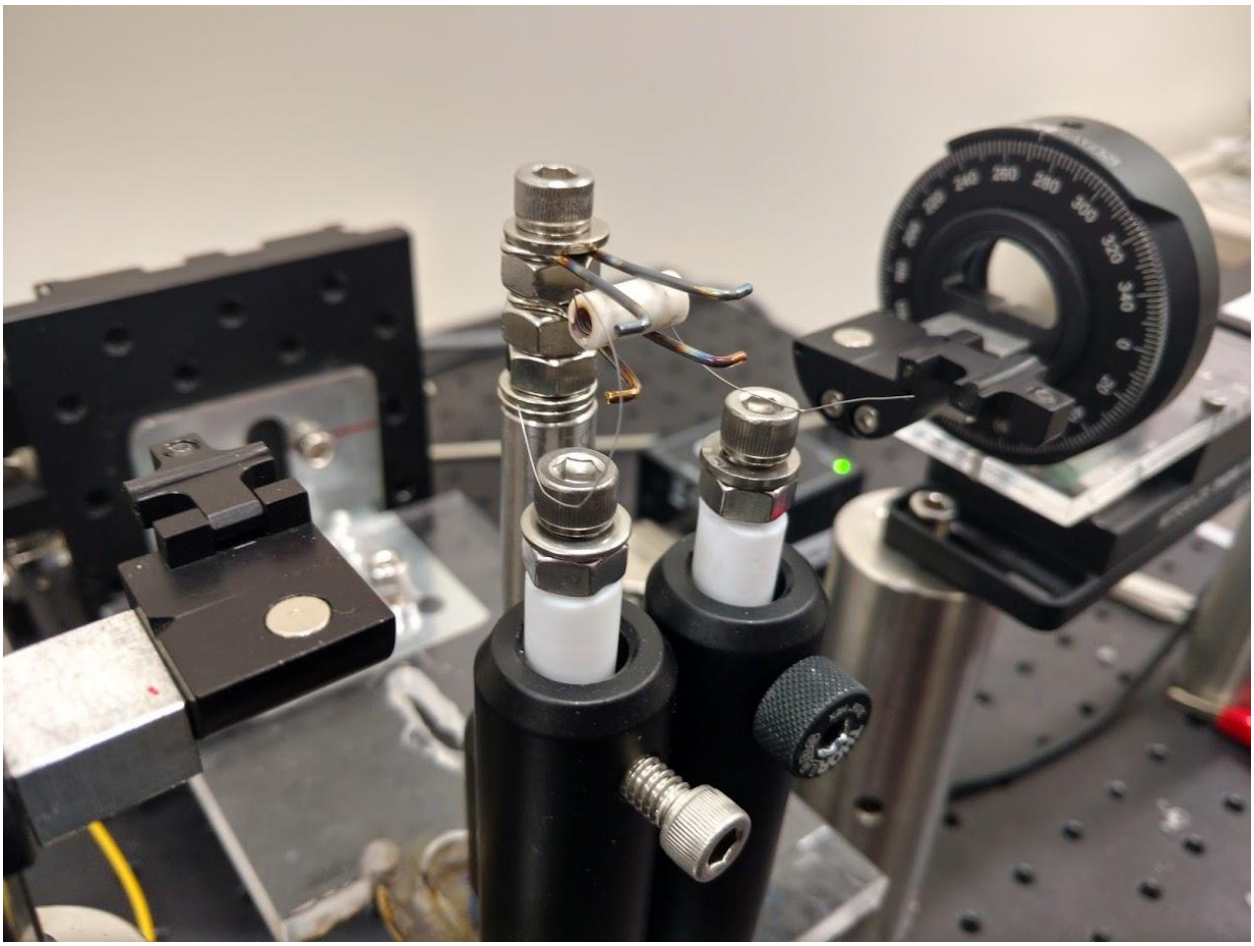

Step 7: Lower the furnace back into place with the vertical stage adjustment and attach the electrical leads to the screw heads.

Replacing the Furnace Holder

Occasionally, the transmission will drop drastically toward the end of the tapering process, or the process may not appear to work at all. The clips holding the furnace in place may need to be replaced. To do so, simply disassemble the post with the clips and reassemble it with new binder clips.